4-2016

Construction of Bicyclo[2.2.2]diazaoctane Alkaloids via Intermolecular [4+2] Cycloadditions

Jacob Gabriel Robins
College of William and Mary

Construction of Bicyclo[2.2.2]diazaoctane Alkaloids via Intermolecular [4+2] Cycloadditions

A thesis submitted in partial fulfillment of the requirement
for the degree of Bachelor of Science in Chemistry from
The College of William and Mary

by

Jacob Gabriel Robins

Accepted for HONORS

Associate Professor Jonathan R. Scheerer, Director

Professor Robert J. Hinkle

Professor John C. Poutsma

Professor Diane C. Shakes

Williamsburg, VA
April 26, 2016

ABSTRACT

The synthesis of bicyclo[2.2.2]diazaoctane prenylated indole alkaloids, containing both *syn* and *anti* ring fusion, is described. More than 100 examples of alkaloids in this family have been isolated and show a variety of potent bioactivities. This strategy utilizes the convergent and atom–economic intermolecular hetero Diels–Alder cycloaddition to construct the bicyclic nucleus from electron–deficient dienophiles and an electron–rich pyrazinone diene. The regiochemical and stereochemical implications of this cyclization are investigated.

TABLE OF CONTENTS

ACKNOWLEDGEMENTS

Firstly, my deepest gratitude goes out to Dr. Scheerer. He has been an outstanding mentor to me and many others over the years. It is a unique opportunity to work with someone who shows such dedication for his work and patience with those of us still learning this craft. I would also like to thank Dr. Robert Hinkle, Dr. J. C. Poutsma, and Dr. Shakes who have graciously served on my committee. Specifically, I owe great deal to Dr. J. C. Poutsma and collaborator Dr. Jennifer Poutsma, who have worked so hard to help me with the computational work. Many other professors have been integral to my education here at William & Mary, and to them I owe so much.

Another round of thanks goes out to all of my lab–mates in Scheerer lab, for all the success we've shared and the many more failures that we've endured. A great deal of this work would never have happened were it not for the dedicated and tireless efforts of Kyu Kim and for to him, I owe many thanks. I would also like to acknowledge Jill Williamson, who has been such a wonderful friend and collaborator, both in lab and in life.

I would not be the man I am today without the kindness and support that I found with the William & Mary Choir and Dr. James Armstrong. The Choir has become a home for me and I have drawn most of my strength from my time there. I cannot imagine my college days without these close friends.

I also must acknowledge the Second Floor Lobby party, including but not limited to John Kean, Marshall Padilla, Allison Kelley, Isaac Alty, John Rose, Margaret Olesen, and many others. Maybe it was just Stockholm's Syndrome during P. Chem., but I treasure the times we have spent together.

Finally, I need to thank my parents and my family, Josh, Leah, Aunt Liz and Uncle Dan, and Aunt Stacey and Uncle Frank. College would have been impossible with your love, care, and support.

To my parents, for instilling in me an appreciation of chemistry and a love for life

LIST OF TABLES

LIST OF FIGURES

LIST OF SCHEMES

Chapter One
Bicyclo[2.2.2]diazaoctane Prenylated Alkaloids

Introduction

Birch and Wright isolate the brevianamides in 1969, finding for the first time natural products which contain the bicyclo[2.2.2]diazaoctane core (**Figure 1.1**).[1] Since then, nearly 100 more alkaloids have been isolated which contain this same molecular scaffold. Some of these natural products, as well unnatural, synthetic cousins, have shown moderate to high biological activity. Because of the variety and intensity of this activity, as well as the intrinsic complexity of the molecular structures, the biosynthetic origin of the [2.2.2]diazabicycle, as well as methods to synthetically produce the core nucleus, have received significant attention. This chapter will summarize the structural diversity, proposed biosynthesis, and biological activity of a selected subset of these alkaloids. Synthetic strategies towards the bicyclic core will be evaluated in Chapter 2.

Figure 1.1 Bicyclo[2.2.2]diazaoctane core

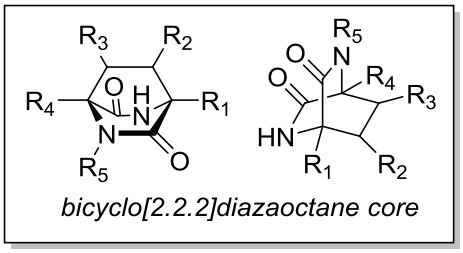

Structural Diversity

The bicyclo[2.2.2]diazaoctane ring system characterizes this class of molecules (selected examples are shown in **Figure 1.2**), structural features differ among them and will be highlighted here.

Figure 1.2 Selected Bicyclo[2.2.2]diazaoctane Alkaloids

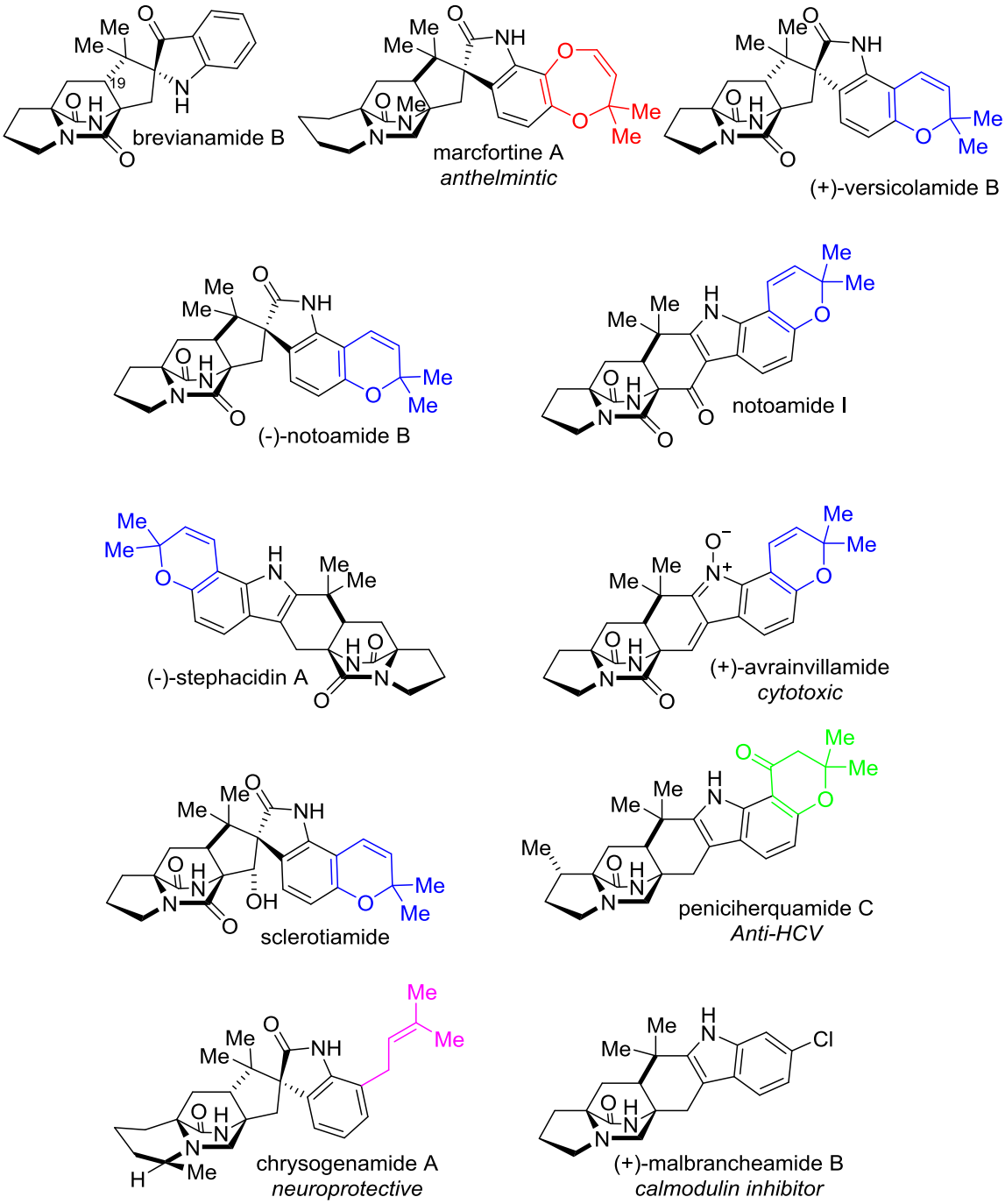

Although all members of this family are derived at least partially from a tryptophan residue, indole oxidation and prenylation varies greatly. The most prevalent substitution is a 2,2–dimethyl–*2H*–chromene, or benzopyran (highlighted in blue). The dioxepin oxidation, highlighted in red, is also observed in a number of diazaoctane alkaloids. Far less common is the 2,2–dimethylchroman–4–one moiety (highlighted in green), present only in the peniciherquamides. The malbrancheamides uniquely attest to indole halogenation. An uncyclized prenyl substitution, highlighted in pink, is present in chyrsogenamide A and some notoamides.

Three possibilities exist for the ring juncture of the tryptophan onto the bicyclic nucleus. First, a 6–membered ring can be attached directly to the indole ring. Secondly, a 5–membered spirocyclic junction onto a 2–oxindole can be seen following a purported biogenic oxidation–rearrangement sequence. The brevianamides uniquely contain a C3 keto indoline oxidation with a spirocyclic fusion. The diastereoselection of the spirocyclic junction likely depends on the C19 diastereochemistry.

Figure 1.3 shows representative diagrams for the *syn* and *anti* diastereomers of the bicyclic core. Examples exist of both diastereomers although the *syn* isomer predominates.

Figure 1.3 Diastereomers of the [2.2.2] system

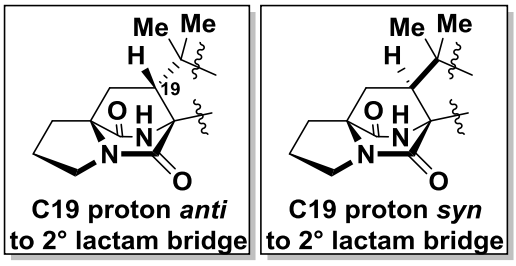

The benzylic locus, which is also the β carbon of the tertiary lactam in diketopiperazine derived bicycles, exhibits a variety of oxidation states. Many alkaloids are found in the lowest, methylene oxidation state but some have been found at the alcohol (e.g., sclerotiamide), vinyl (e.g., avrainvillamide), and ketone (e.g., notoamide I) oxidation states (**Figure 1.2**).

The bicyclic nucleus, while broadly conserved across the family, also exhibits a variety of oxidation states and substitutions. The presence of a two carbon bridge and two nitrogen atoms is common to all bicycles in this family but the six–membered ring which forms first *in* vivo can take two oxidation states: a diketopiperazine or a monoketopiperazine. This translates to the presence or absence, respectively, a carbonyl adjacent to the tertiary amine. The secondary lactam bridge, found in all known examples of this family, has been found with both *N*–methylation (as in marcfortine A) or as the lactim *O*–methyl ether.

Finally, these metabolites also show diversity in ring substitution off of the tertiary lactam. **Figure 1.3** also highlights the proline–derived pyrrolidine ring system. This is by far the most common in the family. Marcfortines A and B and chrysogenamide however contain the 6–membered pipecolic acid–derived piperidine system. Both the proline and pipecolic acid systems can show a range of substitution patterns.

The Malbrancheamides

The malbrancheamides were first isolated in 2006 from *Malbranchea aurantiaca*, which was cultured from Mexican bat guano, and represents the only class of bicyclo[2.2.2]diazaoctane indole alkaloids isolated from a genus other than *Penicillium* or *Aspergillus*.[2, 3] They are also unique in that the malbrancheamides are the only class of these alkaloids which exhibit halogenation on the indole system (**Figure 1.4**). Biologically, malbrancheamide and malbrancheamide B are of particular interest due to their calmodulin inhibitory activity of CaM–dependent phosphodiesterase (PDE1).[4, 6]

Structural features of the malbrancheamides include a monoketopiperazine ring, the aforementioned halogenation, a proline–derived ring, and a *syn* fusion with the bicyclic core.

Figure 1.4 The Malbrancheamides

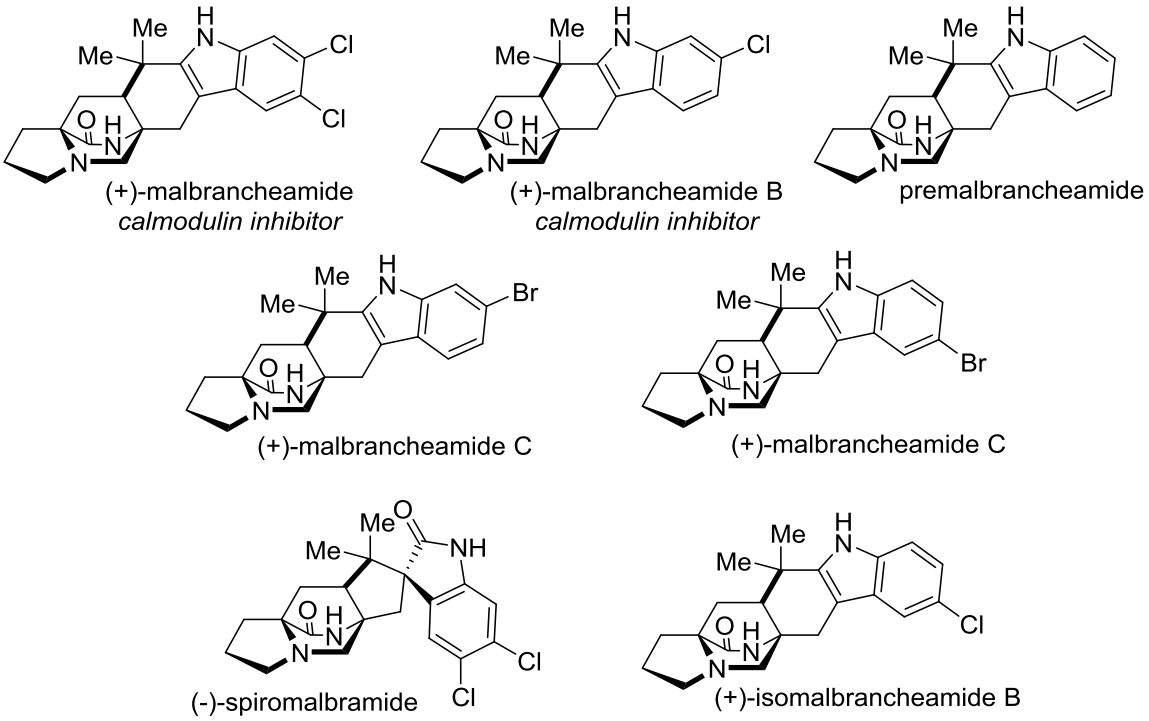

Studies into malbrancheamide biosynthesis by Williams and co–workers have yielded the following proposed pathway (**Scheme 1.1**).[5] Condensation of *L*–tryptophan with *L*–proline and dimethallyl pyrophosphate (DMAPP) affords deoxybrevianamide E and subsequent oxidation to a pyrazinone is followed by putative carbonyl reduction and subsequent intramolecular Diels–Alder (IMDA). A series of halogenases then install the halogen atoms at the necessary sites. Incorporation studies showed that radio–labelled keto–premalbrancheamide was not incorporated by *M. aurantiaca*, suggesting that carbonyl reduction occurs before cycloaddition, as indicated below.

Scheme 1.1 Proposed malbrancheamide biosynthesis

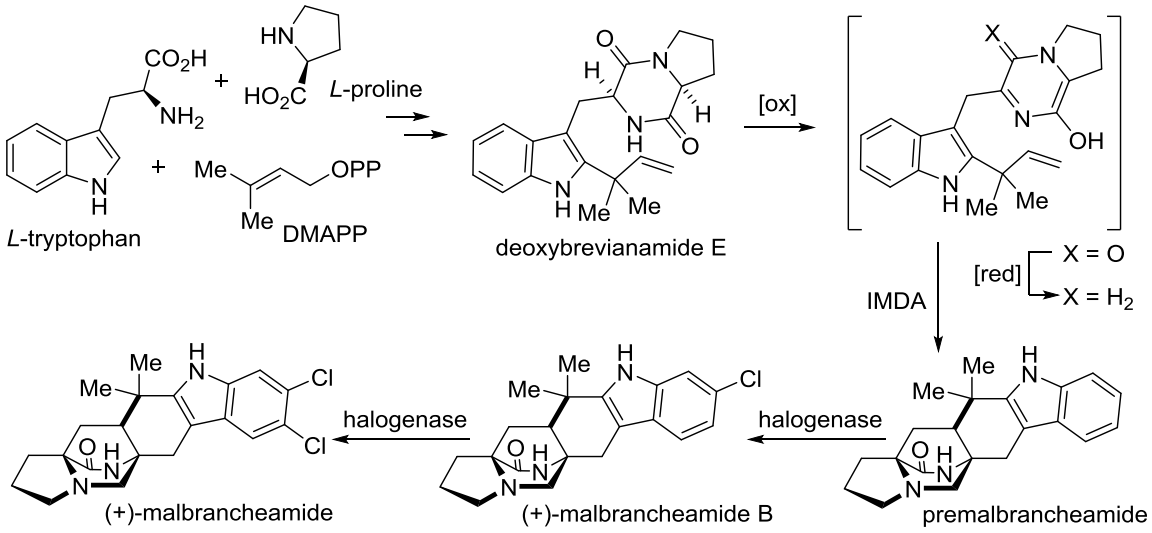

The Marcfortines and Chrysogenamide A

Blue cheese, loved by some and despised by many, was found to contain mold cultures of *Penicillium roqueforti* (now *P. paneum*) from which marcfortines A–C were isolated in 1980 by Polonsky and co–workers.[6] Structurally, the marcfortines and the closely related chrysogenamide A possess the *syn*–fused bicyclo[2.2.2] core, a monoketopiperazine ring, a spiro–oxindole moiety, and a pipecolic acid ring (**Figure 1.5**).

Figure 1.5 Marcfortines A–C and chrysogenamide A

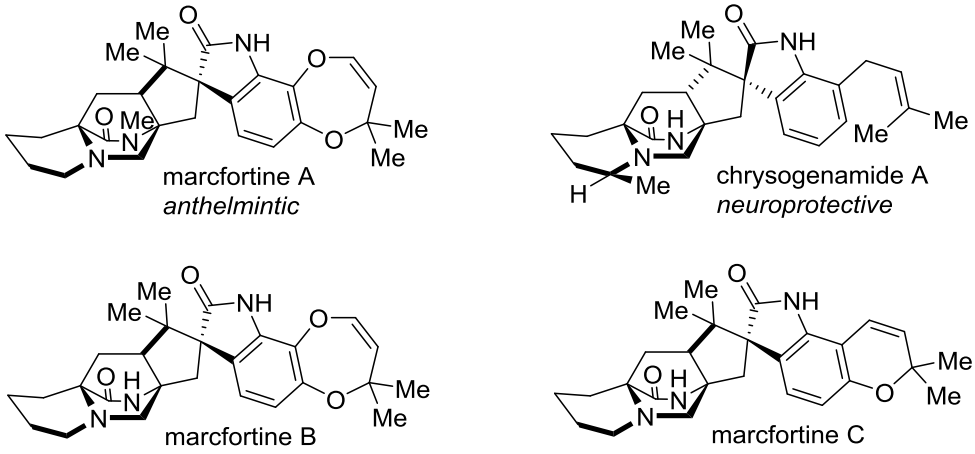

The marcfortines show structural similarity to chrysogenamide A, isolated in 2008 by Zhu et al. from *Penicillium* chrysogenum.[7] While marcfortines A and B exhibit a dioxepin ring and marcfortine C shows the more common pyran moiety, chrysogenamide A is the only alkaloid in this family with an isoprene at the C7 indole position. It is also one of the only members of the family shown to display neurocyte protection in the face of oxidative stress–induced cell death. Chrysogenamide A also possesses the less common *anti*–fused bicyclic core and a substituted pipecolic acid unit, unlike the marcfortines. Marcfortine A displays anthelmintic activity, a trait which is also found in the broad class of paraherquamides, discussed below.

Paraherquamides

Consisting of at least 16 related secondary metabolites, the paraherquamide subfamily is one of the largest and most structurally diverse of the bicyclo[2.2.2]diazaoctane indole alkaloids. Conserved among all members of this subfamily is a monoketopiperazine ring, *syn* fusion like the marcfortines and (excluding VM55599 and pre–paraherquamide) a substituted spiro–oxindole moiety (**Figure 1.6**). Many of the paraherquamides exhibit *N*–methylation on the bridging secondary lactam.

Figure 1.6 Selected paraherquamides and derquantel

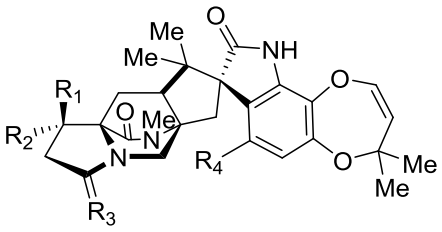

(-)-paraherquamide A, R_1 = OH, R_2 = Me, R_3 = H_2, R_4 = H
(-)-paraherquamide B, R_1 = H, R_2 = H, R_3 = H_2, R_4 = H
paraherquamide H, R_1 = H, R_2 = Me, R_3 = O, R_4 = H
SB203105, R_1 = H, R_2 = Me, R_3 = H_2, R_4 = OH

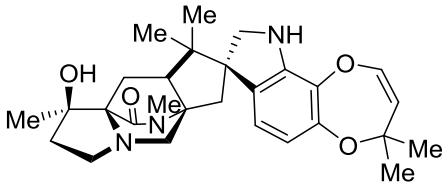

derquantel
(2-deoxyparaherquamide A)

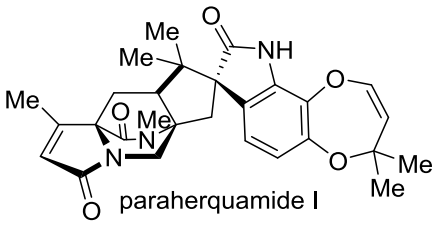

paraherquamide I

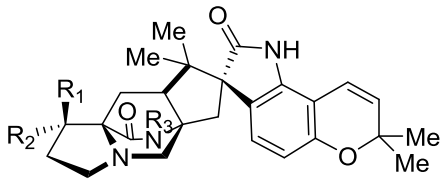

paraherquamide F, R_1 = H, R_2 = Me, R_3 = Me
paraherquamide G, R_1 = OH, R_2 = Me, R_3 = Me
VM55595, R_1 = H, R_2 = Me, R_3 = H

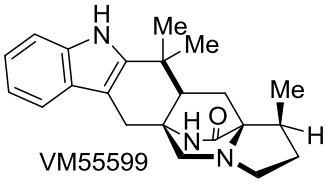

VM55599

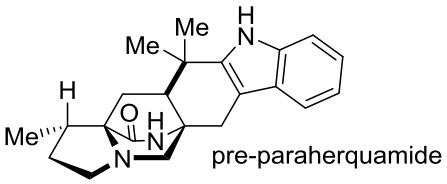

pre-paraherquamide

Paraherquamide A was first isolated from *P. paraherquei* (also called *P. brasilianum*) in 1981, followed by paraherquamides B–G from *P. charlesii*. Paraherquamides H, I and many related compounds have been isolated from the aforementioned soil fungal cultures and others.[8]

Parasitic nematodes pose significant problems to human and animal populations and the potent anthelmintic activity of certain paraherquamides have garnered them significant interest. Specifically, SB200437 (not shown), SB 203105, and paraherquamide A have been shown to act against parasites which have developed resistance to broad–spectrum anthelmintics.[9] However, paraherquamide A also exhibited high toxicity towards healthy cells so Pfizer, interested in capitalizing on the potential market profitability, synthesized derquantel as a safer alternative.[10] Derquantel is now sold as a combination treatment with abamectin under the brand name Startect.[11]

Peniciherquamides and Mangrovamides

Isolated from *Penicillium herqui* in 2015, peniciherquamides A–C are close relatives of the paraherquamides (**Figure 1.7**).[12] Structurally, the peniciherquamides exhibit a *syn*–fused diazabicyclo[2.2.2]octane core, a monoketopiperazine ring with a β–methylproline moiety, and 2,2–dimethylchroman–4–one functionalized spiro–oxindole feature. Peniciherquamide B also uniquely displays *O*–methylation of the secondary lactam.

Figure 1.7 Peniciherquamides A–C and selected mangrovamides

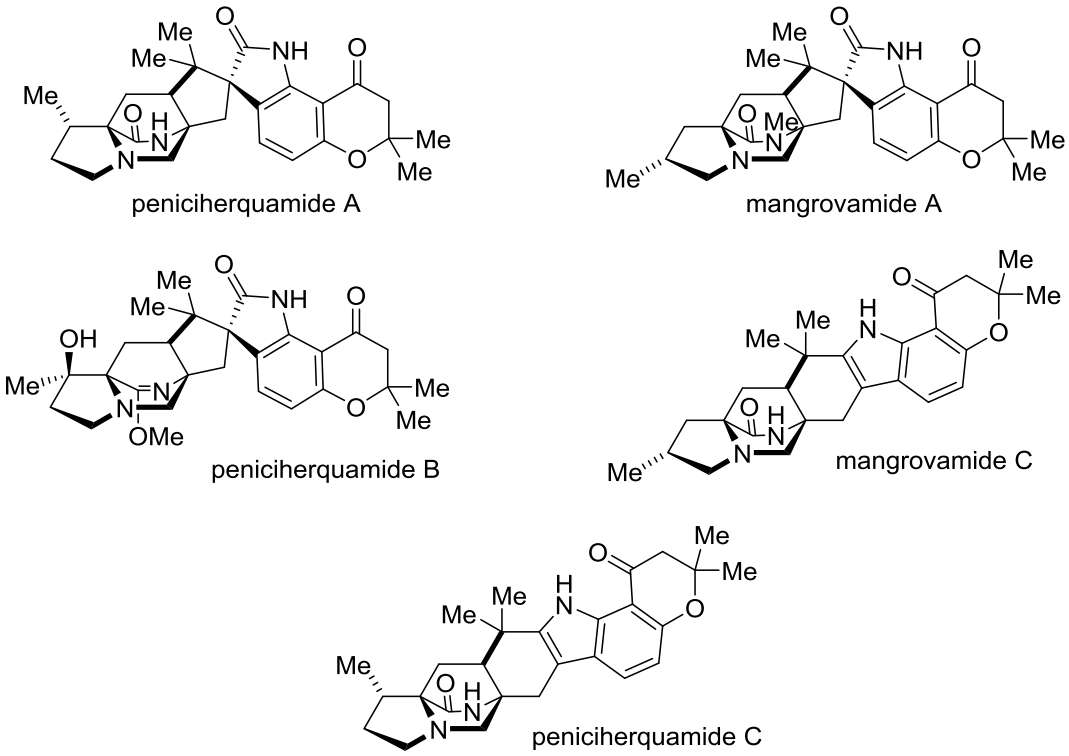

Other natural products in this family with a β–methylproline ring include VM55595, paraherquamide A, and SB203105. The mangrovamides share the unique 2,2–dimethylchroman–4–one moiety with the peniciherquamides, in addition to the *syn*–fused bicycle but feature *N*–methylation (except mangrovamide C) and a γ–methylproline.[13] Peniciherquamide C, however, is unique in that it is the only bicyclo[2.2.2]diazaoctane prenylated indole alkaloid to show significant anti–hepatitis C virus activity (5.1 μM).[12]

The Brevianamides

First isolated from *Penicillium brevicompactum* in 1969 by Birch et al., the brevianamides are quintessential members of the [2.2.2]diazabicyclic alkaloid family (**Figure 1.8**).[1] The brevianamides show no indole substitution, an unsubstituted proline–

derived ring, the unusual *anti* configuration, a unique spiro–indoxyl moiety, and are derived from a diketopiperazine, the first of such molecules to be discussed here. Despite this relative structural simplicity, brevianamides A and D have shown modest antifeedant and insecticidal activity.[14] It is important to note that the brevianamides C and D are artifacts of isolation to light exposure, not natural products.

Figure 1.8 The Brevianamides A–F

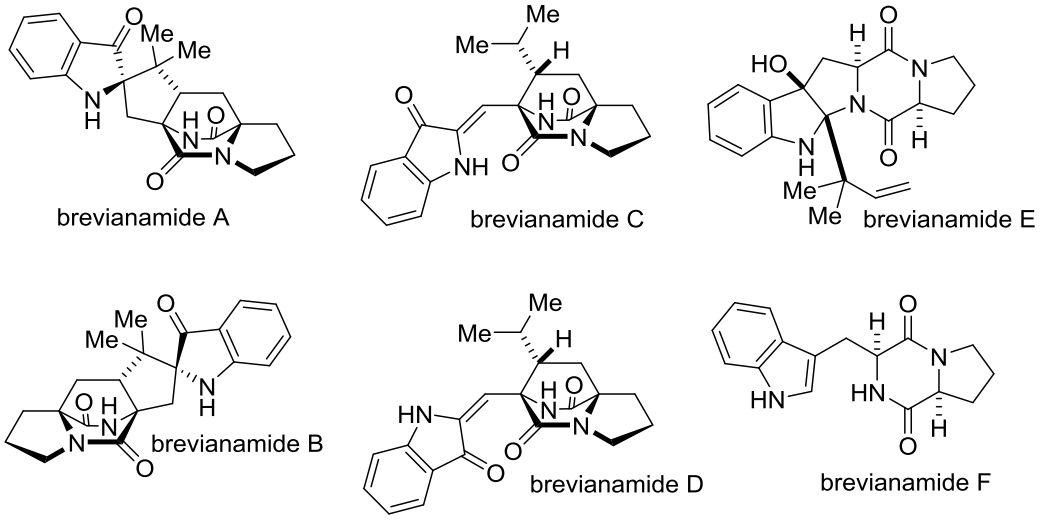

Birch and co–workers undertook a study of the biosynthetic origins of the brevianamides and proposed **Scheme 1.2** as a likely route.[15] They proposed that the condensation of *L*–tryptophan and *L*–proline affords brevianamide F. Subsequent reverse prenylation would afford deoxy brevianamide E. Multi–step oxidation and cyclization would then yield brevianamides A and B.

Scheme 1.2 Birch's proposed brevianamide biosynthesis

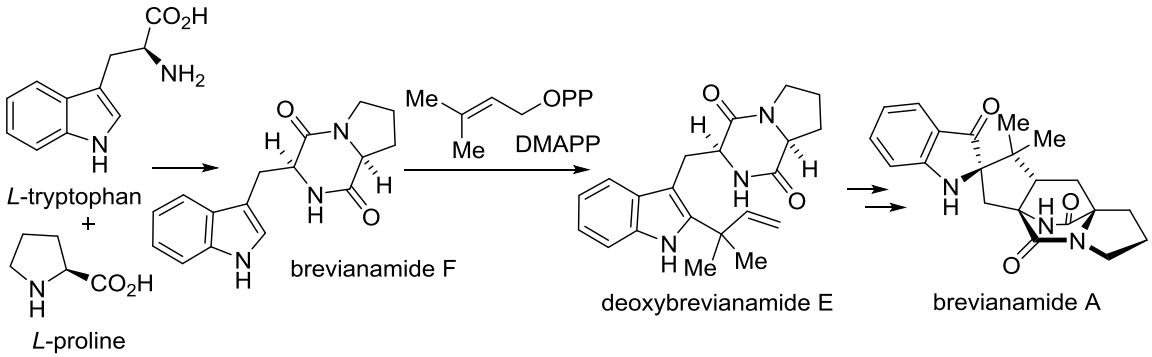

Continued studies by Williams et al. have updated Birch's original proposal and the results of this inquiry is summarized in **Scheme 1.3**.[16] It was observed that radiolabeled deoxybrevianamide E was incorporated as brevianamides A, B, and E, thereby supporting Birch's proposal that it was a precursor to cyclization. However, a racemic mixture of a brevianamide B–type structure **3** which lacked the spiro–oxindole moiety was not incorporated by *Penicillium brevicompactum* into brevianamide B. This suggests that 0indole oxidation occurs prior to cyclization. It was thus proposed that deoxybrevianamide is selectively oxidized to **1** and then further converted to azadiene **2** which participates in an intramolecular Diels–Alder cycloaddition. Synthetic challenges have hindered attempts to conclusively validate this pathway.

Scheme 1.3 Williams's updated brevianamide biosynthesis

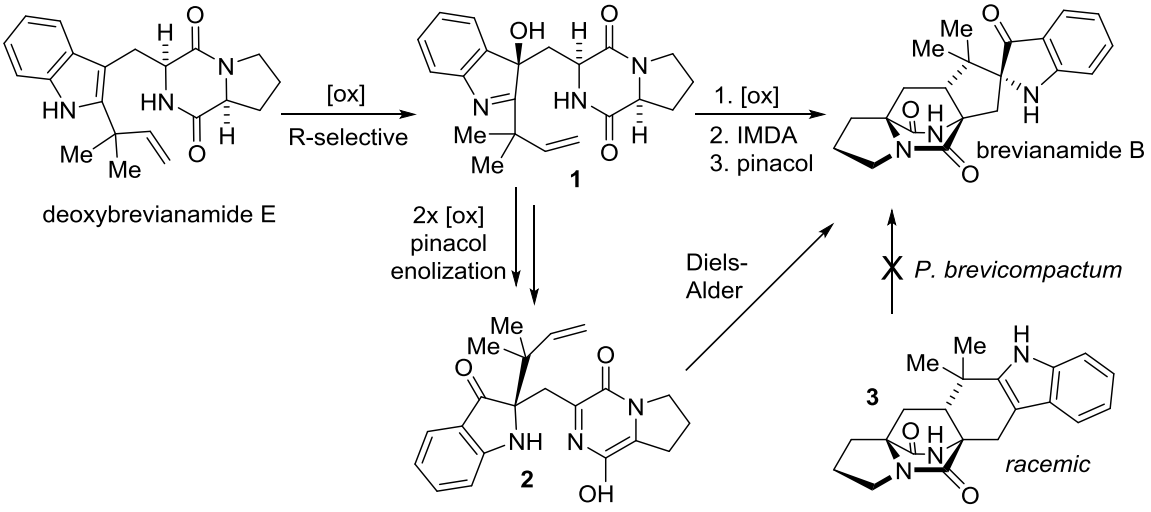

The Stephacidins and Notoamides

The final class of bicyclo[2.2.2]diazaoctane–containing prenylated indole alkaloids to be discussed here are the broad category containing the stephacidins, notoamides, and versicolamides (**Figure 1.9**). Sclerotiamide was the first to be isolated in 1996 from *A. sclerotiorum*,[17a] with the stephacidins A and B later isolated from the terrestrial species *A. ocraceus* WC76466[17b] and avrainvillamide from the marine species *Aspergillus* sp. CNC358.[17c,d] Notoamides A–R, isolated from a variety of both marine and terrestrial fungi, have been key in the continued research into understanding the biosynthesis of this class of molecules. [17e–k] Stephacidin A, notoamide B, and versicolamide B have also been isolated from the terrestrial fungus *A. amoenus* (formerly *A. versicolor*)[17j] and from the marine–derived *A. protuberus* (formerly *Aspergillus* sp. MF297–2).[17h] Closer analysis of these isolates revealed that the compounds isolated from the two species were in fact enantiomers of each other. This represents the first example of enantiomeric reverse prenylated indole alkaloids found in nature.

Figure 1.9 Selected stephacidins, notoamides, and versicolamides

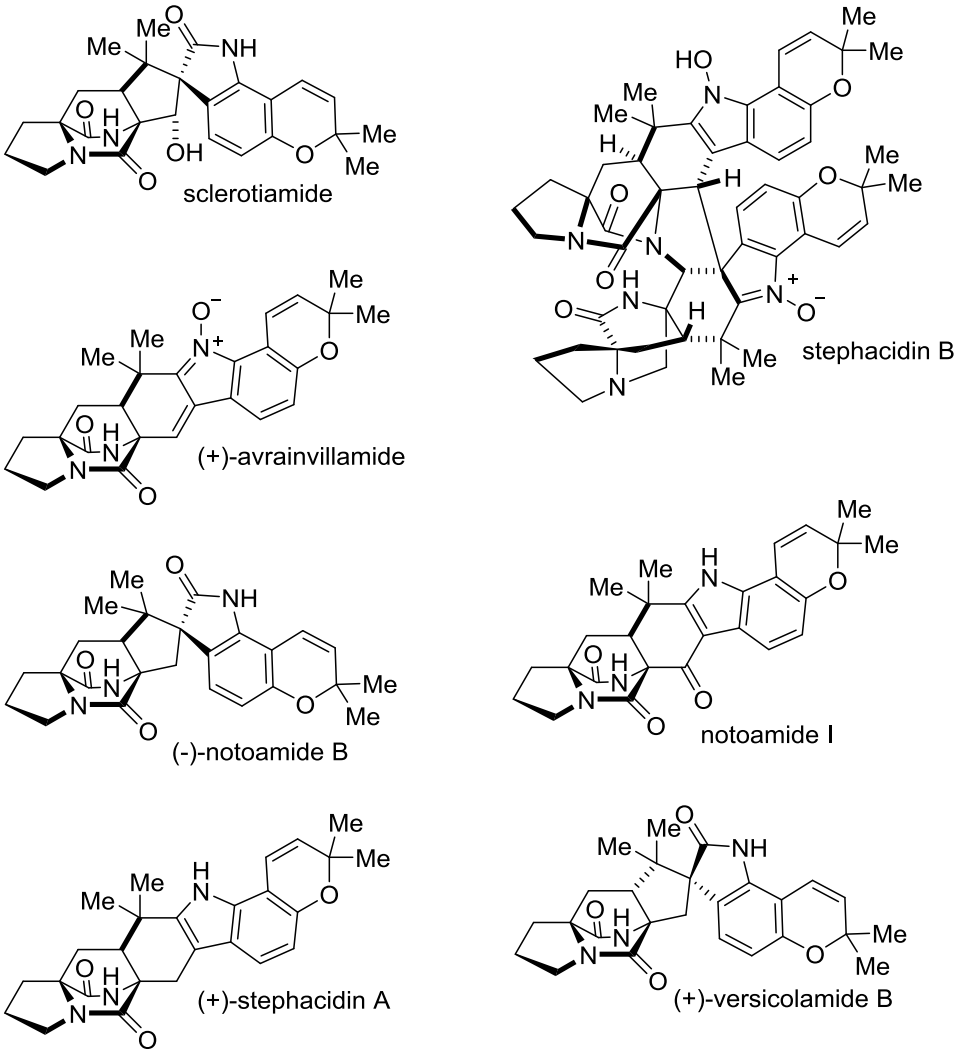

This subclass of molecules displays a diketopiperazine core, like the brevianamides, and an unsubstituted pyrrolidine ring adjacent to the bicyclic core. The versicolamides and the 6–*epi* natural products are unique in the class in that they exhibit *anti* ring fusion to the bicyclic diketopiperazine; the other members of the subclass show the more common *syn* junction. The indole systems of these compounds are always oxygenated, either as the pyran ring or its uncyclized, reverse prenylated precursor as in

notoamide T. Finally, these isolates exhibit two kinds of unions with the indole systems: 5–membered spirocycles and 6–membered rings.

The isolation of notoamide S from *A. amoenus* in 2015 by Williams et al., along with an enantiomeric mixture of 6–*epi*–stephacidin, has proven key in elucidating the proposed biosynthetic pathway proposed below (**Scheme 1.4**).[17l] As before, condensation of tryptophan and proline affords brevianamide F which is converted to deoxybrevianamide E. Unique to this subclass, the indole ring is oxidized and reverse prenylated to yield first 6–hydroxy–deoxybrevianamide E and then the key precursor notoamide S. A two–electron oxidation converts notoamide S into a putative achiral azadiene which then undergoes intramolecular Diels–Alder cycloaddition to yield one or the other enantiomer of notoamide T, depending on the species of fungi in question. Cyclization leads to stephacidin A which can then undergo oxidation and a pinacol rearrangement to yield one or the other enantiomer of notoamide A, or versicolamide B if 6–*epi*–notoamide T was formed.

Alternatively, (+)–stephacidin A can be oxidized to form (+)–avrainvillamide which then dimerizes to form the massive (-)–stephacidin B (**Scheme 1.5**). Because all three of these structures have been isolated, it is clear that this dimerization must occur *in vivo* however the exact mechanism for this is still unclear. Qian–Cutrone and co–workers originally proposed that protonation of one monomer to the *N*–hydroxyindole would lead to electrophilic attack of the olefin of another monomer's center carbocyclic ring.[17b] This would form a secondary carbocation which would then be attacked by the first monomer's secondary lactam bridge to install the five–membered ring, yielding stephacidin B. However, Nussbaum has proposed an alternate strategy whereby one monomer's

secondary lactam nitrogen acts as an aza–Michael addition donor which creates a transient *N*–hydroxyindole on the second monomer.[18] This second monomer then acts as a second aza–Michael addition donor on the first monomer which then forms the final *N*–hydroxyindole system. This is an entirely new system for aza–Michael addition but is corroborated by the evidence from the Myers group that simplified derivatives of these nitrones undergo Michael addition with methanol at room temperature.[19] The Myers group found that the dimerization occurs spontaneously when avrainvillamide is exposed to triethylamine at room temperature.[20] It was later shown that retrodimerization occurs with relative ease *in vivo*, which provides evidence for the hypothesis that avrainvillamide is the actual bioactive agent, not stephacidin B.[21]

Scheme 1.5 Synthesis of stephacidin B

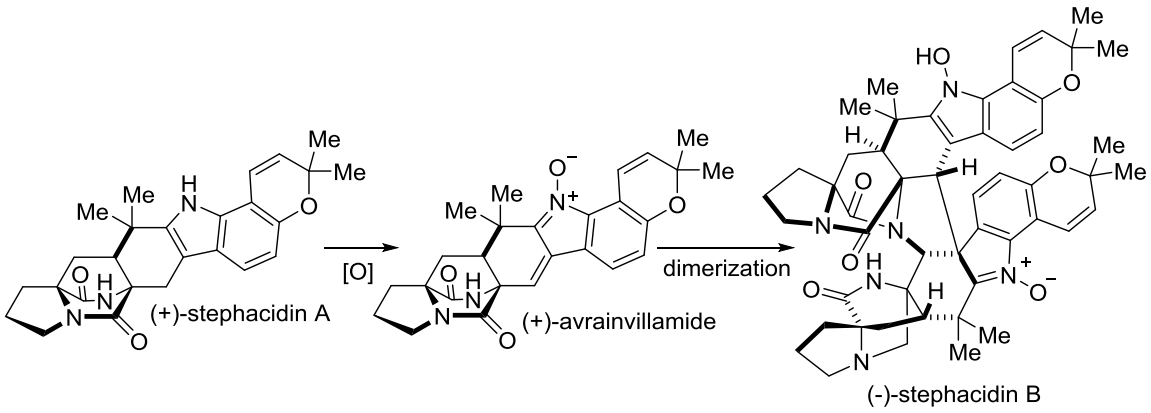

Scheme 1.4 Proposed biosynthesis of stephacidins, notoamides, and versicolamides

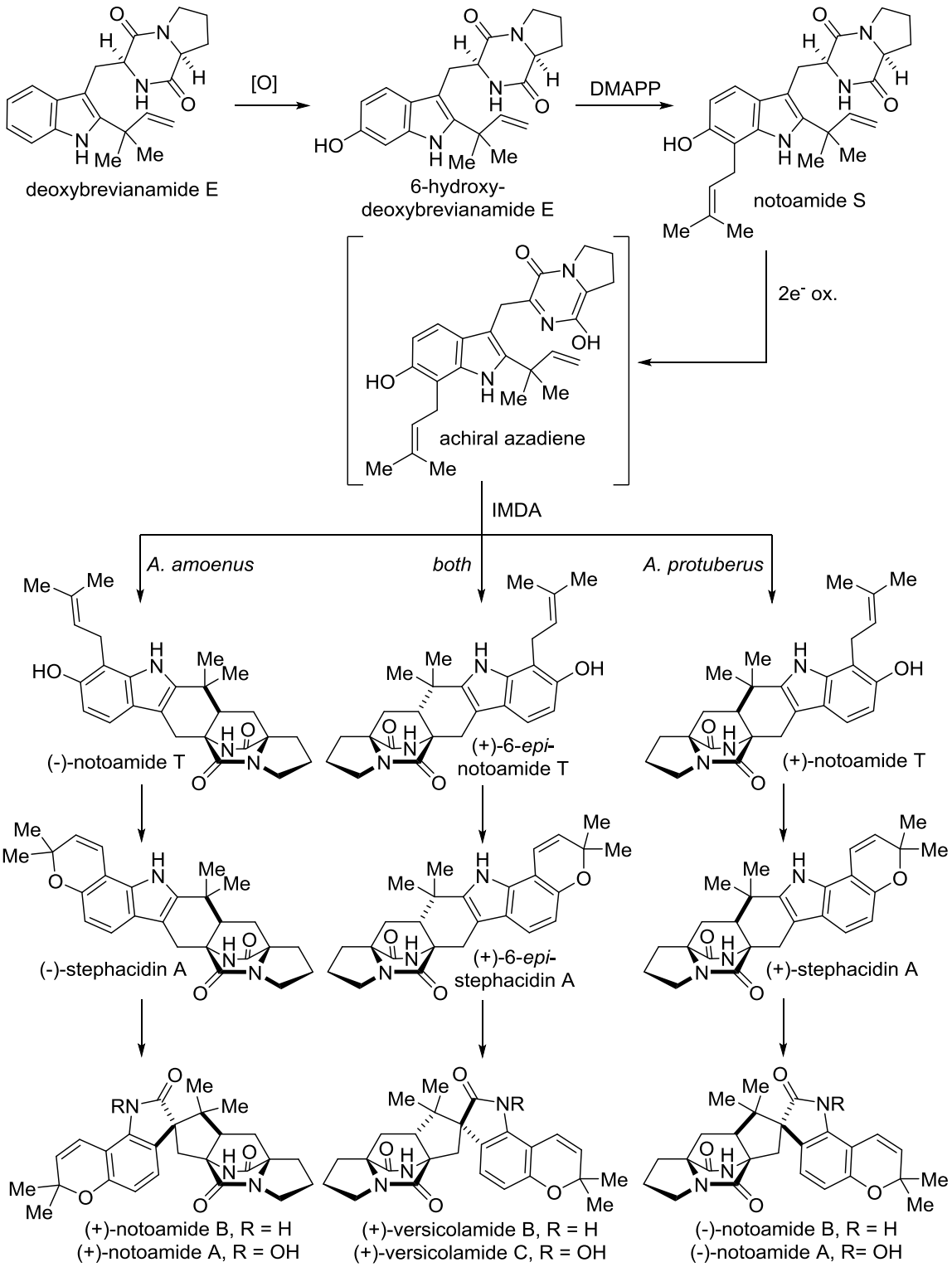

Biological Activity

As has been alluded to above, the bicyclo[2.2.2]diazaoctane alkaloids exhibit a wide range of bioactivity. Activity ranges from antinematodal to antifeedant, from cytotoxic to neuroprotective, and from anti–hepatitis C virus to antibacterial. **Table 1.1** summarizes the available data.

Table 1.1 Bioactivity of selected [2.2.2]-diazaoctane alkaloids

Compound	Bioactivity	Reference
malbrancheamide	calmodulin inhibitor	2
chyrsogenamide A	neuroprotective agent	7
marcfortine A	anthelmintic	6
SB203105	anthelmintic	8
paraherquamide A – G	antinematodal	8e
peniciherquamides C	anti–hepatitis C virus	12
brevianamide A	antifeedant	15
brevianamide D	insecticidal	15
brevianamide F	antibacterial	15
stephacidin A, B	cytotoxic	17
avrainvillamide	cytotoxic, antibacterial	17

The stephacidins and avrainvillamide have been subject to the greatest level of scientific scrutiny because of their extremely potent cytotoxicity (~100 μM)[21] and novel mechanism. After Qian–Cutrone and co–workers[17b], Fenical and co–workers[17c], and Sugie and co–workers[17d] isolated these three compounds, bioactivity surveys showed their cytoxicity against various cancer cell lines, notably the testosterone–sensitive prostate cancer type LNCaP. Synthetic efforts by the Myers group to arrive at a simplified derivative of avrainvillamide and stephacidin B that only contain the 3–alkylidene–*3H*–indole 1–oxide function have shown that this moiety acts a novel Michael acceptor for

nucleophilic alcohols and thiols.[19] This simplified, potentially bioactive structure was tested alongside avrainvillamide in screens of multiple cancer cell lines and using activity–based probes, it was determined that avrainvillamide binds to multiple proteins in cancer cell lysates which contain nucleophilic cysteine residues.[21] Significantly, one such protein was found to be nucleophosmin, a multifunctional protein often used for nuclear transport in conjunction with exportin–1. Overexpression and cytoplasmic localization of mutant nucleophosmin is often seen in patients with acute myeloid leukemia, along with repression of p53 which normally either induces DNA repair or apoptosis of cells containing a large number of carcinogenic mutations. Studies by Myers et al. have shown that avrainvillamide binds to cytosolic nucleophosmin, both wild–type and aberrant form, facilitating its nucleolar relocalization which leads to reduction of cancer–like traits of the cell.[22] This is the first reported case of a small non–petidic molecule acting as an *S*–alkylating agent on the C–terminus of nucleophosmin, leading to the restoration normal cellular function.

REFERENCES

1. Birch, A. J.; Wright, J. J.; *J. Chem. Soc. D.* **1969**, 12, 644b–645.
2. Marínez–Luis, S.; Rodrígues, R.; Acevedo, L.; Gonzáles, M. C.; Lira–Rocha, A.; Mata, R. *Tetrahedron* **2006**, *62*, 1817–1822.
3. Finefield, Jennifer M.; Frisvad, Jens C.; Sherman, David H.; Williams, Robert M. *J. Nat. Prod.* **2012**, *75*, 812–833.
4. Figueroa, M.; Gonzáles, M. D. C.; Mata, R. *Nat. Prod. Res.* **2008**, *22*, 709–714.
5. Ding, Y.; Greshock, T. J.; Miller, K. A.; Sherman, D. H.; Williams, R. M. *Org. Lett.* **2008**, *10*, 4863–4866.
6. (a) Polonsky, J.; Merrien, M. –A.; Prangé, T.; Pascard, C.; Moreau, S. *J. Chem. Soc. Commun.* **1980**, 601–602. (b) Prangé, T.; Billion, M. –A.; Vuilhorgen, M.; Pascard, C.; Polonsky, J. *Tetrahedron Lett.* **1981**, *22*, 1977–1980.
7. Lin, Z.; Wen, J.; Zhu, T.; Fang, Y.; Gu, Q.; Zhu, W. *J. Antibiot.* **2008**, *61*, 81–85.
8. (a) Yamazaki, M.; Okuyama, E.; Kobayashi, M.; Inoue, H. *Tetrahedron Lett.* **1981**, *22*, 135–136. (b) Ondeyka, J. G.; Goegelman, R. T.; Schaeffer, J.M.; Kelemen, L.; Zitano, L. *J. Antibiot.* **1990**, *43*, 1375–1379. (c) Lopez–Gresa, M. P.; Gonzalez, M. C.; Ciavatta, L.; Ayala, I.; Moya, P.; Primo, J. *J. Agric. Food Chem.* **2006**, *54*, 2921–2925. (d) Blanchflower, S. E.; Bank, R. M.; Everett, J. R.; Reading, C. *J. Antibiot*. **1993**, *46*, 1355–1363. (e) Banks, R. M.; Blanchflower, S. E.; Everett, J. R.; Manger, B. R.; Reading, C. *J. Antibiot*. **1997**, *50*, 840–846. (f) Blanchflower, S. E.; Banks, R. M.; Everett, J. R.; Manger, B. R.; Reading, C. *J. Antibiot.* **1991**, *44*, 492–497. (g) Liesch, J. M.; Wichmann, C. F. *J. Antibiot.* **1990**, *43*, 1380–1386. (h) Ding, Y.; Gruschow, S.; Greshock, T. J.; Finefield, J. M.; Sherman, D. H.; Williams, R. M. *J. Nat. Prod*. **2008**, *71*, 1574–1578. (i) Kwon, J.; Young, H. S.; Lee, J. –E.; Seo, E. –K.; Shen, L.; Yuanqiang, G.; Hong, S. –B.; Park, S. –Y.; Lee, D. *J. Nat. Prod*. **2015**, *78*, 2572–2579.
9. Zinser, E. W.; Wolfe, M. L.; Alexander–Bowman, S. J.; Thomas, E. M>; Davis, J. P.; Groppi, V. E.; Lee, B. H.; Thomphson, D. P.; Geary, T. G. *J. Vet. Pharmacol. Ther.* **2002**, *25*, 241–250.
10. Shoop, W. L.; Haines, H. W.; Eary, C. H.; Michael, B. F. *Am. J. Vet. Res.* **1992**, *53*, 2032–2034.
11. (a) Kaminsky, R.; Bapst, B.; Stein, P. A.; Strehlau, G. A.; Allan, B. A.; Hosking, B. C.; Rolfe, P. F.; Sager, H. *Parasitol. Res.* **2011**, *109*, 19−23. (b) Love, S. *AFBM J*. **2010**, *7*, 45−52. (c) Little, P. R.; Hodges, A.; Watson, T. G.; Seed, J. A.; Maeder, S. J. *N. Z. Vet. J.* **2010**, *58*, 121−129.
12. Nishikori, S.; Takemoto, K.; Kamisuki, S.; Nakajima, S.; Kuramochi, K.; Tsukuda, S.; Iwamoto, M.; Katayama, U.; Suzuki, T.; Kobayashi, S.; Watashi, K.; Sugawara, F. *J. Nat. Prod.* **2016**, *79*, 442–446.
13. Yang, B.; Dong, J.; Lin, X.; Zhou, X.; Zhang, Y.; Liu, Y. *Tetrahedron* **2014**, *70*, 3859–3863.
14. Paterson, R. R. M.; Simmonds, M. S. J.; Blaney, W. M. *J Invertebr. Pathol.* **1987**, *50*, 124–133.
15. (a) Birch, A. J.; Wright, J. J. *Tetrahedron* **1970**, *26*, 2329–2344. (b) Baldas, J.; Birch, A. J.; Russell, R. A. *J. Chem. Soc., Perkin Trans. 1* **1974**, 50–52.
16. Sanz–Cervera, J. F.; Glinka, T.; Williams, R. M. *Tetrahedron* **1993**, *49*, 8471–8482.

17. (a) Whyte, A. C.; Gloer, J. B.; Wicklow, D. T.; Dowd, P. F. *J. Nat. Prod.* **1996**, *59*, 1093–1095. (b) Qian–Cutrone, J.; Huang, S.; Shu, Y. –Z.; Vyas, D.; Fairchild, C.; Menendez, A.; Krampitz, K.; Dalterio, R.; Klohr, Steven E.; Gao, Q. *J. Am. Chem. Soc.* **2002**, *124*, 14556–14557. (c) Fenical, W.; Jensen, P. R.; Cheng, X. C. U.S. Patent 6,066,635, 2000. (d) Sugie, Y.; Hirai, H.; Inagaki, T.; Ishiguro, M.; Kim, Y. –J.; Kojima, Y.; Sakakibara, T.; Sakemi, S.; Sugiura, A.; Suzuki, Y.; Brennan, L.; Duignan, J.; Huang, L. H.; Sutcliffe, J.; Kojima, N. J. *J. Antibiot.* **2001**, *54*, 911–916. (e) Kato, H.; Yoshida, T.; Tokue, T.; Nojiri, Y.; Hirota, H.; Ohta, T.; Williams, R. M.; Tsukamoto, S. *Angew. Chem., Int. Ed*. **2007**, *46*, 2254−2256. (f) Tsukamoto, S.; Kato, H.; Greshock, T. J.; Hirota, H.; Ohta, T.; Williams, R. M. *J. Am. Chem. Soc*. **2009**, *131*, 3834−3835. (g) Tsukamoto, S.; Kato, H.; Samizo, M.; Nojiri, Y.; Onuki, H.; Hirota H.; Ohta, T. *J. Nat. Prod*. **2008**, *71*, 2064−2067. (h) Tsukamoto, S.; Kawabata, T.; Kato, H.; Greshock, T. J.; Hirota, H.; Ohta, T.; Williams, R. M. *Org. Lett*. **2009**, *11*, 1297−1300. (i) Tsukamoto, S.; Umaoka, H.; Yoshikawa, K.; Ikeda, T.; Hirota, H. *J. Nat. Prod*. **2010**, *73*, 1438−1440. (j) Greshock, T. J.; Grubbs, A. W.; Jiao, P.; Wicklow, D. T.; Gloer, J. B.; Williams, R. M. *Angew. Chem., Int. Ed*. **2008**, *47*, 3573−3577. (k) Kito, K.; Ookura, R.; Kusumi, T.; Namikoshi, M.; Ooi, T. *Heterocycles* **2009**, *78*, 2101−2106. (l) Kato, H.; Nakahara, T.; Sugimoto, K.; Matsuo, K.; Kagiyama, I.; Frisvad, Jens C.; Sherman, David H.; Williams, Robert M.; Tsukamoto, S. *Org. Lett.* **2015**, *17*, 700–703.
18. Nussbaum, F. *Agnew. Chem. Int. Ed.* **2003**, *42*, 3068–3071.
19. Myers, Andrew G.; Herzon, Seth B. *J. Am. Chem. Soc.* **2003**, *125*, 12080–12081.
20. Herzon, Seth B.; Myers, Andrew G. *J. Am. Chem. Soc.* **2005**, *127*, 5342-5344.
21. Wulff, Jeremy E.; Siegrist, Romain; Myers, Andrew G. *J. Am. Chem. Soc.* **2007**, *129*, 14444–14451.
22. Mukherjee, H.; Chan, K.-P.; Andresen, V.; Hangley, Mariah L.; Gjertsen, Bjørn T.; Myers, Andrew G. *ACS Chem. Biol.* **2015**, *10*, 855–863.

Chapter Two
Previous Synthetic Strategies

Introduction

Selected synthetic methodologies for constructing [2.2.2]diazabicycles are discussed below. Six distinct strategies have been established in the literature and examples representative of each are presented.

Aminoacyl Radical Strategy

A synthesis of the oxidized natural product avrainvillamide was undertaken by the Myer's lab soon after its isolation.[12] An aminoacyl radical was used to construct the [2.2.2]bicyclic manifold found in these alkaloids.

Synthesis began with unsaturated cyclohexanone **1**, made enantioselectively from commercially available starting materials in 4 steps (**Scheme 2.1**). Alkylation with novel electrophile **2** proceeded with complete diastereoselectivity to produce **3**. Strecker–like addition of HCN across the *N*–Boc enamine moiety proceeded cleanly to give **4**. Epimerization to the necessary isomer was followed by chemoselective reduction of the nitrile to primary amide **5**. Exposure to thiophenol and triethylamine induced conjugate addition and led to the formation of hemiaminal **6**. Following Boc deprotection and hemiaminal dehydration, radical initiator **7** was appended to the pyrrolidine ring to afford **8**. Now that the appropriate radical initiator and terminator had been included on the carbon skeleton, the envisioned intramolecular radical cyclization could be attempted. To that end, *t*–amyl peroxybenzoate induced hemolytic bond cleavage which led to attack by the resultant acyl radical to the enamine carbon in a 6–exo fashion (see highlighted bond) and

produced bicycle **9** as a single diastereomer. A 3 step conversion to α–iodoenone **10** was followed by Ullmann coupling with aryl halide **11**. The resultant nitroarene **12** was reduced by zinc powder to afford avrainvillamide as a single enantiomer in 17 steps. Exposure to NEt_3 in acetonitrile at room temperature resulted in dimerization to stephacidin B.

Scheme 2.1 Myer's synthesis of avrainvillamide

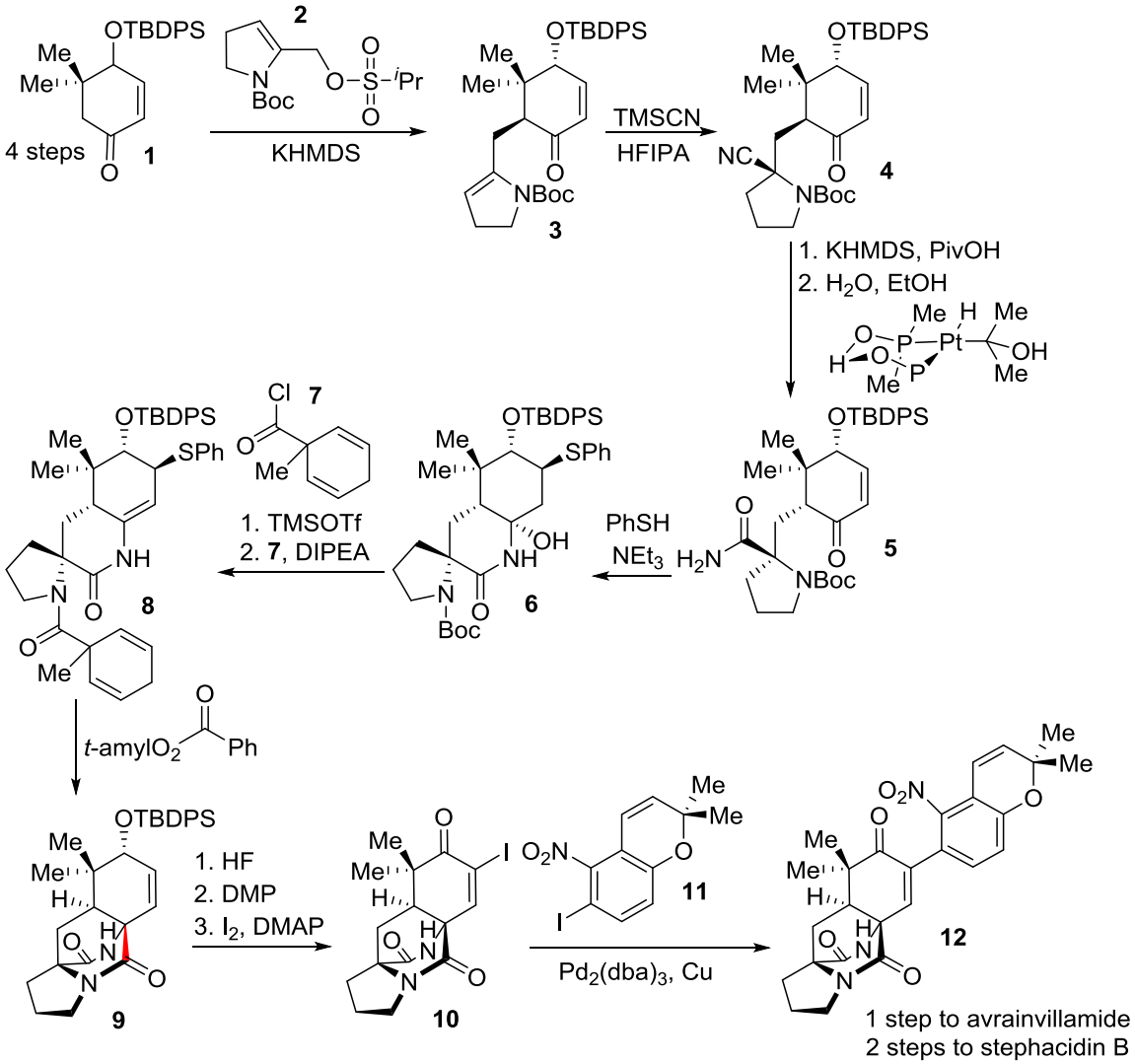

S_N2' Ring Closure

The Williams group developed the first ever total synthesis of any diazabicyclic indole alkaloid by utilizing an intramolecular S_N2' cyclization to establish the [2.2.2]diazaoctane core.[2] The [2.2.2] core is established by enolization of a diketopiperazine followed by intramolecular nucleophilic attack of a pendant allylic chloride (**Scheme 2.2**). This strategy was successfully employed for synthesis of brevianamide B[2] and later extended to paraherquamide B[3] and stephacidin A[4].

Scheme 2.2 Intramolecular S_N2' ring closure

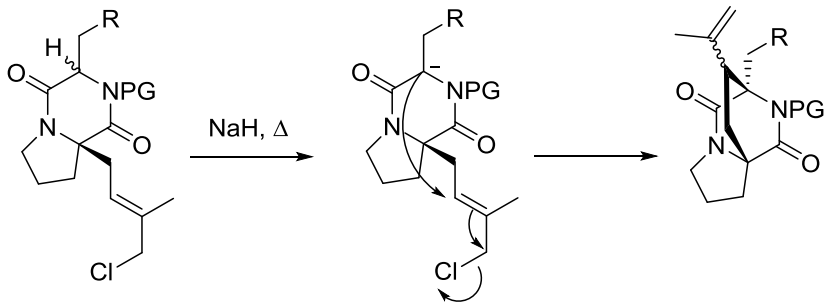

The synthesis of stephacidin A began with the substituted tryptophan **13** (**Scheme 2.3**).[4] Coupling with allyl proline methyl ester **14** yielded dipeptide **15** which was subjected to microwave heating to effect ring closure to diketopiperazines **16a,b**. A 1:1 mixture of *syn* and *anti* isomers were observed and separated. Subsequently, the lactim *O*–methyl ether protecting group was introduced on the secondary lactam and the pendant allyl chain was subjected to Grubbs cross–metathesis. Allyl chloride **17** was prepared in two further steps in anticipation of the S_N2' closure. As was observed in the synthesis of paraherquamide B, S_N2' cyclization of lactim ether protected diketopiperazines results in exclusive selectivity for the *syn* isomer **18**.[3] In contrast, the Williams synthesis of

brevianamide B intercepts an unprotected diketopiperazine intermediate which can produce either diastereomer in varying ratios depending on reaction conditions.[4]

Scheme 2.3 Synthesis of stephacidin A via S_N2' cyclization

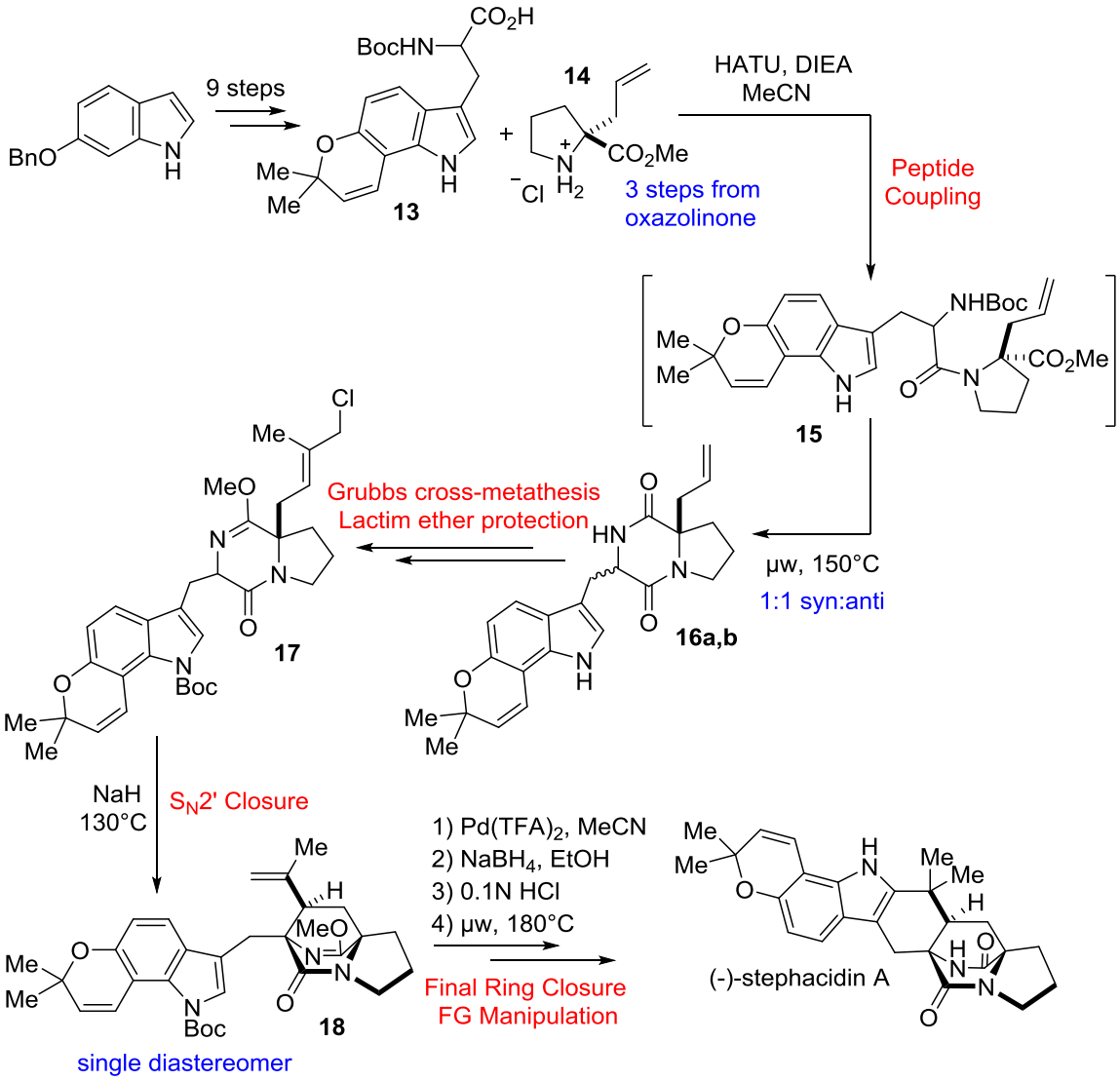

Functional group conversion and closure to the heptacyclic skeleton of stephacidin A was completed with special attention to the acid–sensitive nature of the pyran moiety. This afforded stephacidin A in 17 steps and 6% overall yield with complete selectivity for the *syn* diastereomer.

Oxidative Enolate Heterocoupling

Baran and co–workers devised a route to stephacidin which utilized an intramolecular oxidative heterocoupling between ester and amide enolates to construct the bicyclic core of these indole alkaloids.[5, 6] This work is based on a series of investigations in the Baran group on the propensity of carbonyl enolates to react with heterocyclic aromatic systems under exposure to metal oxidants such as Cu(II).[7]

Carboxybenzyl–protected tryptophan derivative **20** was prepared in 7 steps from a reduced pyroglutamate and a protected iodoaniline (**Scheme 2.4**). This was coupled with proline diester **19** (from *R*–proline in 5 steps) to afford dipeptide **21**. Chemoselective deprotection of the carboxybenzylamine was followed by thermal ring closure to a diketopiperazine. Treatment with MOMCl yielded the *N*–methylmethoxy protected secondary amine **22**. At this point, a screen of various metal oxidants revealed that $Fe(acac)_3$ was the most propitious for bond formation in the key intramolecular oxidative enolate heterocoupling between ester and amide enolates. Bicycle **23** was recovered as a single diastereomer but it is still unclear whether this diastereoselectively is the result of a chelated transition state or is due to the innate bias of this scaffold. In either case, **23** was MOM deprotected, the exocyclic methyl ester was converted to a tertiary alcohol via treatment with methyl Grignard and then to the corresponding prenyl residue after treatment with Burgess reagent. Finally, thermolytic Boc cleavage and formal ene rearrangement likely generated a spirocyclic intermediate which can undergo a 1,2–shift to afford (-)–stephacidin A in 20 steps. This synthetic sample was found to be enantiomeric with an isolated standard from Fenical lab, thereby proving the absolute chemistry of the natural product for the first time.

Scheme 2.4 Oxidative enolate heterocoupling synthesis of stephacidin A

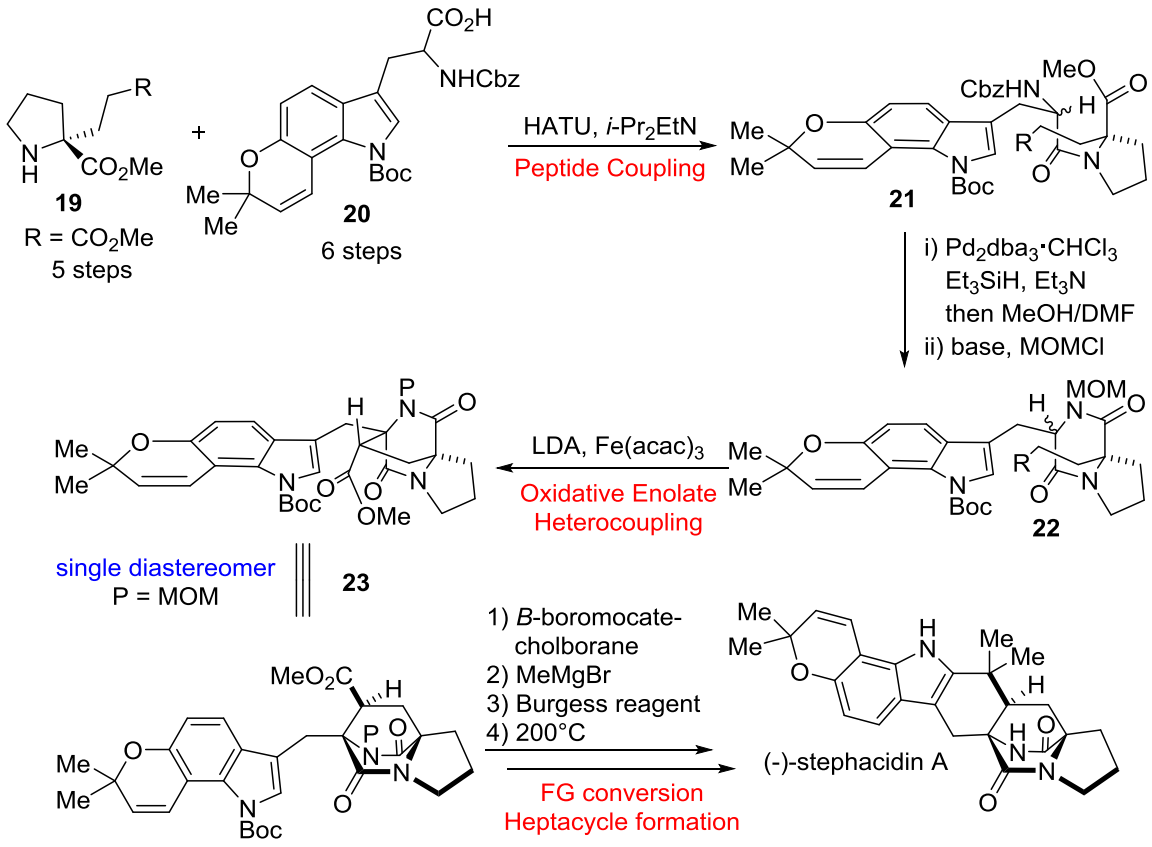

Cationic Cascade

The Simpkins group envisioned a cationic cascade based on an appropriately substituted tryptophan/proline diketopiperazine to forge the characteristic [2.2.2]bicycle.[8] Prenylated proline **23** was synthesized from Seebach proline acetal in 2 steps (**Scheme 2.5**). Coupling with indole pyruvic acid occurred in moderate yield to produce the closed diketopiperazine **24**. Exposure to the Lewis acid TMSOTf induced carbocation formation adjacent to the tertiary lactam. Construction of the bicyclic core was completed by electrophilic attack on the prenyl *pi* system, leading to the formation of a tertiary carbocation which participated in precedented cyclization onto the indole system. In sum,

this pathway yielded bicycles **25a,b** in only 5 steps from commercially available starting materials and a 4:1 diastereomeric ratio, favoring the *syn* C–6 epimer.

The minor, *anti* isomer was used to produce *ent*–brevianamide B in 4 consequent steps. The use of an appropriately substituted indole coupling partner led to the production of *ent*–malbrancheamide B in 10 synthetic steps with an equivalent diastereomeric ratio. Unfortunately, attempts to extend this methodology to the stephacidins did result in productive cyclization due to acid–mediated degradation of the pyran moiety. This shortcoming was overcome by a radical cascade (*vide infra*).

Scheme 2.5 Cationic cyclization to [2.2.2]diazaoctanes

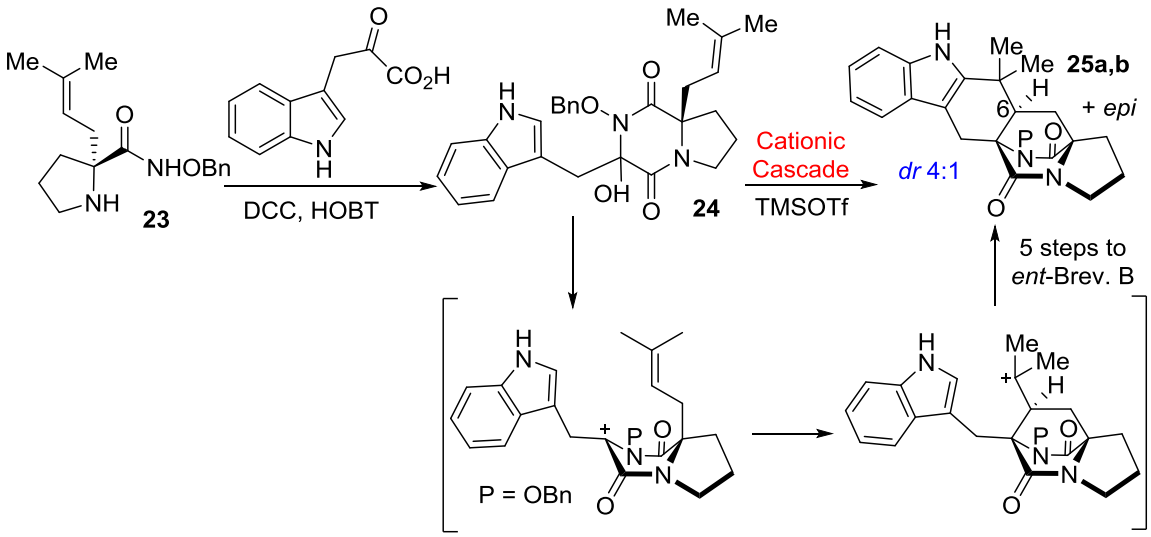

Radical Cascade

The previous two synthesized outlined above place at their core either anionic (enolate) or cationic cyclization strategies. Continued work in the Simpkins group has moved into single–electron, radical cyclization chemistry to produce indoline [2.2.2]bicyclic alkaloids.[9] Previous work in the Baran[10a,b] and Williams[10c] labs have shown the utility of such indoline precursors as stepping stones to the oxidative synthesis of various members of the stephacidin family.

Scheme 2.6 Radical cyclization towards indoline [2.2.2]diazaoctanes

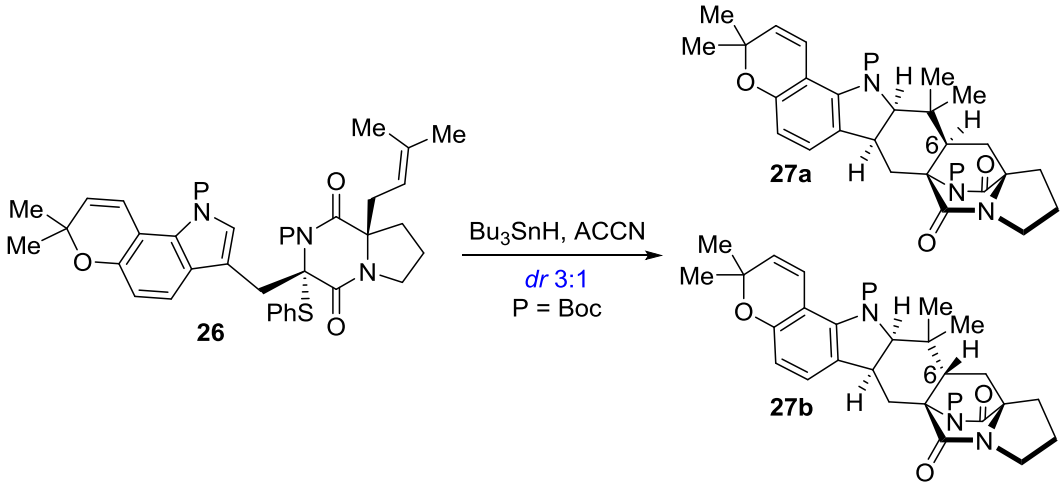

Instead of the α–hydroxy diketopiperazine **24** used in the cationic case, α–sulphenylated diketopiperazines were envisioned as appropriate precursors to stable radical formation. To that end, mixed proline diketopiperazine **26** was synthesized in 13 steps from 6–benzyloxy indole in a manner analogous the α–hydroxy intermediate used previously (**Scheme 2.5**). Exposure to reductive Bu_3SnH conditions induced sequential 6–*exo* and 6–*endo* cyclization produce indolines **27a,b** in approximately 3:1 diastereomeric ratio favoring the *syn* isomer (**Scheme 2.6**). Although this represents a marked decrease in selectivity from the cationic methodology discussed earlier, the benzopyran moiety found in the stephacidins is preserved under these acid–free conditions and subsequent DDQ dehydrogenation and Boc deprotection yielded (-)–stephacidin A from **27a**. Extension of this work utilizing the persistent radical effect has enabled to construction of bridged diketopiperazines of bridge length greater than 2 and containing heteroatoms.[11]

Intramolecular Diels–Alder Cycloadditions

As was shown in Chapter 1, the prevailing understanding of the scientific community is that the [2.2.2]diazabicyclic alkaloids are produced by fungi via an intramolecular hetero Diels–Alder cycloaddition (*vide supra*). Efforts to complete biomimetic synthesis of these alkaloids using a variety of intramolecular cycloaddition conditions have been undertaken by multiple groups and will be discussed below.

The Williams lab keyed in on this powerful, two carbon–carbon bond forming reaction in their synthesis of brevianamide B.[12] *Epi*–deoxybrevianamide E was protected as the lactim *O*–methyl ether and dehydrogenation with DDQ afforded **29** (**Scheme 2.7**). Subsequent exposure to aqueous KOH led to the formation of azadiene **30** which spontaneously cyclized to give **31** and **32** as a 2:1 mixture of *syn* and *anti*. Although only single isomers are observed in the biosynthesis of these and related alkaloids, laboratory conditions were not able to replicate the same extent of diastereofacial selectivity. 4 steps were then required to complete the total synthesis of brevianamide B from minor isomer **32**.

The observed preference for the *syn* fused bicycle has allowed this methodology to be applied more broadly to those alkaloids which also exhibit this fusion. For example, Scheerer lab developed a stereoselective domino reaction sequence which constructs the molecular scaffold common to these alkaloids (**Scheme 2.8**).[13] Specifically, a chiral aminal auxiliary was incorporated in the pyrrolidine ring which enforces stereofacialselectivity. To that end, diketopiperazine **34** was synthesized in 4 steps from *L*–serine methyl ester and exposed to NaOMe to effect enolization. Condensation with indole aldehyde **33** affords **35**

Scheme 2.7 Biomimetic Diels–Alder towards racemic brevianamide B

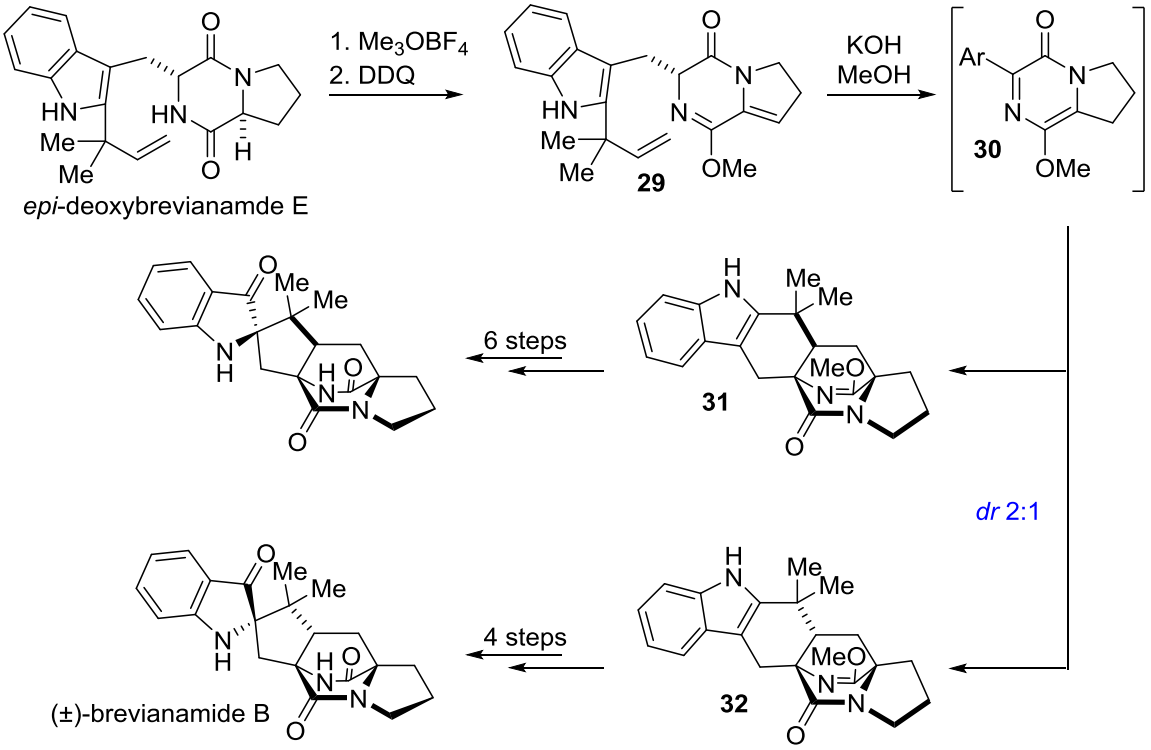

Scheme 2.8 Chiral auxiliary–enforced IMDA synthesis of malbrancheamide

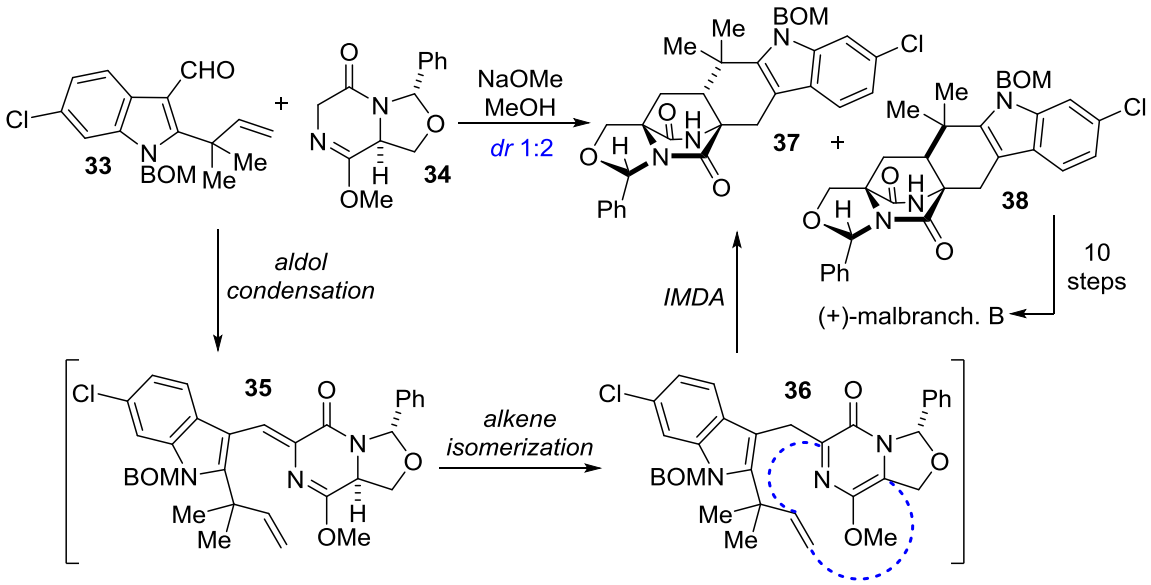

(not isolated) which undergoes alkene isomerization to pyrazinone **36**. At this point, [4+2] cyclization occurred to afford diastereomers **37** and **38** as a 2:1 mixture favoring the *syn* isomer. After lactim ether hydrolysis, the diastereomers were separated and 9 further steps led to the formal synthesis of *syn* fused malbrancheamide B.

Finally, the Williams group extended their previous methodology to the total synthesis of stephacidin A.[14] Gramine derivative **39** was coupled with β–hydroxy *L*–proline **40** to afford a dipeptide (**Scheme 2.9**). Heating in morpholine prompted cyclization to diketopiperazine **41**. Mitsonobu–type elimination led to the formation of enamine **42** which could be isolated but at elevated temperatures was found to directly participate in the Diels–Alder cycloaddition. (+)–stephacidin A and its C6 epimer were isolated in a 2.4:1 diastereomeric ratio, a *dr* which seems to be consistent across several related examples.

Scheme 2.9 Improved IMDA towards stephacidin A

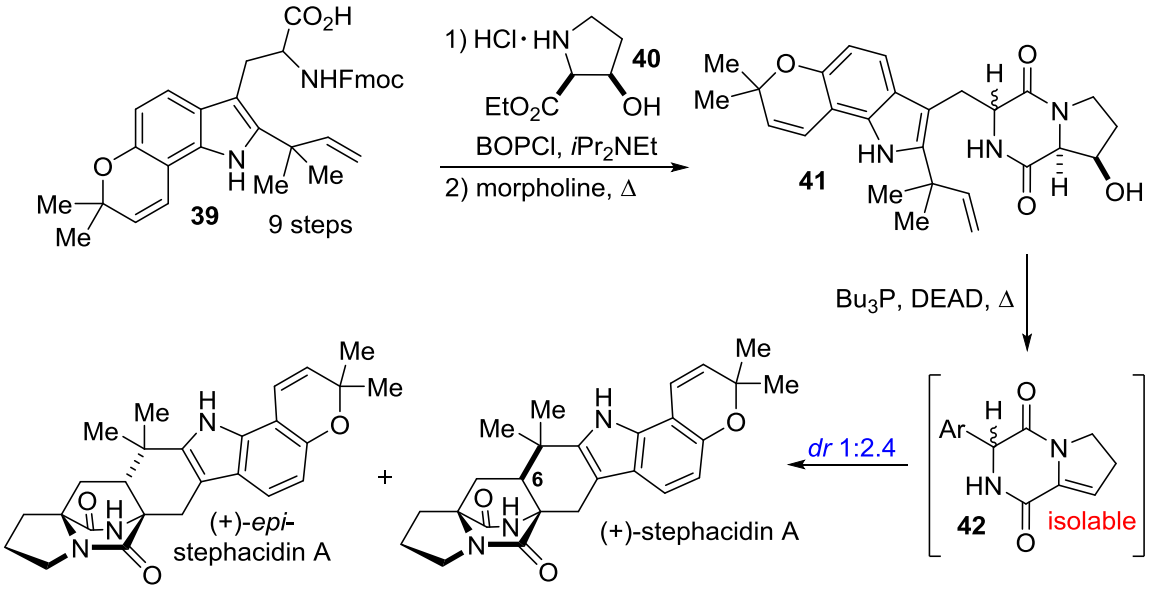

REFERENCES

1. Herzon, Seth B.; Myers, Andrew G. *J. Am. Chem. Soc.* **2005**, *127*, 5342–5344.
2. Williams, R. M.; Glinka, T.; Kwast, E. *J. Am. Chem. Soc.* **1988**, *110*, 5927–5929.
3. Cushing, T. D.; Sanz–Cervera, J. F.; Williams, R. M. *J. Am. Chem. Soc.* **1993**, *115*, 9323–9324.
4. Artman, Gerald D., III; Grubbs, Alan W.; Williams, Robert M. *J. Am. Chem. Soc.* **2007**, *129*, 6336–6342.
5. Baran, Phil S.; Guerrero, Carlos A.; Ambhaikar, Narendra B.; Hafensteiner, Benjamin D. *Angew Chem. Int. Ed.* **2005**, *44*, 606–609.
6. Baran, Phil S.; Hafensteiner, Benjamin D.; Ambhaikar, Narendra B.; Guerrero, Carlos D.; Gallaher, John D. *J. Am. Chem. Soc.* **2006**, *128*, 8678–8693.
7. (a) Baran, P. S.; Richter, J. M. *J. Am. Chem. Soc.* **2004**, *126*, 7450–7451. (b) Baran, P. S.; Richter, J. M. *J. Am. Chem. Soc.* **2005**, *127*, 8678–8693.
8. Frebault, Frédéric C.; Simpkins, Nigel S. *Tetrahedron* **2010**, *66*, 6585–6596.
9. (a) Simpkins, Nigel; Pavlakos, Ilias; Male, Louise. *Chem. Commun.* **2012**, *48*, 1958–1960. (b) Simpkins, Nigel S.; Pavlakos, Ilias; Weller, Michael D.; Male, Louise. *Org. Biomol. Chem.* **2013**, *11*, 4957–4970.
10. (a) Baran, P. S.; Guerrero, D. A.; Hafensteiner, B. D.; Ambhaikar, N. B. *Angew. Chem., Int. Ed.*, **2005**, *44*, 3892–3895. (b) Baran, P. S.; Hafensteiner, D. D.; Ambhaikar, N. B.; Guerrero, C. A., Gallagher, J. D. *J. Am. Chem. Soc.* **2006**, *128*, 8678–8693. (c) Artman, G. D.; Grubbs, A. W.; Williams, R. M. *J. Am. Chem. Soc.* **2007**, *129*, 6336–6342.
11. Amatov, T.; Pohl, R.; Císařová, I.; Jahn, U. *Agnew. Chem. Int. Ed.* **2015**, *54*, 12153–12157.
12. Williams, Robert M.; Sanz–Cervera, Juan F.; Sancenón, F.; Marco, J. Alberto; Halligan, K. *J. Am. Chem. Soc.* **1998**, *120*, 1090–1091.
13. Laws, Stephen W.; Scheerer, Jonathan R. *J. Org. Chem.* **2013**, *78*, 2422–2429.
14. (a) Greshock, Thomas J.; Grubbs, Alan W.; Tsukamoto, Sachiko; Williams, Robert M. *Agnew. Chem. Int. Ed.* **2007**, *46*, 2262–2265. (b) Greshock, Thomas J.; Williams, Robert M. *Org. Lett.* **2007**, *9* (21), 4255–4258.

Chapter Three
Intermolecular Diels–Alder Cyclizations of Pyrazinones

Introduction and Retrosynthesis

Inspired by the efforts of various laboratories to construct the bicyclo[2.2.2]diazaoctane core of these alkaloids via an intramolecular Diels–Alder cycloaddition[1], we turned our attention to the intermolecular case.[2] We theorized that this bimolecular reaction might improve the somewhat poor diastereoselectivity (~2:1 favoring the *syn* isomer) observed in nearly all biomimetic intramolecular variants with reverse prenylated indole. Although the regiochemistry of the cycloaddition was unclear at the outset, the intermolecular strategy might offer a concise entry to the diazabicyclic core.

The [2.2.2]diazabicycles **1** and **2** contain the carbon framework that is found in all natural products of this family. *Syn*–configured **1** can be reduced to the monoketopiperazine premalbrancheamide, which is the biogenic precursor to malbrancheamides A and B.[3] *Anti*–configured **2**, while not a natural product, has been converted in a few short steps to brevianamide B.[4] **1** and **2** can be viewed as model compounds that represent the most simple *syn* and *anti* configured structures that contain all rings apparent in the natural product family.

Figure 3.1 [2.2.2]diazabicycles with *syn* and *anti* fusion

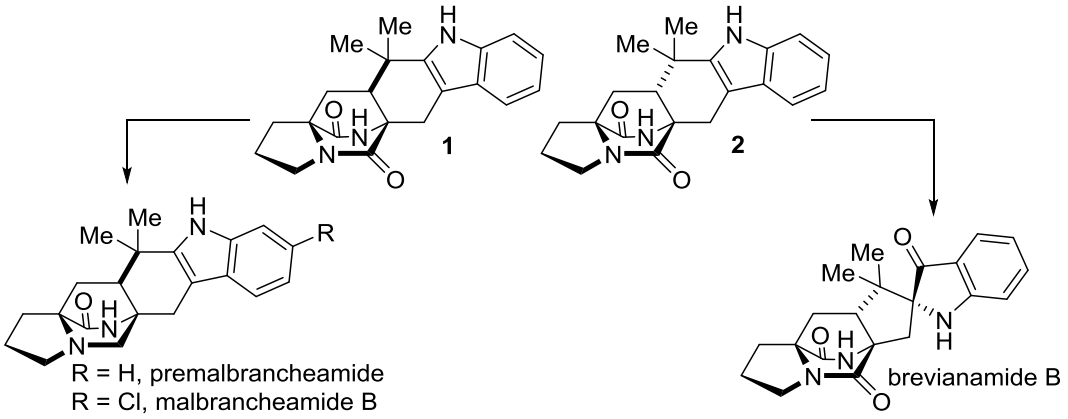

Previous work in the Scheerer lab has established that pyrazinone precursors can be prepared in a one–pot aldol–condensation/alkene isomerization domino sequence. The coupling of a protected diketopiperazine with indole aldehyde would therefore afford pyrazinone **3**. This is now ideally prepared for an intermolecular Diels–Alder reaction with any range of acrylate derived dienophiles to yield bicycle **4**. The regiochemical and stereochemical outcomes of this cycloaddition, in addition to questions regarding reactivity, were unclear at the start of this project. Acrylate dienophiles or their synthetic equivalents were prioritized because treatment with an organometallic reagent (e.g., MeMgBr) would afford a tertiary alcohol that is capable of engaging in Friedel–Crafts cyclization to complete the ring systems of **1** and **2.** Spectroscopic comparison of these pentacycles to known standards would prove the stereochemistry of the products of our synthesis.

Scheme 3.1 Retrosynthesis of [2.2.2]diazabicycles

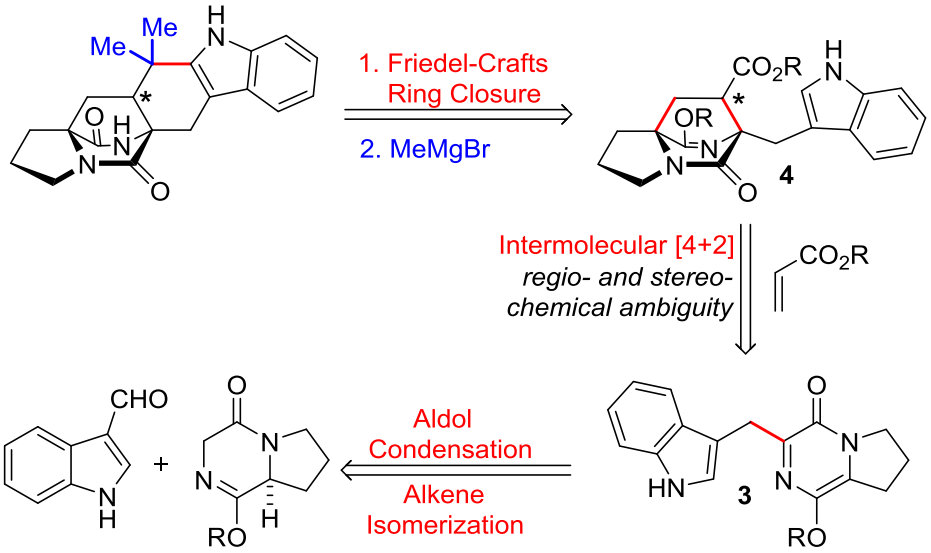

Formal Synthesis of Brevianamide B and Premalbrancheamide

We began our studies with the synthesis of diketopiperazine **6**, which is derived from *L*–proline methyl ester in 3 steps (**Scheme 3.2**). Exposure of **6** to LiHMDS at –78°C led to aldol addition to aldehyde **5**. Trapping of the intermediate aldol addition product with acetic anhydride led to the isolation of β–acetoxy **7** as a mixture of 4 diastereomers. An unpurified mixture was treated with the mild nitrogenous base DBU which induced elimination of the acetoxy residue and alkene isomerization to afford pyrazinone **8**. While this azadiene was not amenable to silica gel chromatography and decomposed when exposed to air for a few hours, we were able to purify via recrystallization to obtain a homogenous material.

Diels–Alder cycloaddition was first attempted with ethyl acrylate and the observed cycloadducts were afforded as a 3:1:1 mixture. The major isomer **9** was isolated in 48% yield and corresponds to the *endo* transition state. We could improve the diastereoselectivity by utilizing Oppolzer's sultam acrylamide to deliver **10** as a single

diastereomer. Unfortunately, **9** and **10** exhibited the undesired regiochemistry whereby the carboxyl functionality is not positioned proximal to the indole nucleus. The regiochemistry apparent in **9** and **10** does not allow for easy synthesis of **1** or **2**.

Scheme 3.2 Intermolecular [4+2] cycloadditions with acrylates

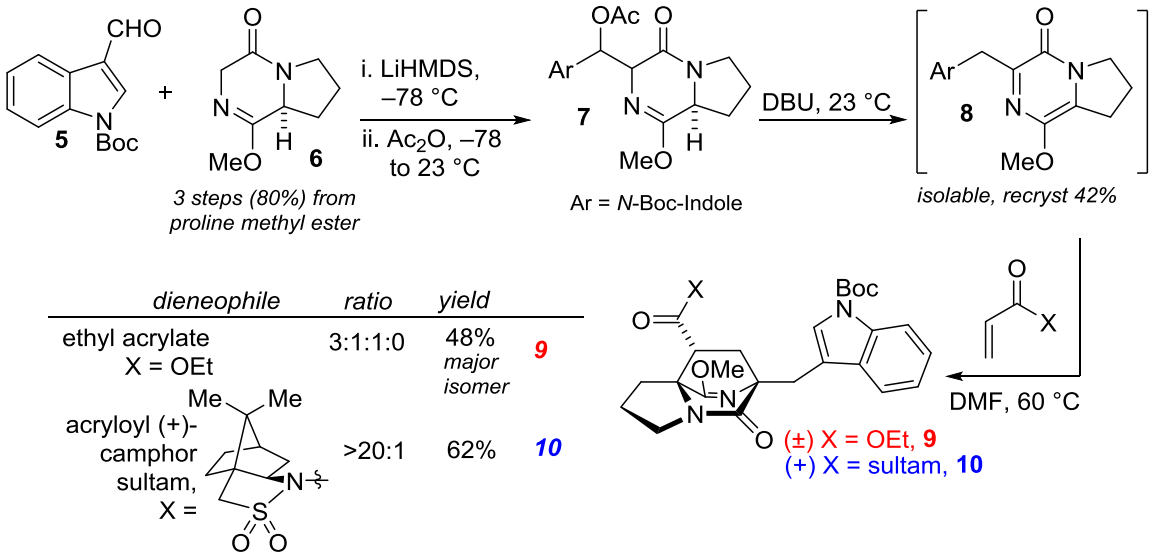

Computational studies into the transition state energies of similar cycloadducts has been pursued to provide greater understanding of the intermolecular pyrazinone Diels–Alder cycloaddition. **Figure 3.2** shows the calculated transition state for the addition of ethyl acrylate to α–methyl pyrazinone which would produce the cycloadduct with identical regio– and stereochemistry as **9**. The potential energy surface shown in **Figure 3.3** shows roughly even spacing of the four reactant geometries. The calculated transition state for the isomer corresponding to **9** lies at least 3.6 kJ mol^{-1} lower in energy than the other transition states. Products **A2** and **A4** have approximately equal transition state energies, which could indicate a 1:1 ratio. The transition state calculated for **A3** was found nearly 3 kJ mol^{-1} higher than the other examples. From this data, we can conclude that the major isomer of this cycloaddition corresponds to **9** and that two other products, which correspond to both

diastereomers of the regioisomer, would form in an approximately 1:1 ratio. The fourth isomer may or may not be formed. This corroborates our experimental observations excellently. The other calculated transition states and IRC graphs for all 4 isomers can be found in Appendix II.

Figure 3.2 Exemplary calculated transition state for pyrazinone [4+2] additions

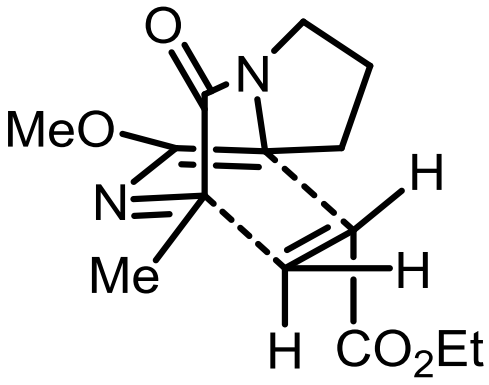

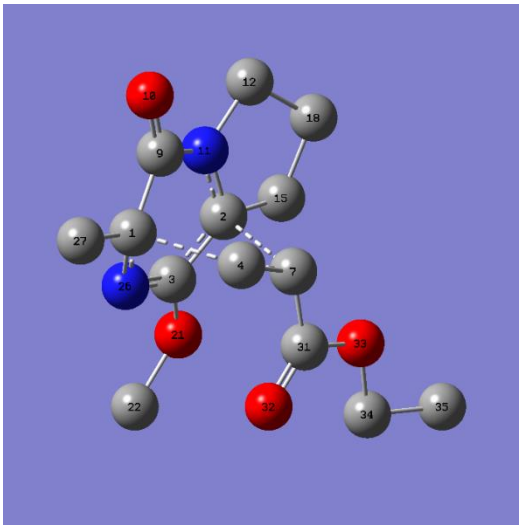

We found that the desired regiochemistry was obtained when we utilized methyl 2–nitroacrylate as the dienophile (**Scheme 3.3**). This substrate was significantly more reactive than the other acrylates studied and underwent cycloaddition at ambient temperatures or lower. Cooling the reaction solution to –10 °C and warming to room temperature overnight afforded cycloadducts **11** and **12** as a 4:1 mixture in 84% overall yield. Unfortunately, these isomers were not readily separable by column chromatography, although it was possible to isolate an analytic quantity of **11** for spectroscopic purposes.

Figure 3.3 Potential Energy Surface for ethyl acrylate cycloaddition

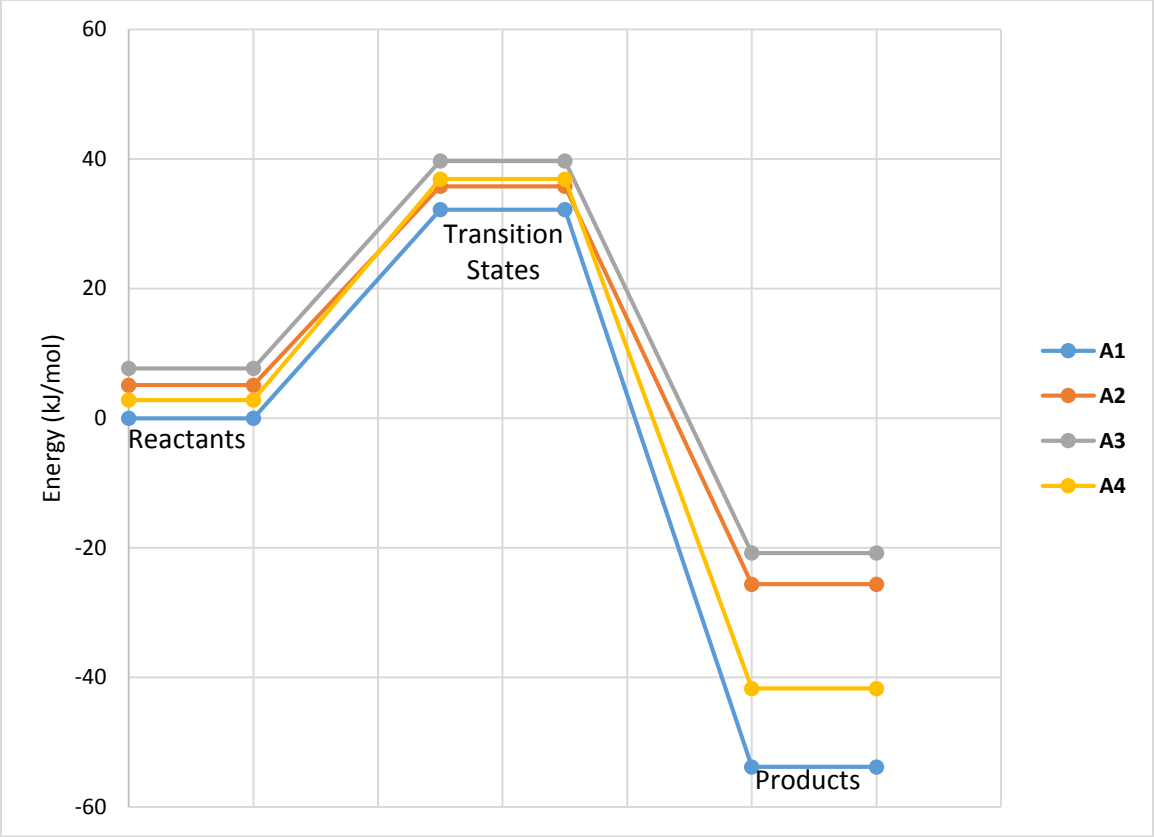

Attempted radical reduction of the secondary nitro group in cycloadduct **11** with Bu_3SnH and AIBN in refluxing toluene (110 °C) resulted in the isolation of only the elimination product **13**. Reduction at lower temperatures (70–80 °C) also led to **13** as the major product, however a small quantity of *syn*–isomer **15** (ca. 10% yield) was also observed, thereby validating our stereochemistry from the cycloaddition. It is useful to note that while this cycloaddition proceeds in good regioselection and the strong preference of the nitro group for the *endo* transition state enforces the formation of only the *syn* diastereomer, a far cry from the ~2:1 *dr* observed in the intramolecular case.

Scheme 3.3 [4+2] cycloaddition with nitro acrylate and nitro–group reduction

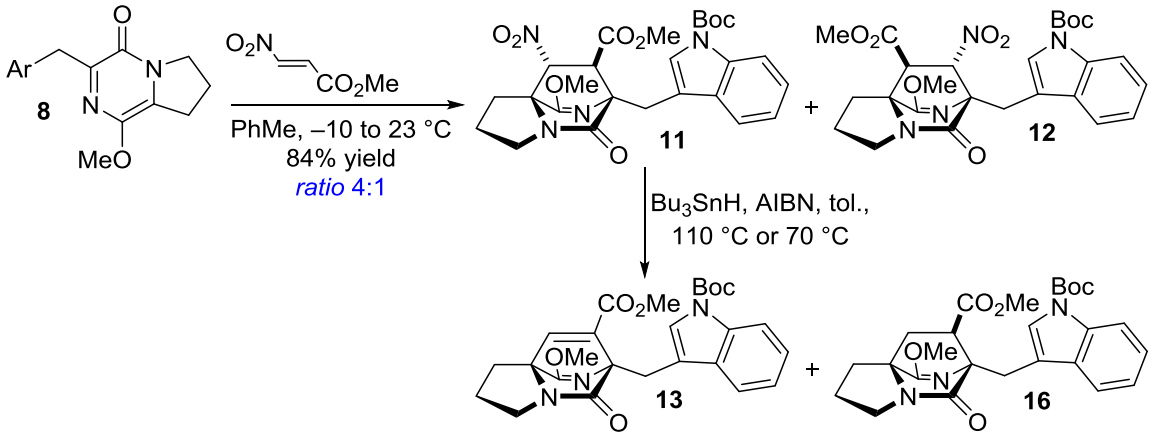

Scheme 3.4 Endgame of formal syntheses of brevianamide B and premalbrancheamide

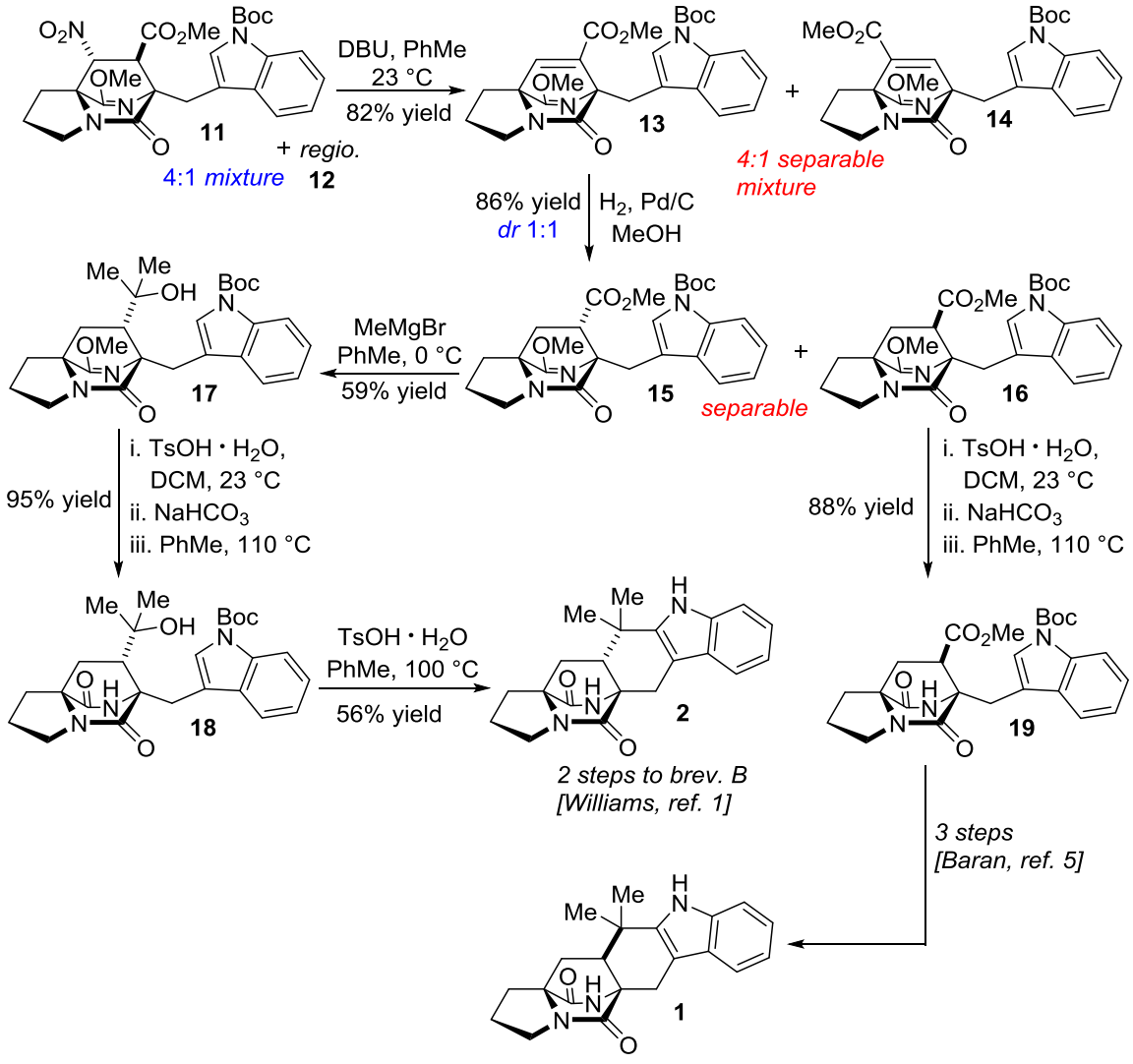

Radical reduction was not a tenable route to arrive at saturated methyl ester cycloadducts **15** and **16** (see **Scheme 3.4**). It was therefore most operationally simple to treat the 4:1 mixture of **11** and **12** with stoichiometric DBU, inducing nitro group elimination to afford α,β–unsaturated methyl esters **13** and **14** as an easily separable 4:1 mixture. Hydrogenation with palladium on carbon of **13** led to the isolation of saturated methyl esters **15** and **16** in a 1:1 ratio.

The ready availability of both *syn* and *anti* diastereomers allowed us to move forward with the formal syntheses of brevianamide B and premalbrancheamide. **15** was treated with excess methyl Grignard to afford the tertiary alcohol **17**. Acidic cleavage of the lactim ether in **17** was preformed prior to Friedel–Crafts annulation. Their Friedel–Crafts alkylation of **18** was promoted with *p*–toluenesulfonic acid in refluxing toluene and delivered the desired *anti* fused **2** in 83% yield. The spectral data for **2** was identical to an authentic standard provided by Williams. Acidic hydrolysis of the lactim either functionality in **16** let us intercept known lactam **19**, an intermediate previously prepared by Baran *et al.* in the syntheses of complex alkaloids in this family[5]

Our synthesis of **2** and **19** represent 12–step formal syntheses of brevianamide B and pre–malbrancheamide, representative of *anti*– and *syn*–fused [2.2.2] diazabicyclic alkaloid natural products. We have provided further insight into pyrazinone Diels–Alder cycloadditions and shown that 2–nitroacrylate dienophiles can be used to provide the desired regiochemistry and produce only the *syn* fused bicyclic nucleus in six steps from proline methyl ester.

Future Work and Early Attempts toward Improved Selectivity

Obviously, our synthetic methodology leaves much to be desired in the way of diastereoselectivity. Although the intermolecular Diels–Alder with 2–nitroacrylate produces two regioisomers with excellent diastereoselectivity for each, the elimination of the nitro functionality under basic conditions destroys the stereochemical bias imparted by this cycloaddition. Initial attempts at radical reduction of the nitro group proceeded in poor yield and could not be improved. The following pages will detail our initial work to improve our selectivity and ideas about what could be attempted in the future.

We hypothesized that the organoiridium Crabtree's catalyst might act to diastereoselectively add hydrogen across α,β–unsaturated methyl ester **13**. Alcohols, esters, ureas and a variety of other Lewis–basic functionalities have been evaluated as directing groups for iridium hydrogenation catalysts.[6] However, lactams and lactims have not yet been investigated for this reactivity. Our bicycle provides an ideal substrate to test whether the iridium complex has a preference to bind a tertiary lactam over and secondary lactim to deliver hydrogen across as double bond selectively. Exposure of **13** to hydrogen gas with Crabtree's catalyst at room temperature afforded exclusively the *syn* isomer **16** but only in 15% yield (**Scheme 3.5**). This result is far from ideal, but we believe that further investigation with other catalytic systems, such as ruthenium complexes, may reveal more desirable reactivity.

Scheme 3.5 Attempts with directed hydrogenation

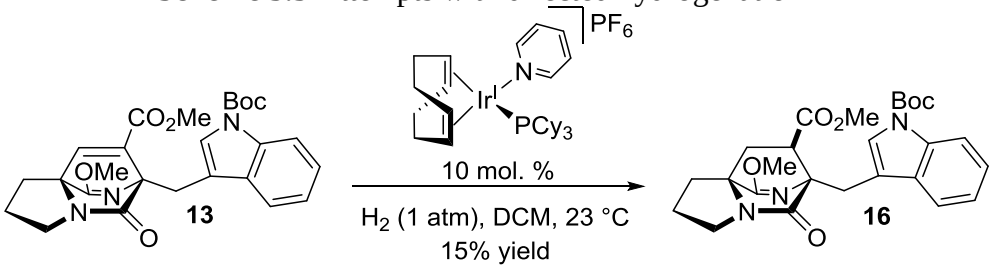

Following the failure of directed hydrogenation to proceed in good yield, we attempted a new approach whereby conjugate hydride addition to the same α,β–unsaturated methyl ester would produce an enolate might possibly be selectively protonated in order to form **15** or **16**. We initially explored Stryker's reagent, a hexameric copper (I) hydride source which has been used in conjugate hydride addition to various α,β–unsaturated carbonyl compounds.[7] We observed that treatment of **13** with stoichiometric reagent in deoxygenated toluene at room temperature afforded a 1:3 ratio of **15** and **16**, favoring the *syn* isomer, in near quantitative yields (**Scheme 3.6**). Unfortunately, we were not able to replicate this result because the reagent decomposed within a week, despite our careful exclusion of oxygen in a Schlenk flask. Other reagents that promote conjugate addition of hydride were examined, including *N*–selectride. In the event, conjugate reduction at –78 °C followed by cold methanol quench afforded a similar 1:3 ratio of *anti*:*syn* isomers, in significantly reduced yields (48% overall). The observed selectivity was not consistent in our hands and subsequent reduction attempts demonstrated little selectivity (1:1). These results indicate some promise for the selective protonation of the derived enolate of **13** and that a preference for the *syn* isomer might be obtained with continued effort.

Scheme 3.6 Conjugate hydride additions to **13**

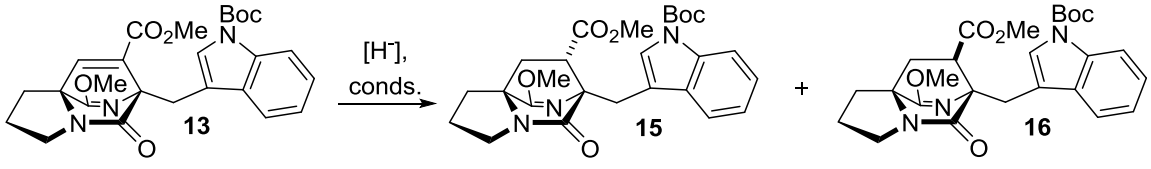

[H⁻]	*solvent*	*temp.*	***15*:*16***	*yield*
$[(Ph_3P)CuH]_6$	PhMe	23 °C	1:3	97%
N-Selectride	THF	–78 °C	1:3 -or- 1:1	<50%

We have also evaluated a number of alternative dienophiles for cycloaddition to pyrazinone **8**. **Table 3.1** lists all dienophiles tested at this time for thermal Diels–Alder cycloaddition. Ethyl acrylate gives a 3:1:1 ratio and 2–nitroacrylate gives a 4:1 regioisomeric ratio with only the *syn* isomer represented. The cycloaddition appears to prefer electron–deficient dienophiles although it is sensitive to nonbonding interactions. Tertiary alcohol substitution would ideally intercept **18** or its *anti* isomer and proceed with our above synthesis however no cycloaddition was observed, with either a nitro or carboxyl electron withdrawing group. It may be useful to investigate the utility of chiral nitroacrylate dienophiles which may be able to access either enantiomeric series of natural products. Lewis acid–catalyzed or radical–cation initiated[8] Diels–Alder cycloadditions with **8** and either *p*–methoxystyrene or *p*–allylanisole proceeded either with polymerization of dienophile or degradation of azadiene starting material. Intermolecular [4+2] cycloadditions to diketopiperazine azadienes such as **8** remain a persistent challenge in current synthetic methodology.

Conclusion

The formal syntheses of brevianamide B and premalbrancheamide have been reported. The [2.2.2]diazaoctane core was constructed via an intermolecular Diels–Alder cycloaddition to a diketopiperazine pyrazinone. When 2–nitroacrylate was utilized as dienophile, the reaction produced only the *syn* diastereomer, although that selectivity could not be maintained in the course of the synthetic procedure.

Table 3.2 Scope of [4+2] annulation with pyrazinone **8**

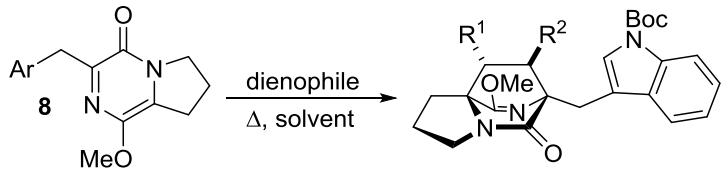

dienophile	*solvent/conds.*	*temp.*	*time*	*result*
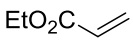	DMF	60 °C	O/N	3:1:1, wrong *regio.* 48% major **9**
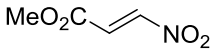	toluene	-10 to 23 °C	O/N	4:1 **11**:**12** *regio.* 89% overall
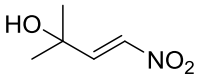	DMF	80 °C	3 days	Decomposition
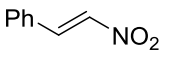	DMF	80 °C	3 days	Decomposition <5% cycloadduct?
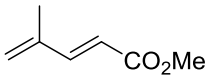	toluene	110 °C	O/N	Complex mixture
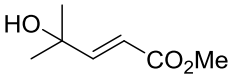	DMF	130 °C	3 days	Boc cleavage
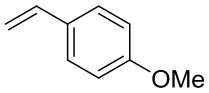	$N(p\text{-}BrPh)_3SbCl_6$ DCM	0 °C	4 hours	Recovered sm
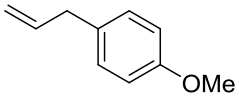	$N(p\text{-}BrPh)_3SbCl_6$ DCM	0 °C	4 hours	Recovered sm
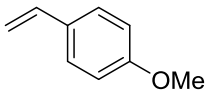	TMSOTf, DCM $Cu(OTf)_2$, DCM $Sc(OTf)_3$, DCM	-78 to 23 °C	O/N	Polymerization Recovered sm
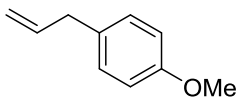	TMSOTf, DCM $Cu(OTf)_2$, DCM	23 °C	4 hours	Degredation

Experimentals

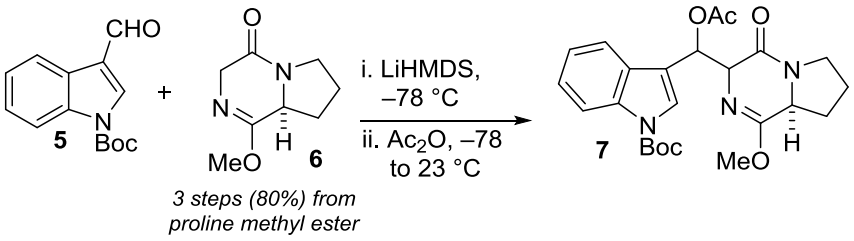

tert-Butyl 3-(Acetoxy((8aS)-1-methoxy-4-oxo-3,4,6,7,8,8ahexahydropyrrolo[1,2-a]pyrazin-3-yl)methyl)-1H-indole-1-carboxylate (7). To DKP **6** (2.16 g, 12.9 mmol) in THF (71 mL) at −78 °C was added LiHMDS (14.1 mL, 1 M in THF) dropwise and the mixture stirred for 30 min at −78 °C. *N*–Boc–indole carboxaldehyde **5** (3.31 g, 13.5 mmol) was added as a solution in THF (10 mL) dropwise over 5 min, and the reaction was stirred for an additional 30 min at −78 °C. Ac_2O (1.82 mL, 19.3 mmol) and pyridine (1.55 mL, 19.3 mmol) were each added dropwise over 5 min, and the cold bath was removed. The reaction was allowed to warm to rt and stir for 16 h and was then diluted with HCl (20 mL, 0.1 M) and extracted with EtOAc (3 × 30 mL). The combined organic extracts were washed with satd aqueous $NaHCO_3$ (50 mL), saturated NaCl (50 mL), dried (Na_2SO_4), filtered, and concentrated *in vacuo* to afford the β–acetoxy product as a mixture of four diastereomers. The resulting residue was purified by flash column chromatography on silica gel (gradient elution: 30% → 100% EtOAc in hexanes). The four diastereomers were collected together to afford a pale yellow amorphous solid (5.32 g, 91% yield): mp 58.0−59.1 °C; TLC (80% EtOAc in hexanes) R_f 0.25−0.35 (UV/CAM); IR (film) 2980, 2945, 2886, 1732, 1676, 1657, 1451, 1368, 1338, 1310, 1252, 1219, 1152, 1080, 1017, 947, 853, 839, 764, 747, 700, 631, 600, 592 cm^{-1}; ^1H NMR (400 MHz, CDCl3) 8.13−8.01 (m, 1H), 7.96−7.91 (m, 1H), 7.74−7.52 (m, 1H), 7.32− 7.18 (m, 2H), 6.89−6.41 (m, 1H), 4.77−4.28 (m, 1H),

4.05−3.94 (m, 1H), 3.79−3.72 (m, 3H), 3.70−3.63 (m, 1H), 3.50−3.31 (m, 1H), 2.31−2.22 (m, 1H), 2.16−2.01 (m, 3H), 1.93−1.69 (m, 2H), 1.62− 1.29 (m, 1H), 1.66−1.64 (m, 9H); ^{13}C NMR (100 MHz, CDCl3): δ 170.2, 169.8, 169.4, 165.9, 165.5, 165.2, 165.1, 163.4, 163.1, 162.5, 162.4, 149.6, 149.7, 149.5, 135.3, 135.1, 129.8, 129.5, 128.9, 128.6, 125.6, 125.4, 125.0, 124.7, 124.6, 124.4, 124.3, 124.1, 122.7, 122.6, 122.5, 122.3, 121.8, 120.8, 120.4, 120.0, 118.6, 116.9, 116.8, 116.7, 115.2, 115.1, 114.8, 84.1, 83.6, 83.6, 71.1, 71.0, 70.4, 66.0, 65.8, 63.7, 63.4, 56.9, 56.8, 56.6, 56.3, 53.8, 53.7, 53.6, 44.6, 44.4, 44.3, 44.2, 29.6, 29.4, 29.1, 28.7, 28.3, 28.2, 28.1, 22.6, 22.4, 21.9, 21.7, 21.3, 21.2, 21.1; exact mass calcd for $C_{24}H_{29}N_3O_6Na$ $[M + Na]^+$ 478.1949, found 478.1946.

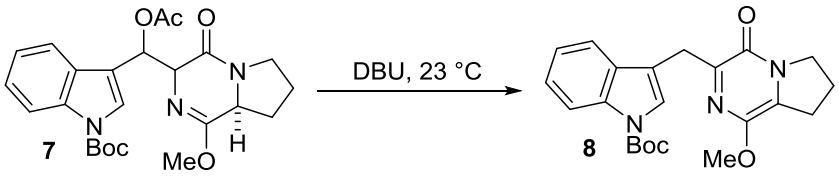

tert-Butyl 3-((1-Methoxy-4-oxo-4,6,7,8-tetrahydropyrrolo- [1,2-a]pyrazin-3-yl)methyl)-1H-indole-1-carboxylate (8). A flame–dried flask was charged with β–acetoxy aldol addition product **7** (1.37 g, 3.00 mmol), wrapped in aluminum foil, flushed with N2 gas for 10 min, and dissolved in PhMe (15 mL) and DMF (3 mL). To the reaction flask was added DBU (0.89 mL, 6.00 mmol), and the reaction was stirred for 16 h, diluted with HCl (20 mL, 0.2 M), and extracted with EtOAc (3 × 30 mL). The combined organic extracts were washed with satd aqueous $NaHCO_3$ (50 mL) and saturated NaCl (50 mL), dried (Na_2SO_4), filtered, and concentrated *in vacuo* to afford pyrazinone 14 as a yellow amorphous solid (1.12 g, 94% yield). The resulting product (0.91 g, quant mass recovery, ca. 95% pure by 1 H NMR) was recrystallized (hexanes/EtOAc) to afford analytically pure **5** (0.38 g, 42% yield) as a yellow amorphous solid. Pyrazinone **5** can be stored (in the dark)

for several weeks under inert gas at −15 °C without appreciable degradation: TLC (100% EtOAc) R_f 0.40 (UV/CAM); IR (film) 2976, 2939, 1730, 1653, 1584, 1579, 1452, 1369, 1349, 1256, 1157, 1080, 1046, 1016, 855, 750 cm^{-1}; ^1H NMR (400 MHz, CDCl3) δ 8.10 (s, 1H), 7.75 (d, *J* = 7.3 Hz, 1H), 7.61 (s, 1H), 7.29−7.19 (m, 2H), 4.19 (s, 2H), 4.14 (t, *J* = 7.0 Hz, 2H), 3.82 (s, 3H), 3.04 (t, *J* = 7.4 Hz, 2H), 2.21 (q, *J* = 7.4 Hz, 2H), 1.65 (s, 9H); ^{13}C NMR (100 MHz, CDCl3) δ 154.0, 149.8, 149.6, 142.5, 135.5, 130.8, 125.4, 124.2, 124.1, 122.2, 120.0, 116.7, 115.0, 83.3, 54.8, 49.5, 28.4, 28.2, 28.1, 21.6; exact mass calcd for $C_{22}H_{25}N_3O_4$ $[M + Na]^+$ 418.1743, found 418.1735.

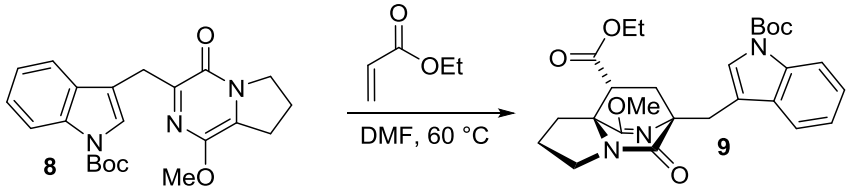

Ethyl (6R*,8R*,8aS*)-6-((1-(tert-Butoxycarbonyl)-1H-indol-3- yl)methyl)-9-methoxy-5-oxo-2,3,5,6,7,8-hexahydro-1H-6,8a- (azenometheno)indolizine-8-carboxylate (9). A flame–dried flask was charged with pyrazinone **8** (227 mg, 0.575 mmol) and fitted with a reflux condenser. The starting material was dissolved in DMF (3.8 mL, 0.15 M), and the reaction vessel was degassed (evacuated and backfilled with N_2 × 5). Ethyl acrylate (0.12 mL, 114 mg, 1.14 mmol) was added, and the reaction vessel was heated at 60 °C for 24 h, cooled to rt, and concentrated *in vacuo* to afford a brown oil. Analysis of the unpurified reaction mixture reveals a 3:1:1 mixture of diastereomers. Purification by flash column chromatography on silica gel (gradient elution: 30% → 100% EtOAc in hexanes) afforded product **9** (138 mg, 48% yield) as a colorless oil: TLC (60% EtOAc in hexane) R_f 0.30 (CAM); IR (film) 2985, 2945, 2876, 1736, 1683, 1642, 1456, 1416, 1308, 1260, 1156, 1085, 1016, 852, 768, 745 cm^{-1}; ^1H NMR (400 MHz, CDCl3) 8.10 (br s, 1H),

7.78 (d, *J* = 7.5 Hz, 1H), 7.68 (s, 1H), 7.24 (m, 2H), 4.05 (m, 2H), 3.75 (s, 3H), 3.50−3.30 (m, 2H), 3.44 (d, *J* = 14.8 Hz, 1H), 3.34 (d, *J* = 14.8 Hz, 1H), 2.78 (dd, *J* = 9.8, 5.5 Hz, 1H), 2.61 (m, 1H), 2.05−1.85 (m, 4H), 1.80 (dd, *J* = 13.2, 5.5 Hz, 1H), 1.64 (s, 9H), 1.18 (t, *J* = 7.2 Hz, 3H); ^{13}C NMR (100 MHz, CDCl3) δ 172.3, 163.0, 160.8, 149.5, 134.9, 132.1, 130.3, 129.0, 128.4, 128.2, 125.3, 124.7, 123.0, 118.9, 116.1, 155.5, 115.1, 104.8, 83.7, 65.6, 60.7, 54.3, 43.8, 35.0, 32.4, 29.0, 28.2, 28.1, 20.2, 14.0; exact mass calcd for $C_{27}H_{33}N_3O_6$ $[M + Na]^+$ 518.2261, found 518.2259.

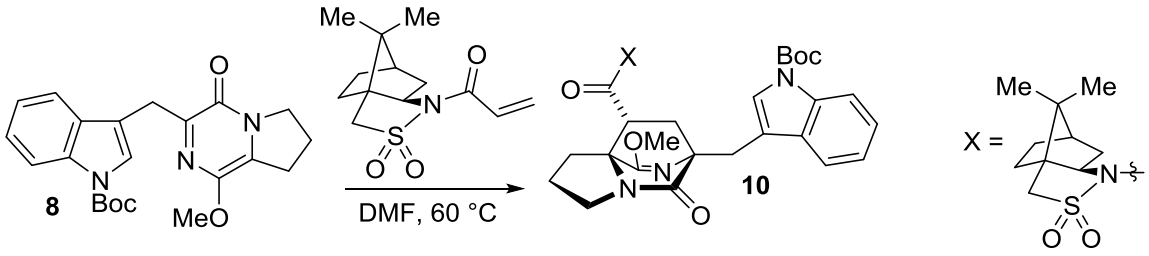

tert-Butyl 3-(((6R,8R,8aS)-8-((7aR)-8,8-Dimethyl-2,2-dioxidohexahydro-3H-3a,6-methanobenzo[c]isothiazole-1-carbonyl)- 9-methoxy-5-oxo-2,3,7,8-tetrahydro-1 H -6,8a- (azenometheno)indolizin-6(5H)-yl)methyl)-1H-indole-1-carboxylate (10). To a flame–dried flask were added acryloyl (+)–camphorsultam (135 mg, 0.51 mmol) and pyrazinone **8** (188 mg, 0.48 mmol). The flask was fitted with a condenser and flushed with N_2. The reactants were dissolved in DMF (3.2 mL, 0.15 M), and the vessel was evacuated and backfilled with N_2 (×5) before heating to 60 °C. After being heated for 24 h, the reaction mixture was cooled to rt and concentrated *in vacuo* to afford a brown oil. Analysis of the unpurified reaction mixture by ^{1}H NMR reveals a single cycloadduct as well as some unreacted sultam dienophile. Purification by flash column chromatography on silica gel (gradient elution: 30% → 70% EtOAc in hexanes) afforded cycloadduct **10** (260 mg, 62% yield) as a colorless oil: TLC (80% EtOAc in hexane) R_f 0.3 (CAM); $[\alpha]_D^{25}$ = +59 (*c* 1.0,

CH_2Cl_2); IR (film) 3854, 3744, 3061, 2986, 2882, 2360, 2337, 1730 1683, 1648, 1635, 1452, 1363, 1351, 1308, 1298, 1268, 1258, 1218, 1164, 1135, 1083, 1015, 987, 768, 735, 667, 533 cm^{-1}; ^1H NMR (400 MHz, CDCl3) 8.1 (s, 1H), 7.77 (d, *J* = 1.14 Hz, 1H), 7.66 (s, 1H), 7.23 (m, 2H), 3.77 (s, 3H), 3.75 (m, 1H), 3.52−3.42 (m, 4H), 3.38 (d, *J* = 13.7 Hz, 1H), 3.30 (d, *J* = 14.8 Hz, 1H), 2.47 (dd, *J* = 11.7, 6.6 Hz, 1H), 2.15−1.81 (m, 10H), 1.68 (dd, *J* = 13.3, 5.5 Hz, 1H), 1.66 (s, 9H), 1.30 (m, 2H), 1.15 (s, 3H), 0.96 (s, 3H); ^{13}C NMR (100 MHz, CDCl3) δ 172.2, 170.9, 169.5, 149.8, 135.1, 132.1, 125.5, 123.6, 121.9, 120.4, 116.5, 114.8, 83.1, 66.3, 66.2, 65.4, 54.5, 53.1, 49.0 48.2, 47.7, 44.6, 43.2, 38.5, 34.9, 32.9, 28.8, 28.2, 27.2, 26.3, 24.4, 20.9, 19.8; exact mass calcd for $C_{35}H_{44}N_4O_7S$ $[M + Na]^+$ 687.2823, found 687.2813.

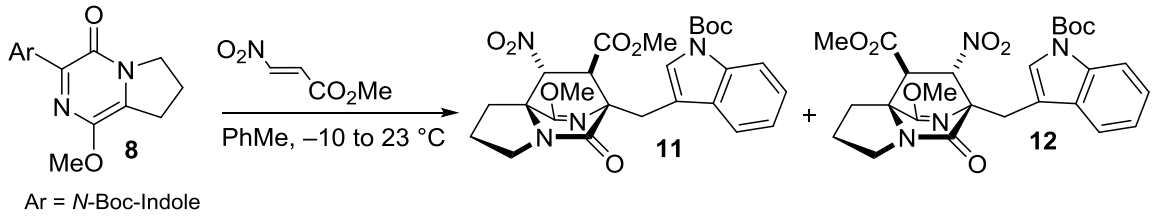

Methyl (6S*,7R*,8R*,8aS*)-6-((1-(tert-Butoxycarbonyl)- 1H-indol-3-yl)methyl)-9-methoxy-8-nitro-5-oxo-2,3,5,6,7,8- hexahydro-1H-6,8a-(azenometheno)indolizine-7-carboxylate (11) and Methyl (6S*,7S*,8S*,8aS*)-6-((1-(tert-Butoxycarbonyl)-1H-indol-3-yl)methyl)-9-methoxy-7-nitro-5-oxo-2,3,5,6,7,8-hexahydro-1H-6,8a-(azenometheno)indolizine-8-carboxylate (12). A dry flask was charged with pyrazinone **8** (531 mg, 1.34 mmol) and flushed with N_2 gas for 30 min and dissolved in toluene (7 mL). A separate flask was charged with nitroacrylate (158 mg, 1.21 mmol) and flushed with N_2 gas for 30 min and dissolved in toluene (2 mL). The reaction flask containing pyrazinone 14 was cooled to −10 °C (ice/salt bath). The nitroacrylate solution was

dropwise to the reaction vessel over 10 min. The reaction was allowed to stir and slowly warm to rt overnight (16 h). The solution was concentrated *in vacuo* to afford a brown oil, which contained the two regioisomeric cycloadducts **11** and **12** in a 4:1 ratio (as judged by ^{1}H NMR on the unpurified reaction mixture). The resulting residue was purified by flash column chromatography on silica gel (gradient elution: 10% → 80% EtOAc in hexanes). A small amount of pure **11** (40 mg) was obtained for analytical purposes and the bulk of the material was obtained as a yellow oil that was comprised of a 4:1 mixture of **11** and **12** (593 mg, 84% yield): TLC (80% EtOAc in hexanes) R_f 0.30, 0.35 (CAM/UV). IR (film) 3052, 2980, 2950, 1733, 1704, 1641, 1608, 1559, 1477, 1452, 1410, 1370, 1309, 1219, 1197, 1158, 1086, 1016, 979, 937, 897, 857, 811, 768, 747, 703, 656 cm^{-1}; ^{1}H NMR (400 MHz, CDCl3): δ 8.13 (d, *J* = 5.9 Hz, 1H), 7.76 (d, *J* = 1.6, 1H), 7.74 (d, *J* = 7.8 Hz, 1H), 7.29 (dt, *J* = 8.2, 1.2 Hz, 1H) 7.21 (dt, *J* = 7.8, 0.8 Hz, 1H), 5.05 (d, *J* = 4.3 Hz, 1H), 3.77 (s, 3H) 3.76 (s, 3H), 3.62− 3.52 (m, 3H), 3.34 (d, *J* = 4.3 Hz, 1H), 3.30 (d, *J* = 15.7 Hz, 1H), 2.72−2.66 (m, 1H), 2.25−2.00 (m, 3H), 1.68 (s, 9H); ^{13}C NMR (100 MHz, CDCl3): δ 169.6, 169.1, 168.7, 149.7, 135.1, 132.0, 125.5, 124.0, 121.9, 120.5, 115.3, 114.9, 88.9, 83.3, 68.6, 65.3, 55.4, 53.1, 51.0, 44.0, 28.2, 27.2, 26.8, 24.3; exact mass calcd for $C_{26}H_{30}N_4O_8Na$ $[M + Na]^+$ 549.1953, found 549.1956.

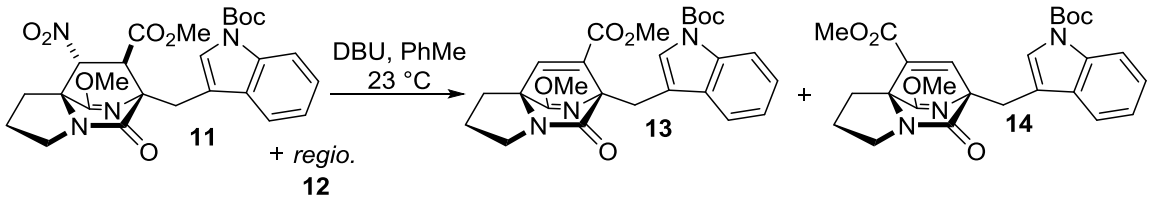

Methyl (6S*,8aS*)-6-((1-(tert-Butoxycarbonyl)-1H-indol-3-yl)methyl)- 9-methoxy-5-oxo-2,3,5,6-tetrahydro-1H-6,8a-(azenometheno)indolizine-7-carboxylate (13) and Methyl (6S*,8aS*)-6-((1-(tert-Butoxycarbonyl)-1H-indol-3- yl)methyl)-9-methoxy-5-oxo-2,3,5,6-tetrahydro-1H-6,8a- (azenometheno)indolizine-8-carboxylate (14). A flask was charged with cycloadducts **11** and **12** (ratio 4:1, 588 mg, 1.12 mmol), flushed with N_2 gas, and dissolved in PhMe (18 mL). To the reaction vessel was added DBU (277 μL, 1.86 mmol), and the reaction mixture was stirred for 16 h at rt, diluted with HCl (0.1 M, 10 mL), and extracted with EtOAc (3 × 15 mL). The combined organic portions were washed with saturated $NaHCO_3$ (20 mL) and saturated NaCl (20 mL), dried (Na_2SO_4), filtered, and concentrated *in vacuo* to give the α,β–unsaturated methyl ester regioisomers **13** and **14** in a 4:1 ratio as judged by ^{1}H NMR on the unpurified reaction mixture. The residue was purified by flash column chromatography on silica gel (gradient elution: 20% → 80% EtOAc in hexanes) to afford the minor regioisomer **14** as a light yellow oil (62.1 mg, 12% yield) and **13** as a pale yellow powder (376 mg, 70% yield). Spectroscopic data reported for **14**: TLC (40% EtOAc in hexanes) R_f 0.45 (CAM/UV); IR (film) 2890, 2884, 1721, 1688, 1634, 1607, 1451, 1369, 1339, 1327, 1308, 1267, 1256, 1244, 1157, 1086, 1044, 1003, 984, 910, 856, 746, 732, 665 cm^{-1}; ^{1}H NMR (400 MHz, CDCl3): δ 8.10 (d, *J* = 7.0 Hz, 1H), 7.83 (d, *J* = 7.5 Hz, 1H), 7.68 (s, 1H), 7.50 (s, 1H) 7.33−7.29 (m, 1H), 7.27−7.23 (m, 1H), 3.80 (s, 3H), 3.73 (d, *J* = 12.1 Hz, 3H), 3.59 (dd, *J* = 15.3, 1.2 Hz, 2H), 3.49−3.44 (m, 1H) 3.19−3.12 (m, 1H) 2.87−2.76 (m, 2H) 2.14−2.04 (m, 1H), 1.98−1.87 (m, 1H) 1.66

(s, 9H); ^{13}C NMR (100 MHz, CDCl3): δ 175.4, 169.6, 162.8, 152.8, 149.8, 138.2, 135.1, 131.7, 124.9, 124.1, 122.3, 120.0, 116.1, 115.0, 83.4, 74.0, 69.4, 56.3, 51.8, 43.0, 28.2, 26.7, 25.6, 25.4; exact mass calcd for $C_{26}H_{29}N_3O_6$ $[M + Na]^+$ 502.1949, found 502.1944. Spectroscopic data reported for α,β–unsaturated methyl ester **13**: mp 94.0−95.0 °C; TLC (40% EtOAc in hexanes) R_f 0.28 (CAM/UV); IR (film) 2980, 2949, 2882, 1722, 1690, 1640, 1607, 1451, 1370, 1339, 1304, 1256, 1221, 1155, 1080, 1017, 995, 978, 930, 907, 856, 835, 764, 739, 619 cm^{-1} ; ^{1}H NMR (400 MHz, CDCl3): δ 8.06 (s, 1H), 7.81 (dd, *J* = 7.1, 1.3 Hz, 1H), 7.62 (s, 1H), 7.28–7.20 (m, 2H), 7.13 (s, 1H), 4.07 (dd, *J* = 15.6, 0.8 Hz, 1H), 3.79 (s, 3H), 3.64 (dd, *J* = 15.6, 0.8 Hz, 1H), 3.40 (s, 3H), 3.40−3.35 (m, 1H), 3.25−3.19 (m, 1H), 2.74 (m, 1H), 2.25−2.18 (m, 1H), 2.10−2.00 (m, 2H), 1.63 (s, 9H); ^{13}C NMR (100 MHz, CDCl3): δ 174.4, 169.7, 164.6, 150.0, 147.5, 144.4, 135.1, 132.3, 124.5, 124.0, 122.1, 120.7, 117.6, 114.9, 83.1, 75.7, 67.6, 56.3, 52.1, 42.7, 28.4, 26.8, 25.5, 25.3; exact mass calcd for $C_{26}H_{29}N_3O_6$ $[M + Na]^+$ 502.1949, found 502.1944.

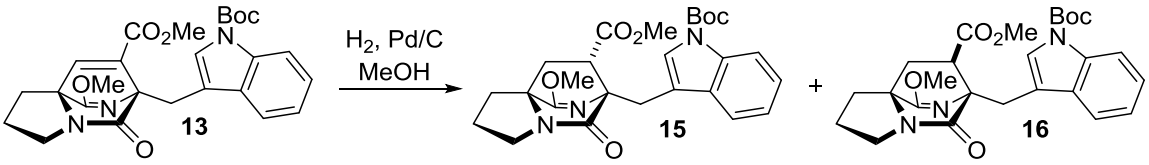

Methyl (6S*,7S*,8aS*)-6-((1-(tert-Butoxycarbonyl)-1H-indol- 3-yl)methyl)-9-methoxy-5-oxo-2,3,5,6,7,8-hexahydro-1H-6,8a- (azenometheno)indolizine-7-carboxylate (15) and Methyl (6S*,7R*,8aS*)-6-((1-(tert-Butoxycarbonyl)-1H-indol-3-yl)- methyl)-9-methoxy-5-oxo-2,3,5,6,7,8-hexahydro-1H-6,8a-(azenometheno)indolizine-7-carboxylate (16). Unsaturated ester **13** (182 mg, 0.378 mmol) was dissolved in MeOH (4 mL) at rt, and 10% Pd/C (25 mg) was added. One balloon of H_2 gas was used to sparge the reaction mixture (10 min); a second balloon was

maintained above the reaction mixture during the course of the reaction to provide an atmosphere of H_2. When TLC indicated consumption of starting material (1 h), the reaction mixture was filtered through Celite, and the filter pad was washed with MeOH. After removal of the solvent *in vacuo*, a white powder was obtained that contained an equal mixture of diastereomers as judged by ^{1}H NMR on the unpurified reaction mixture. The mixture was purified by flash chromatography on silica gel (20% to 100% EtOAc in hexanes) to afford **15** (77 mg, 43% yield) and **16** (78 mg, 43% yield), both obtained as a colorless amorphous solids. Spectroscopic data for **15**: TLC (60% EtOAC in hexanes) R_f 0.36 (CAM/UV); IR (film) 2980, 2948, 2883, 1732, 1730, 1695, 1687, 1641, 1476, 1457, 1452, 1416, 1371, 1360, 1308, 1257, 1213, 1185, 1161, 1084, 1016, 913, 857, 768, 745, 701, 672 cm^{-1}; ^{1}H NMR (400 MHz, CDCl3): δ 8.07 (d, *J* = 5.8 Hz, 1H), 7.76 (s, 1H), 7.74 (d, *J* = 2.0 Hz, 1H), 7.24−7.19 (m, 2H), 3.78 (s, 3H), 3.54 (d, *J* = 14.8 Hz, 1H), 3.47 (s, 3H), 3.44−3.31 (m, 2H), 3.22 (d, *J* = 14.9 Hz, 1H), 3.06 (q, *J* = 4.7 Hz, 1H), 2.65−2.58 (m, 1H), 2.09−1.87 (m, 5H), 1.63 (s, 9H); ^{13}C NMR (100 MHz, CDCl3): δ 172.4, 171.0, 169.9, 149.9, 134.9, 132.3, 125.7, 123.6, 121.9, 120.3, 116.7, 114.8, 82.8, 69.3, 64.1, 54.7, 51.8, 45.8, 43.4, 37.3, 28.6, 28.2, 27.5, 24.4; exact mass calcd for $C_{26}H_{31}N_3O_6Na$ $[M + Na]^+$ 504.2105, found 504.2102. Spectroscopic data for **16**: TLC (60% EtOAC in hexanes) R_f 0.43, (CAM/UV); IR (film) 2979, 2948, 2881, 1731, 1693, 1690, 1689, 1452, 1437, 1419, 1370, 1343, 1301, 1258, 1218, 1162, 1120, 1084, 1045, 1013, 990, 856, 767, 747, 666 cm^{-1}; ^{1}H NMR (400 MHz, CDCl3): δ 8.09 (s, 1H), 7.79 (d, *J* = 7.8 Hz, 1H), 7.68 (s, 1H), 7.25 (t, *J* = 6.2 Hz, 1H), 7.19 (t, *J* = 7.8 Hz, 1H), 3.75 (s, 1H), 3.71 (s, 3H), 3.68 (s, 3H), 3.29 (d, *J* = 15.3 Hz, 1H), 2.76 (q, *J* = 5.1 Hz, 1H), 2.60− 2.54 (m, 1H), 2.08−1.83 (m, 5H), 1.66 (s, 9H); ^{13}C NMR (100 MHz, CDCl3): δ 172.9, 172.4, 169.8, 149.9, 135.2, 132.3,

125.5, 123.8, 121.8, 121.1, 116.5, 114.8, 83.1, 68.9, 63.3, 54.7, 52.1, 45.2, 43.5, 36.3, 28.7, 28.2, 27.2, 24.6; exact mass calcd for $C_{26}H_{31}N_3O_6Na$ $[M + Na]^+$ 504.2105, found 504.2102.

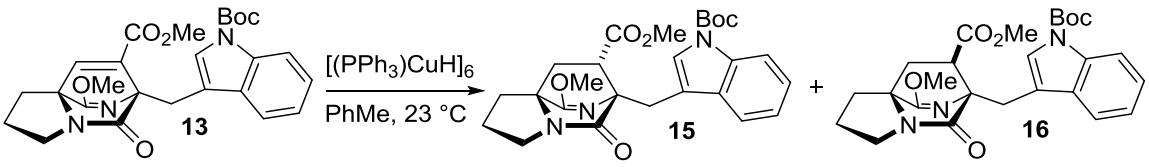

Methyl (6S*,7S*,8aS*)-6-((1-(tert-Butoxycarbonyl)-1H-indol- 3-yl)methyl)-9-methoxy-5-oxo-2,3,5,6,7,8-hexahydro-1H-6,8a- (azenometheno)indolizine-7-carboxylate (15) and Methyl (6S*,7R*,8aS*)-6-((1-(tert-Butoxycarbonyl)-1H-indol-3-yl)- methyl)-9-methoxy-5-oxo-2,3,5,6,7,8-hexahydro-1H-6,8a-(azenometheno)indolizine-7-carboxylate (16). Unsaturated methyl ester **13** (20.2 mg, 0.042 mmol) was added to a flame–dried reaction flask and dissolved in dry toluene (1 mL). The solution was sparged with Ar gas for 10 minutes. In a separate flame–dried flask, (triphenylphosphine)copper hydride hexamer (37.4 mg, 0.21 mmol) was dissolved in dry toluene (1 mL) and sparged with Ar gas for 10 minutes. The copper solution was added dropwise to the solution of starting material. The mixture was allowed to stir at rt for 1 h then diluted with NH_4Cl (5 mL), and extracted with EtOAc (3 × 10 mL). The combined organic layers were washed with saturated NaCl (40 mL), dried (Na_2SO_4), filtered, and concentrated *in vacuo*. Analysis of the unpurified reaction mixture by ^1H NMR shows a 3:1 ratio of *syn* and *anti* products, as well as some residual PPh_3. Purification by flash chromatography on silica gel (25% → 100% EtOAc in hexanes) afforded **15** (7.5 mg, 37% yield) and **16** (12.1, 60% yield), both as colorless amorphous solids. *Vide infra* for spectroscopic information.

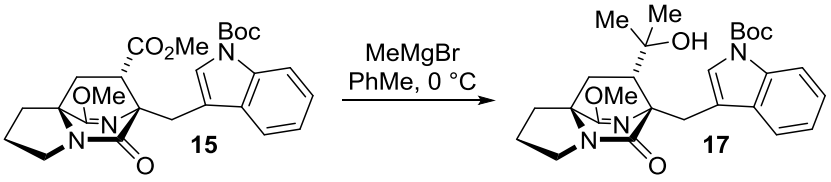

tert-Butyl 3-(((6S*,7S*,8aS*)-7-(2-Hydroxypropan-2-yl)-9- methoxy-5-oxo-2,3,7,8-tetrahydro-1H-6,8a-(azenometheno)- indolizin-6(5H)-yl)methyl)-1H-indole-1-carboxylate (17). A flame–dried flask was charged with **15** (12.5 mg, 0.026 mmol) and flushed with N_2 gas for 10 min, dissolved in toluene (0.52 mL), and cooled to 0 °C. To this solution was added MeMgBr (74 μL, 0.104 mmol, 1.4 M in THF). The reaction was stirred for 1 h at 0 °C, diluted with NH_4Cl (10 mL), and extracted with EtOAc (3 × 10 mL). The combined organic layers were washed with saturated NaCl (40 mL), dried (Na_2SO_4), filtered, and concentrated *in vacuo*. The resulting product was purified by flash chromatography on silica gel (50% → 100% EtOAc in hexanes) to afford the derived lactim tertiary alcohol **17** as a white foam (7.4 mg, 59% yield): TLC (80% EtOAc in hexanes) R_f 0.35 (CAM/UV); IR (film) 3406, 2976, 2945, 2880, 1726, 1661, 1451, 1424, 1368, 1354, 1256, 1207, 1155, 1103, 1080, 1011, 955, 924, 924, 856, 820, 743 cm^{-1}; ^1H NMR (400 MHz, CDCl3) δ 8.05 (br s, 1H), 7.84−7.82 (m, 1H), 7.69 (s, 1H), 7.24−7.18 (m, 2H), 3.75 (d, *J* = 14.8 Hz, 1H), 3.69 (s, 3H), 3.51 (d, *J* = 14.9 Hz, 1H), 3.47−3.41 (m, 1H), 3.28−3.22 (m, 1H), 2.50 (dt, *J* = 12.9, 7.4 Hz, 1H), 2.35 (dd, *J* = 9.8, 6.2 Hz, 1H), 2.04 (dd, *J* = 12.9, 9.8, 1H), 1.97−1.82 (m, 3H), 1.76 (br s, 1H), 1.63 (s, 9H), 1.41 (dd, *J* = 12.9, 6.2 Hz, 1H), 1.32 (s, 3H), 1.22 (s, 3H); ^{13}C (100 MHz, CDCl3) δ 171.5, 169.8, 150.0, 134.8, 132.6, 125.5, 123.3, 121.7, 120.7, 118.8, 114.7, 82.7, 74.2, 71.7, 63.4, 54.1, 51.9, 43.2, 37.9, 31.2, 28.6, 28.2, 25.9, 24.2; exact mass calcd for $C_{27}H_{35}N_3O_5Na$ $[M + Na]^+$ 504.2469, found 504.2468.

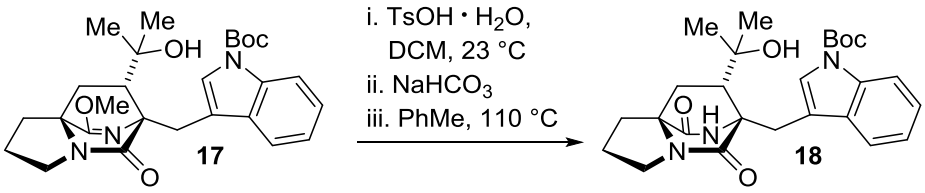

tert-Butyl 3-(((6S,7S,8aS)-7-(2-Hydroxypropan-2-yl)-5,9-dioxotetrahydro-1H-6,8a-(epiminomethano)indolizin-6(5H)-yl)- methyl)-1H-indole-1-carboxylate (18). A reaction flask was charged with lactim tertiary alcohol **17** (15.8 mg, 0.033 mmol) and flushed with N_2 gas for 10 min, dissolved in CH_2Cl_2 (3.5 mL), and cooled to 0 °C. To the reaction flask was added *p*–TsOH·H2O (7.3 mg, 0.038 mmol). The reaction was stirred and slowly warmed to ambient temperature over 6 h. The reaction mixture was diluted with satd aq $NaHCO_3$ (10 mL), and extracted with EtOAc (4 × 10 mL). The combined organic layers were washed with saturated NaCl (40 mL), dried (Na_2SO_4), filtered, and concentrated *in vacuo*. The resulting product (which contained some amino methyl ester) was dissolved in toluene (3 mL) and stirred at 110 °C for 18 h. The solution was concentrated *in vacuo* to obtain lactam tertiary alcohol **18** (15.5 mg, 95% yield) which was used without further purification: TLC (80% EtOAc in hexanes) R_f 0.32 (CAM/UV); IR (film) 3393, 2928, 1688, 1682, 1674, 1451, 1367, 1339, 1310, 1258, 1221, 1153, 1085, 1022, 961, 934, 856, 802, 745, 694, 665, 592 cm^{-1}; ^1H NMR (400 MHz, CDCl3) δ 8.12 (d, *J* = 7.4 Hz, 1H), 7.64 (s, 1H), 7.60 (d, *J* = 7.1 Hz, 1H), 7.33−7.16 (m, 2H), 5.70 (br s, 1H), 4.01 (d, *J* = 15.6 Hz, 1H), 3.64−3.52 (m, 2H), 3.40 (dt, *J* = 11.8, 6.6 Hz, 1H), 2.65 (dt, *J* = 12.9, 7.4 Hz, 1H), 2.36 (s, 1H), 2.31 (dd, *J* = 10.2, 6.6 Hz, 1H), 2.13 (dd, *J* = 13.3, 10.2 Hz, 1H), 1.97 (apparent quint, *J* = 7.0 Hz, 2H), 1.82−1.74 (m, 2H), 1.66 (s, 9H), 1.45 (s, 3H), 1.30 (s, 3H); ^{13}C NMR (100 MHz, CDCl3) δ 172.4, 169.3, 149.6, 135.1, 131.5, 126.8,

124.5, 122.9, 118.0, 115.5, 114.6, 83.7, 73.8, 66.8, 65.8, 50.7, 44.2, 36.2, 32.0, 28.2, 24.1, 23.7, 23.5; exact mass calcd for $C_{26}H_{33}N_3O_5Na$ $[M + Na]^+$ 490.2312, found 490.2312.

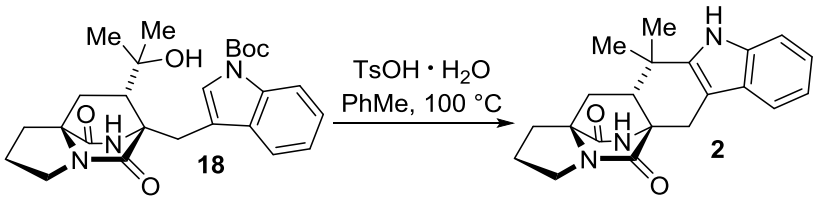

12,12-Dimethyl-2,3,11,12,12a,13-hexahydro-1H,5H,6H- 5a,13a-(epiminomethano)indolizino[7,6-b]carbazole-5,14- dione (2). A reaction flask was charged with lactam tertiary alcohol **18** (11.5 mg, 0.025 mmol), fitted with a reflux condenser, and flushed with N_2 gas for 10 min. PhMe (3.7 mL) and *p*–TsOH·H2O (4.7 mg, 0.025 mmol) were added, and the reaction vessel was heated to 100 °C for 6 h. After being cooled to rt, the reaction was diluted with satd aqueous $NaHCO_3$ (10 mL) and extracted with EtOAc (3 × 10 mL). The combined organic layers were washed with saturated NaCl (40 mL), dried (Na_2SO_4), filtered, and concentrated *in vacuo* to obtain **2** as a white powder (7.1 mg, 83% yield). The material thus obtained was >95% pure as judged by ^{1}H NMR and further purification was not performed: TLC (100% EtOAc) R_f 0.45 (CAM/UV); IR (film) 3325, 3310, 3233, 3221, 3210, 2990, 2947, 2901, 1656, 1670, 1451, 1404, 1369, 1339, 1300, 1258, 1196, 1161, 1092, 1011, 922, 860, 802, 772, 748, 718, 698, 644, 594 cm^{-1}; ^{1}H NMR (400 MHz, CDCl3) δ 7.89 (br s, 1H), 7.52 (d, *J* = 7.8 Hz, 1H), 7.32 (d, *J* = 7.9 Hz, 1H), 7.18 (td, *J* = 7.5, 1.3 Hz, 1H), 7.12 (td, *J* = 7.5, 1.2 Hz, 1H), 5.88 (br s, 1H), 3.93 (d, *J* = 18 Hz, 1H), 3.54 (t, *J* = 6.9 Hz, 2H), 2.91 (d, *J* = 18 Hz, 1H), 2.81 (quint, *J* = 6.7 Hz, 1H), 2.34 (dd, *J* = 9.8, 4.3 Hz, 1H), 2.18−1.99 (m, 4H), 1.89−1.82 (m, 1H), 1.33 (s, 3H), 1.28 (s, 3H); ^{13}C NMR (100 MHz, CDCl3) δ 172.7, 169.0, 139.6, 136.4, 127.2, 122.1, 119.7, 118.3, 110.7, 103.6, 67.1, 61.6, 45.7, 44.2, 34.5, 32.6, 29.1, 29.0, 25.3, 24.5, 23.9.

exact mass calcd for spray dimer $C_{42}H_{46}N_6O_4Na$ $[M + M + Na]^+$ 721.3473, found 721.3476. The spectral data for **2** were identical with an authentic sample provided by Williams (Colorado State University).

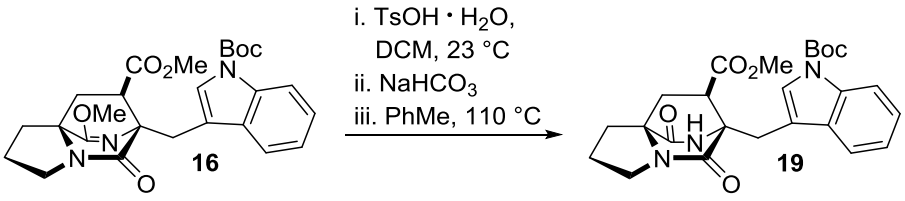

Methyl (6S,7R,8aS)-6-((1-(tert-Butoxycarbonyl)-1H-indol-3- yl)methyl)-5,9-dioxohexahydro-1H-6,8a-(epiminomethano)- indolizine-7-carboxylate (19). A reaction flask was charged with lactim methyl ester **16** (48 mg, 0.099 mmol) and flushed with N_2 gas for 10 min, dissolved in CH_2Cl_2 (10 mL), and cooled to 0 °C. To the reaction flask was added *p*–TsOH·H2O (24 mg, 0.13 mmol), and the reaction was stirred for 6 h while slowly warming to rt. The reaction mixture was diluted with satd aq $NaHCO_3$ (10 mL) and extracted with EtOAc (4 × 10 mL). The combined organic layers were washed with saturated NaCl (40 mL), dried (Na_2SO_4), filtered, and concentrated *in vacuo*. The resulting product (which contained some amino methyl ester) was dissolved in toluene (10 mL) and stirred at 110 °C for 18 h. The solution was concentrated *in vacuo* to obtain the lactam **19** as a white powder (15.7 mg, 88% yield). The material thus obtained was >95% pure as judged by ^{1}H NMR, and further purification was not performed: TLC (70% EtOAc in hexanes) R_f 0.30 (CAM/UV); IR (film) 3175, 3117, 3082, 3051, 2978, 2936, 2882, 1736, 1724, 1690, 1450, 1385, 1362, 1312, 1254, 1196, 1153, 1092, 1308, 1018, 964, 934, 922, 899, 849, 837, 768, 745, 691, 563 cm^{-1}; ^{1}H NMR (400 MHz, CDCl3) δ 8.15 (d, *J* = 8.2 Hz, 1H), 7.71 (s, 1H), 7.59 (d, *J* = 7.5 Hz, 1H), 7.36 (td, *J* = 7.6, 1.2 Hz, 1H), 7.29 (td, *J* = 7.6, 1.2 Hz, 1H), 5.75 (br s, 1H), 3.82 (s, 3H), 3.66−3.53 (m, 3H), 3.30 (dd, *J* = 9.8, 4.7 Hz,

1H), 3.19 (d, *J* = 15.6 Hz, 1H), 2.73−2.66 (m, 1H), 2.28−2.15 (m, 2H), 2.10− 1.98 (m, 2H), 1.85−1.79 (m, 1H), 1.69 (s, 9H); ^{13}C NMR (100 MHz, CDCl3) δ 172.3, 171.6, 166.4, 149.4, 135.4, 130.8, 126.2, 125.0, 123.3, 118.1, 115.7, 112.4, 84.1, 66.1, 63.4, 52.7, 48.2, 44.3, 34.8, 28.9, 28.2, 24.3, 24.0. exact mass calcd for $C_{25}H_{29}N_3O_6Na$ $[M + Na]^+$ 490.1949, found 490.1948. Spectral data agrees with that reported by Baran.[5]

REFERENCES

1. (a) Williams, Robert M.; Sanz–Cervera, Juan F.; Sancenón, F.; Marco, J. Alberto; Halligan, K. *J. Am. Chem. Soc.* **1998**, *120*, 1090–1091. (b) Laws, Stephen W.; Scheerer, Jonathan R. *J. Org. Chem.* **2013**, *78*, 2422–2429. (c) Greshock, Thomas J.; Grubbs, Alan W.; Tsukamoto, Sachiko; Williams, Robert M. *Agnew. Chem. Int. Ed.* **2007**, *46*, 2262–2265. (d) Greshock, Thomas J.; Williams, Robert M. *Org. Lett.* **2007**, *9* (21), 4255–4258. (e) Williams, R. M.; Kwast, E. *Tetrahedron Lett.* **1989**, *30*, 451–454.
2. Robins, Jacob G.; Kim, Kyu J.; Chinn, Alex J.; Woo, John S.; Scheerer, Jonathan R. *J. Org. Chem.* **2016**, *81*, 2293–2301.
3. Ding, Y.; Greshock, T. J.; Miller, K. A.; Sherman, D. H.; Williams, R. M. Org. Lett. **2008**, *10*, 4863−4866.
4. Adams, L. A.; Valente, M. W. N.; Williams, R. M. Tetrahedron **2006**, *62*, 5195−5200.
5. (a) Baran, P.S.; Hafensteiner, B.D.; Ambhaikar, N. B.; Guerrero, C. A.; Gallagher, J. D. *J. Am. Chem. Soc.* **2006**, *128*, 8678–8693. (b) Baran, P. S.; Guerrero, C. A.; Ambhaikar, N. B.; Hafensteiner, B. D. *Agnew Chem., Int. Ed.* **2005**, *44*, 606–609.
6. (a) Church, T. L; Andersson, P. G. *Coord. Chem. Rev.* **2008**, *252*, 513–531. (b) Hsung, R. P.; Song, Z. *Org. Lett.* **2007**, 9 (11), 2199–2202.
7. Mahoney, W. W.; Brestensky, D.M.; Stryker, J. M. *J. Am. Chem. Soc.* **1998**, *110*, 291.
8. Bellville, D. J.; Wirth, D. D.; Bauld, N. L. *J. Am. Chem. Soc*. **1981**, *103*, 718–720.

Appendix I
Supporting Information for Chapter Three

General Information. All reactions were carried out under an atmosphere of nitrogen in flame–dried or oven–dried glassware with magnetic stirring unless otherwise indicated. Acetonitrile, THF, toluene, and Et_2O were degassed with argon and purified by passage through a column of molecular sieves and a bed of activated alumina.[1] Dichloromethane was distilled from CaH_2 prior of use. All reagents were used as received unless otherwise noted. Flash column chromatography[2] was performed using silica gel (230–400 mesh). Analytical thin layer chromatography was performed on 60Å glass plates. Visualization was accomplished with UV light, anisaldehyde, ceric ammonium molybdate (CAM), potassium permanganate, or ninhydrin, followed by heating. Film (or KBr pellet) infrared spectra were recorded using a FTIR spectrophotometer. Optical rotations were determined by a digital polarimeter at 25 °C. ^{1}H NMR spectra were recorded on a 400 MHz spectrometer and are reported in ppm using solvent as an internal standard ($CDCl_3$ at 7.26 ppm) or tetramethylsilane (0.00 ppm). Proton–decoupled ^{13}C NMR spectra were recorded on a 400 MHz spectrometer and are reported in ppm using solvent as an internal standard ($CDCl_3$ at 77.0 ppm). All compounds were judged to be homogeneous (>95% purity) by ^{1}H and ^{13}C NMR spectroscopy unless otherwise noted as mixtures. Mass spectra data analysis was obtained through positive electrospray ionization (ICR–MS w/ NaCl).

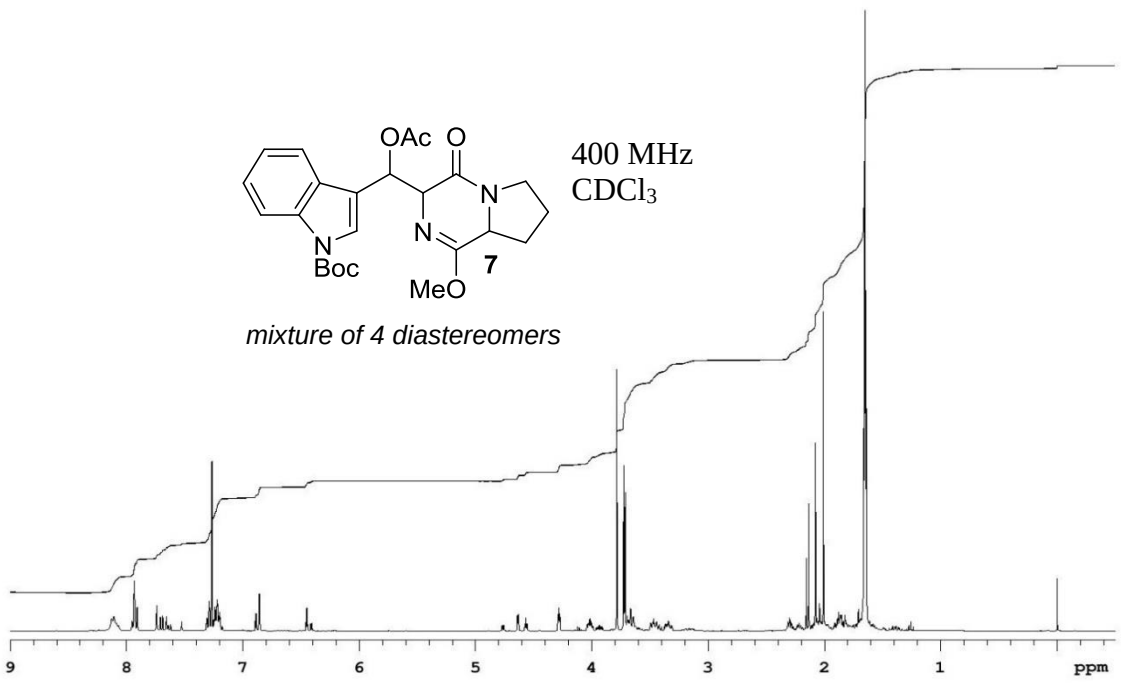
OAc
O
N
N
N
Boc
MeO
7
400 MHz
CDCl3
mixture of 4 diastereomers
9
8
7
6
5
4
3
2
1
ppm

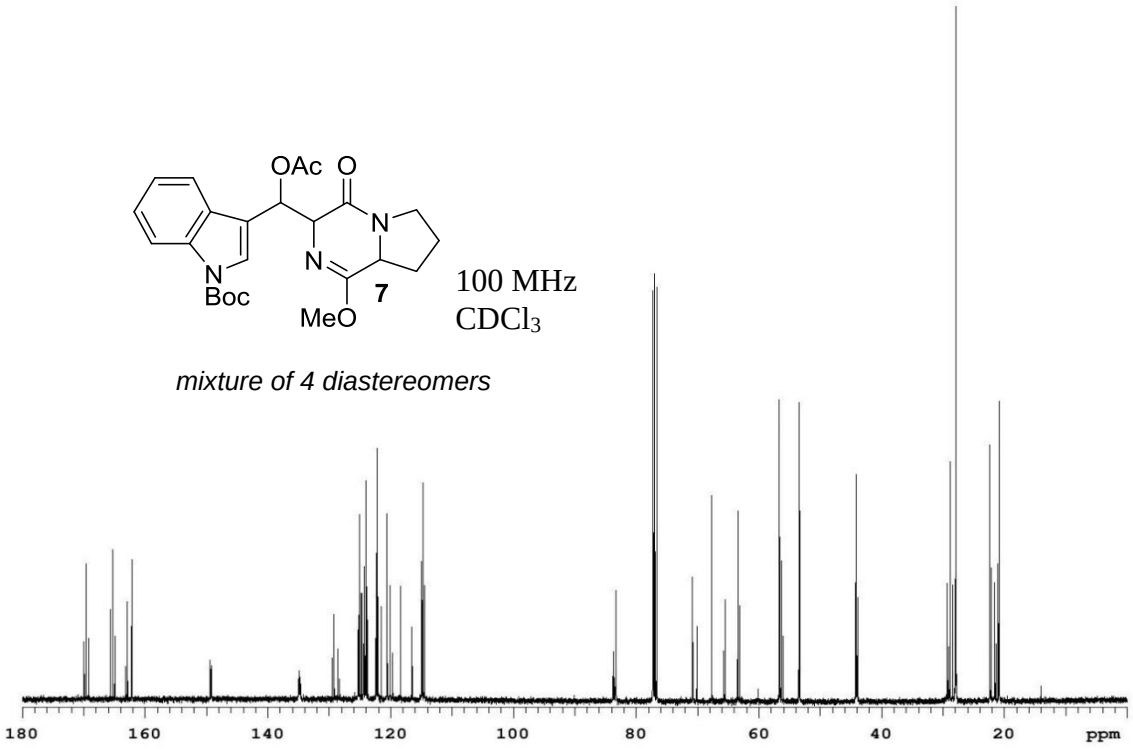
OAc
O
N
N
N
Boc
MeO
7
100 MHz
CDCl3
mixture of 4 diastereomers
180
160
140
120
100
80
60
40
20
ppm

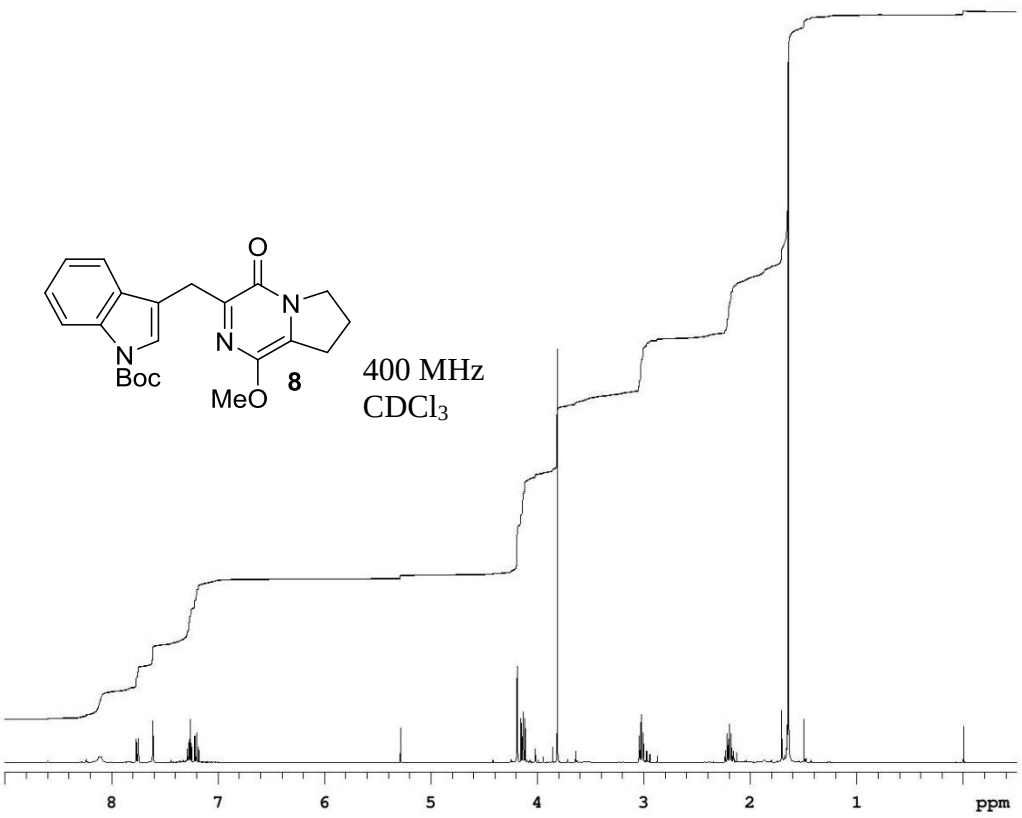
O
N
N
Boc
MeO
8
400 MHz
CDCl3
8
7
6
5
4
3
2
1
ppm

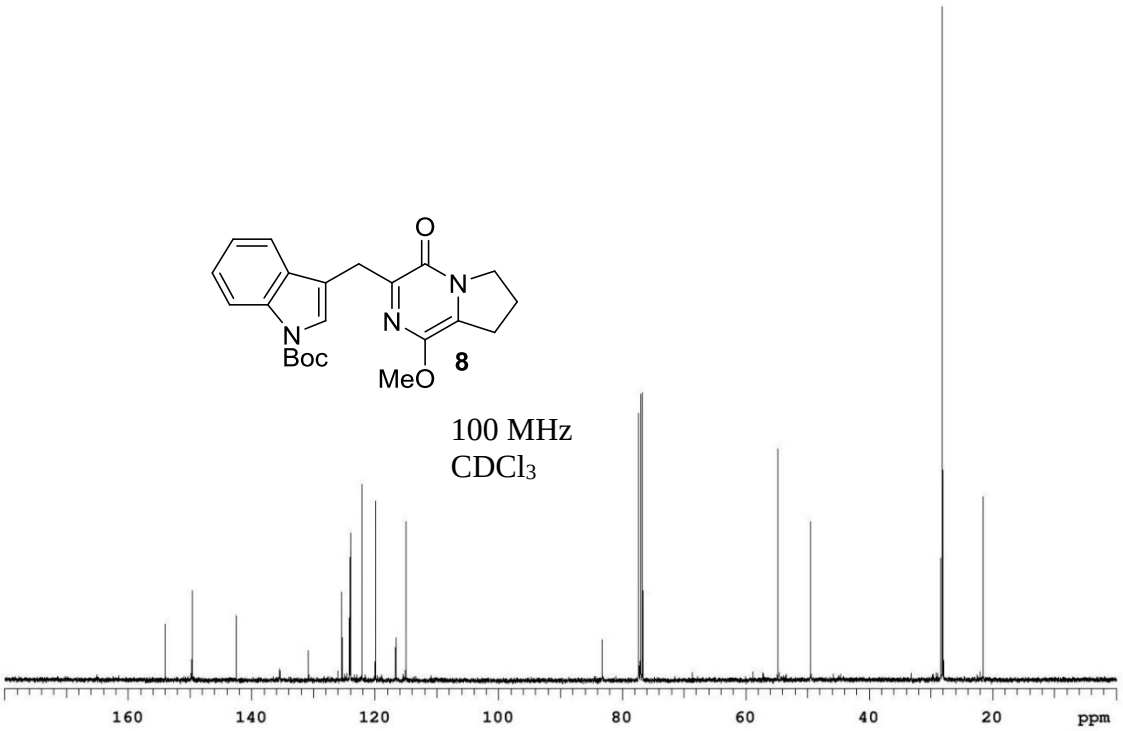
O
N
N
Boc
MeO
8
100 MHz
CDCl3
160
140
120
100
80
60
40
20
ppm

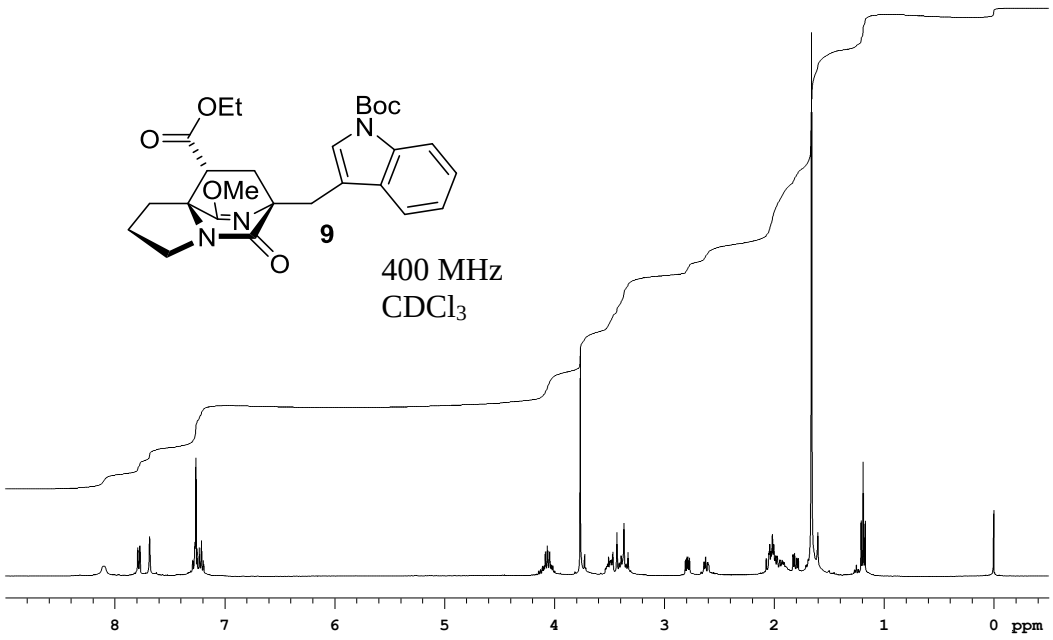

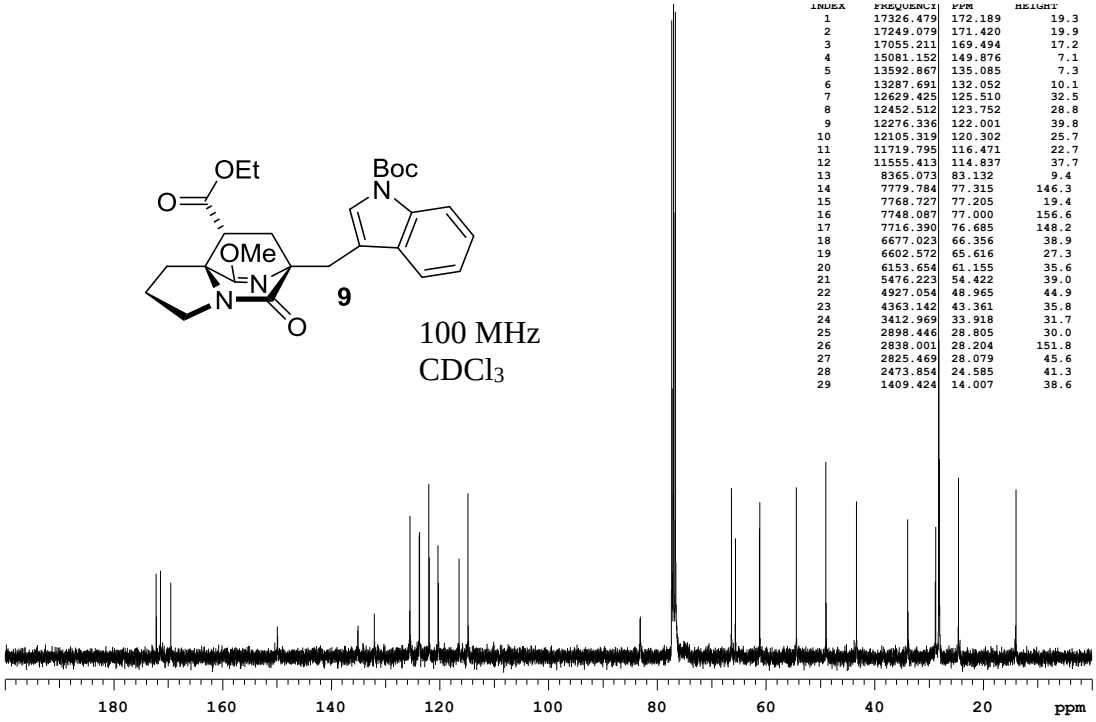

INDEX	FREQUENCY	PPM	HEIGHT
1	17326.479	172.189	19.3
2	17249.079	171.420	19.9
3	17055.211	169.494	17.2
4	15081.152	149.876	7.1
5	13592.867	135.085	7.3
6	13287.691	132.052	10.1
7	12629.425	125.510	32.5
8	12452.512	123.752	28.8
9	12276.336	122.001	39.8
10	12105.319	120.302	25.7
11	11719.795	116.471	22.7
12	11555.413	114.837	37.7
13	8365.073	83.132	9.4
14	7779.784	77.315	146.3
15	7768.727	77.205	19.4
16	7748.087	77.000	156.6
17	7716.390	76.685	148.2
18	6677.023	66.356	38.9
19	6602.572	65.616	27.3
20	6153.654	61.155	35.6
21	5476.223	54.422	39.0
22	4927.054	48.965	44.9
23	4363.142	43.361	35.8
24	3412.969	33.918	31.7
25	2898.446	28.805	30.0
26	2838.001	28.204	151.8
27	2825.469	28.079	45.6
28	2473.854	24.585	41.3
29	1409.424	14.007	38.6

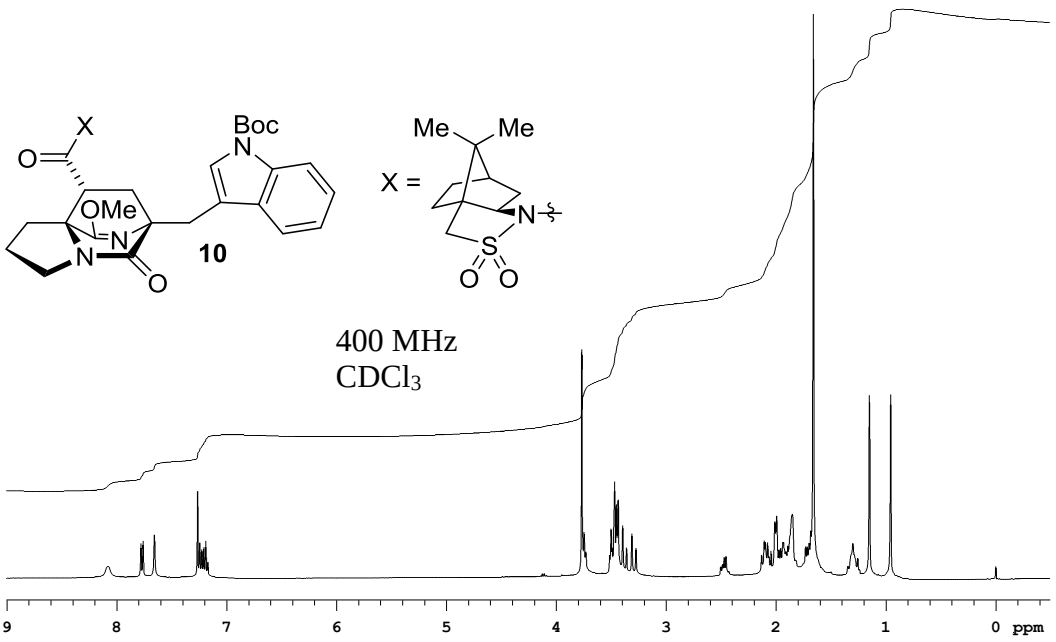

INDEX	FREQUENCY	PPM	HEIGHT	INDEX	FREQUENCY	PPM	HEIGHT
1	17325.004	172.175	16.335		2451.739	24.365	32.3
2	17193.056	170.864	20.936		2105.284	20.922	42.4
3	17058.897	169.530	20.937		1993.976	19.816	42.1
4	15078.940	149.854	8.2				
5	13598.027	135.136	5.5				
6	13291.377	132.089	11.7				
7	12628.688	125.503	36.1				
8	12439.980	123.628	31.1				
9	12272.650	121.965	34.6				
10	12117.113	120.419	31.8				
11	11719.795	116.471	21.1				
12	11549.516	114.778	34.9				
13	8348.856	82.970	12.9				
14	7780.521	77.322	75.0				
15	7768.727	77.205	22.1				
16	7748.087	77.000	78.9				
17	7716.390	76.685	77.0				
18	6671.126	66.297	35.8				
19	6665.966	66.246	38.2				
20	6584.144	65.433	42.2				
21	5482.120	54.481	36.7				
22	5349.435	53.162	33.6				
23	4931.477	49.009	34.3				
24	4854.814	48.247	46.0				
25	4797.317	47.675	34.2				
26	4492.879	44.650	33.5				
27	4350.611	43.236	31.8				
28	3877.367	38.533	33.6				
29	3509.535	34.878	29.3				
30	3308.296	32.878	28.2				
31	2896.235	28.783	28.7				
32	2840.212	28.226	141.0				
33	2739.224	27.222	40.0				
34	2649.293	26.329	29.4				

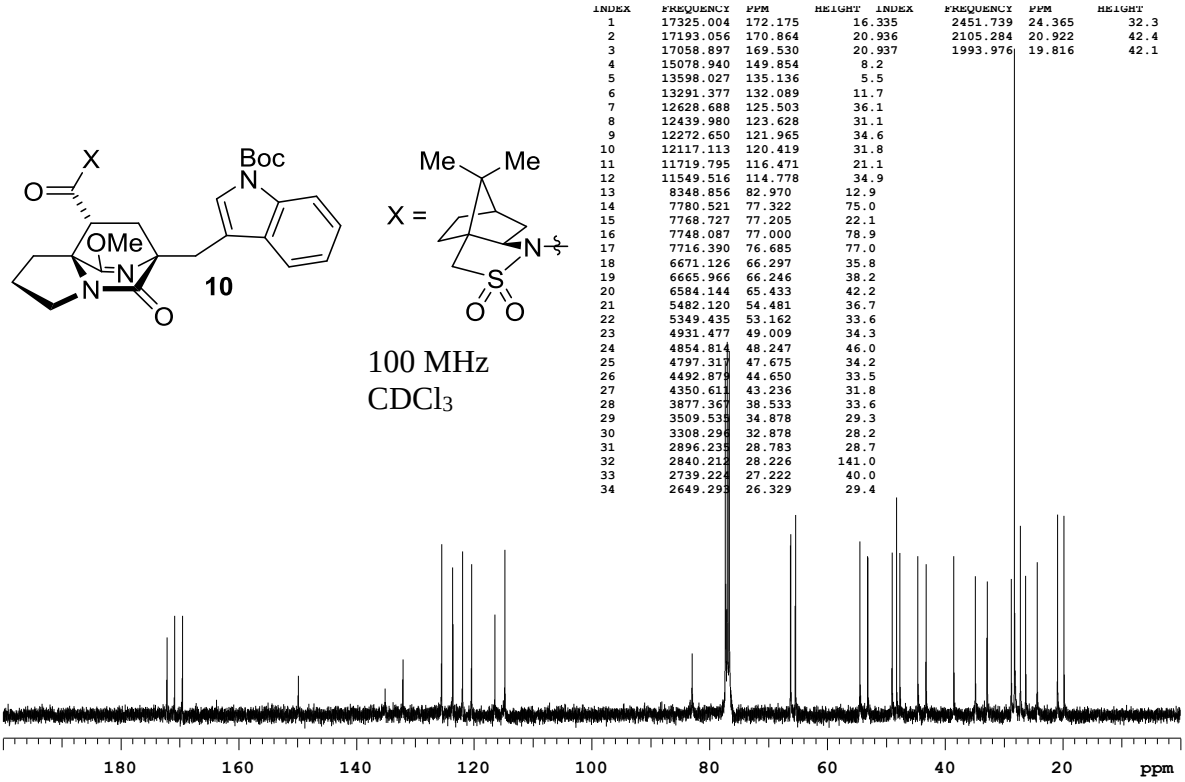

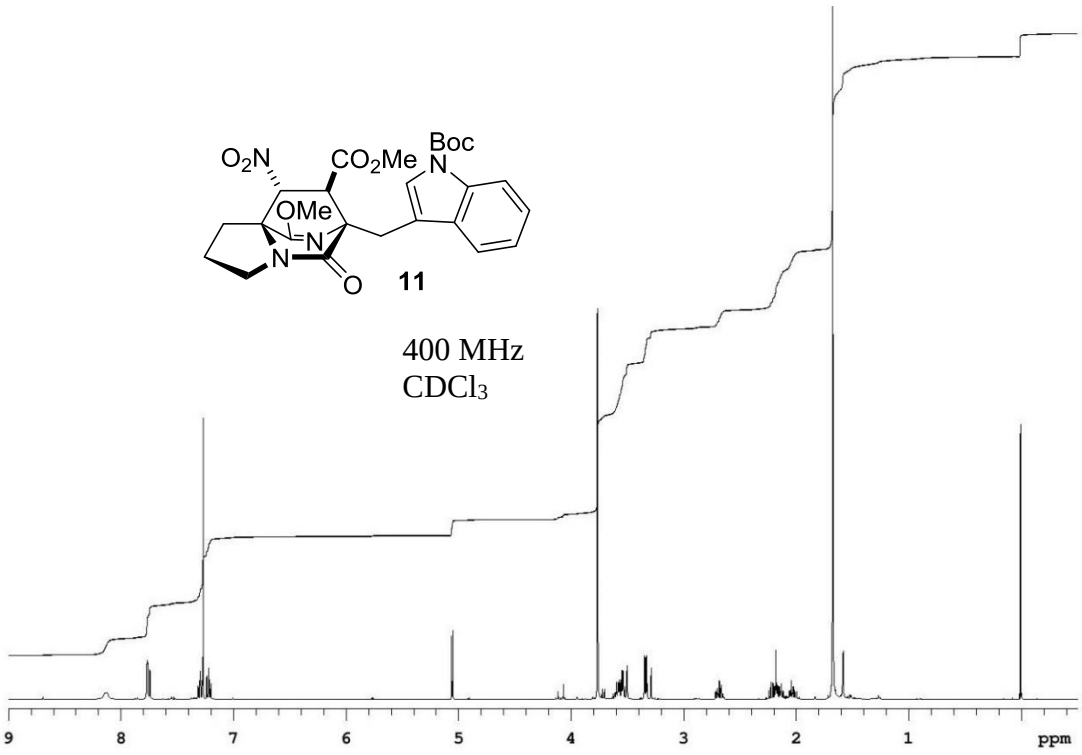
O2N
CO2Me
Boc
N
OMe
N
N
O
11
400 MHz
CDCl3
9
8
7
6
5
4
3
2
1
ppm

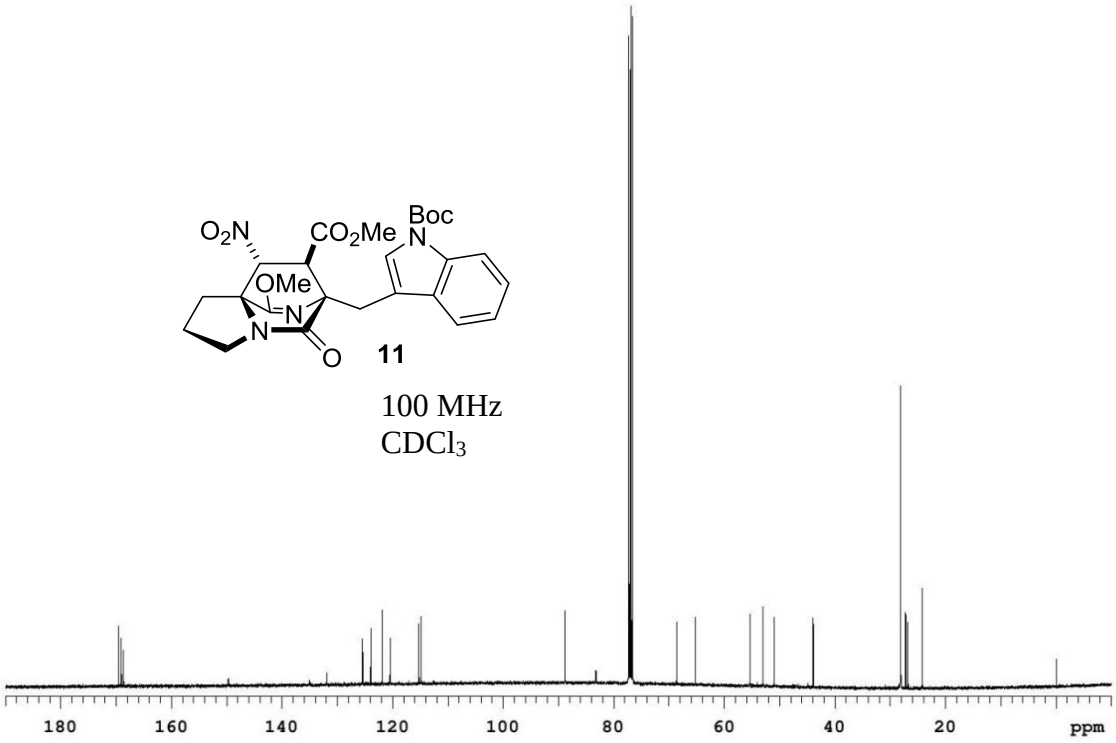
O2N
CO2Me
Boc
N
OMe
N
N
O
11
100 MHz
CDCl3
180
160
140
120
100
80
60
40
20
ppm

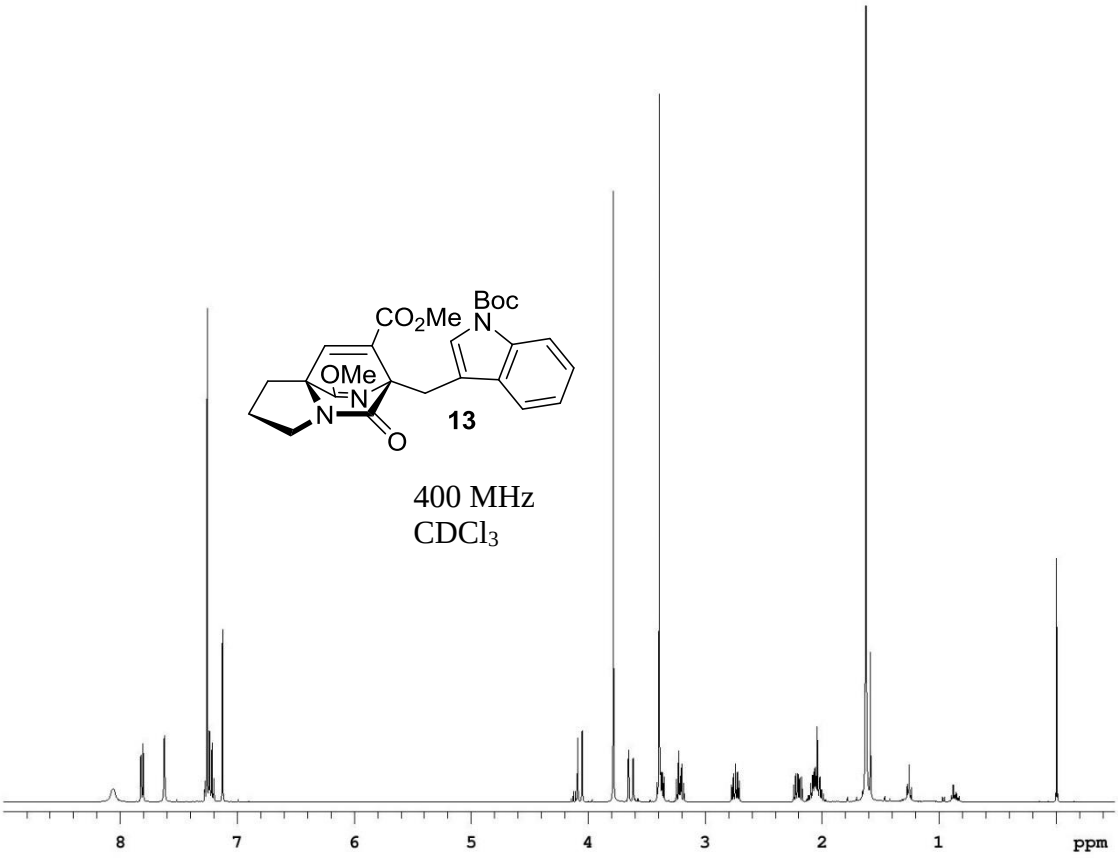
CO2Me
Boc
N
OMe
N
N
O
13
400 MHz
CDCl3
8
7
6
5
4
3
2
1
ppm

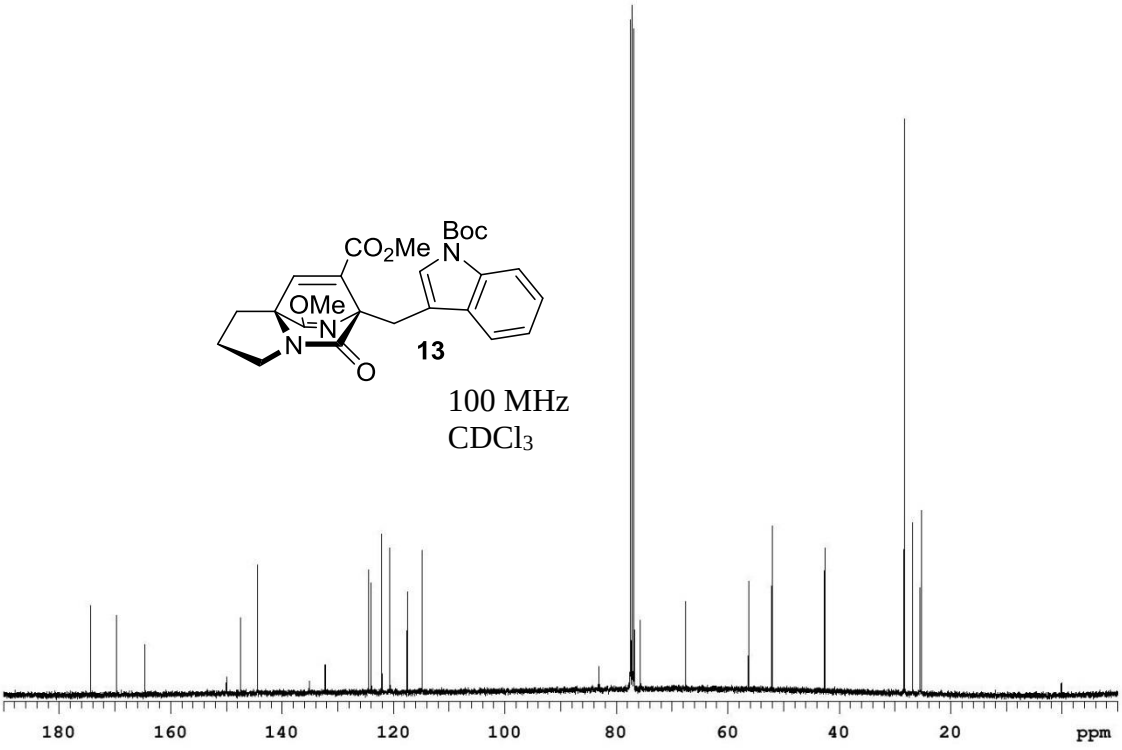
CO2Me
Boc
N
OMe
N
N
O
13
100 MHz
CDCl3
180
160
140
120
100
80
60
40
20
ppm

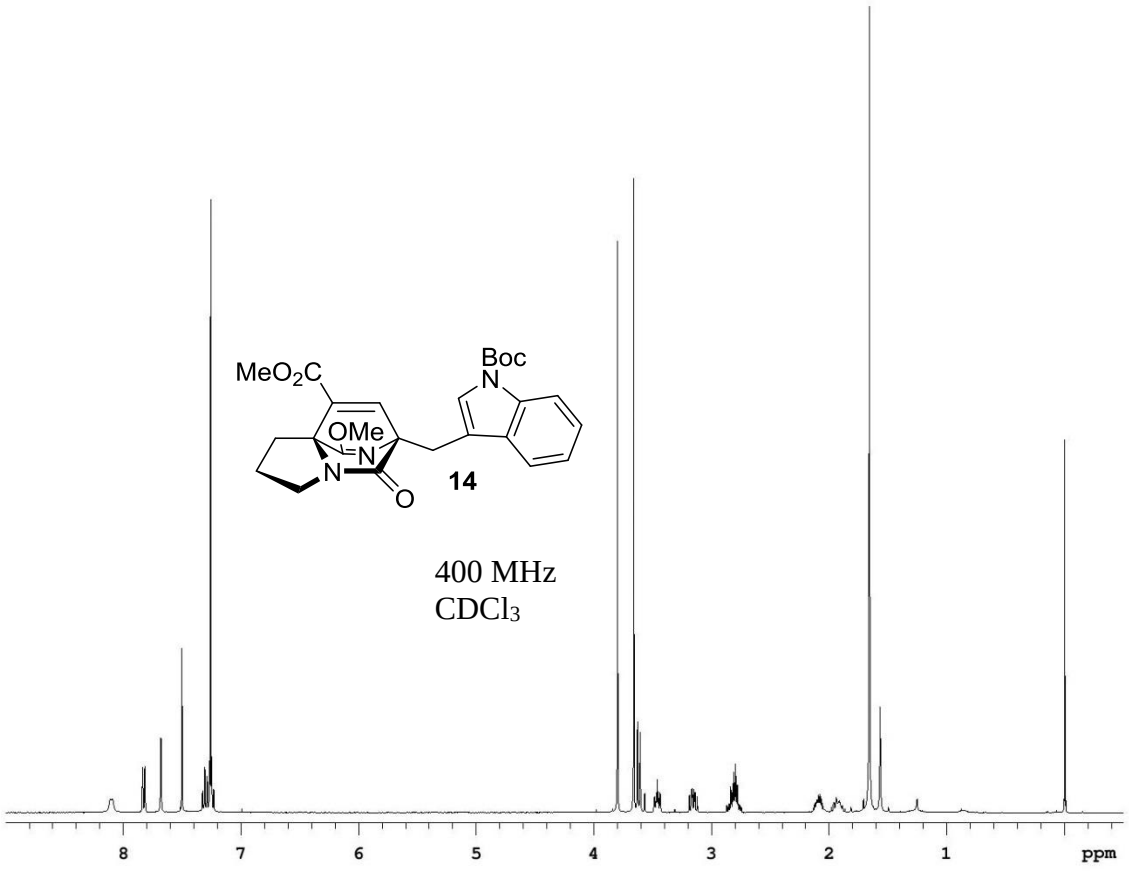
MeO2C
Boc
N
OMe
N
N
O
14
400 MHz
CDCl3
8
7
6
5
4
3
2
1
ppm

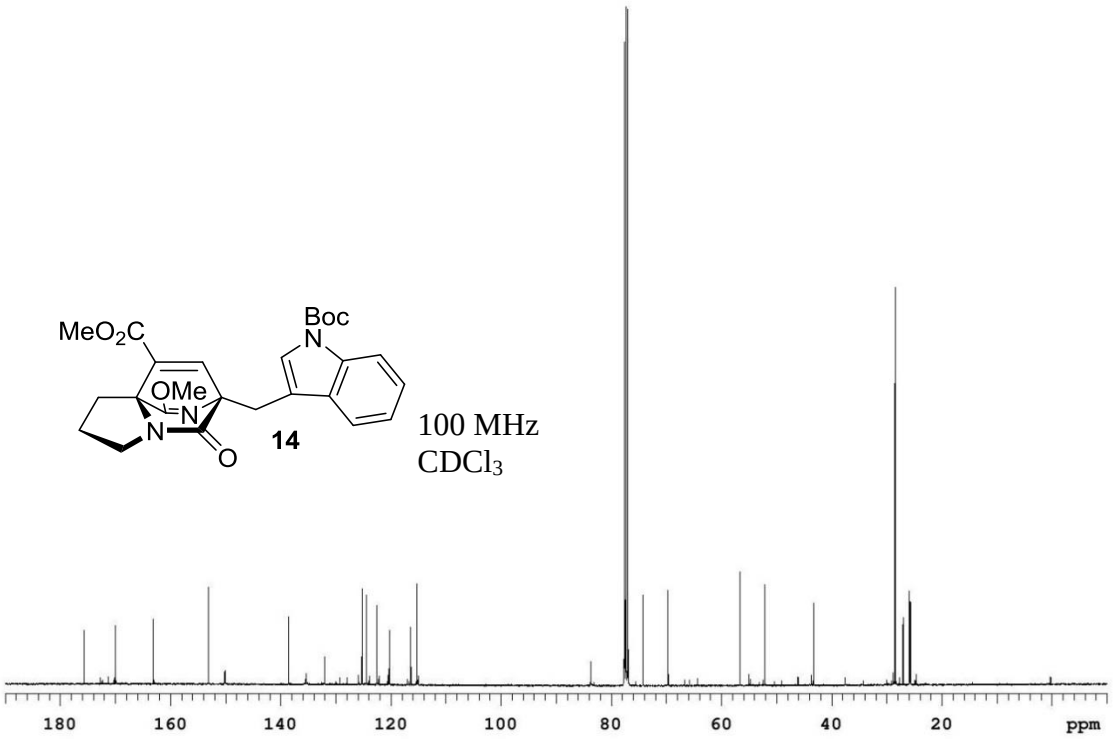
MeO2C
Boc
N
OMe
N
N
O
14
100 MHz
CDCl3
180
160
140
120
100
80
60
40
20
ppm

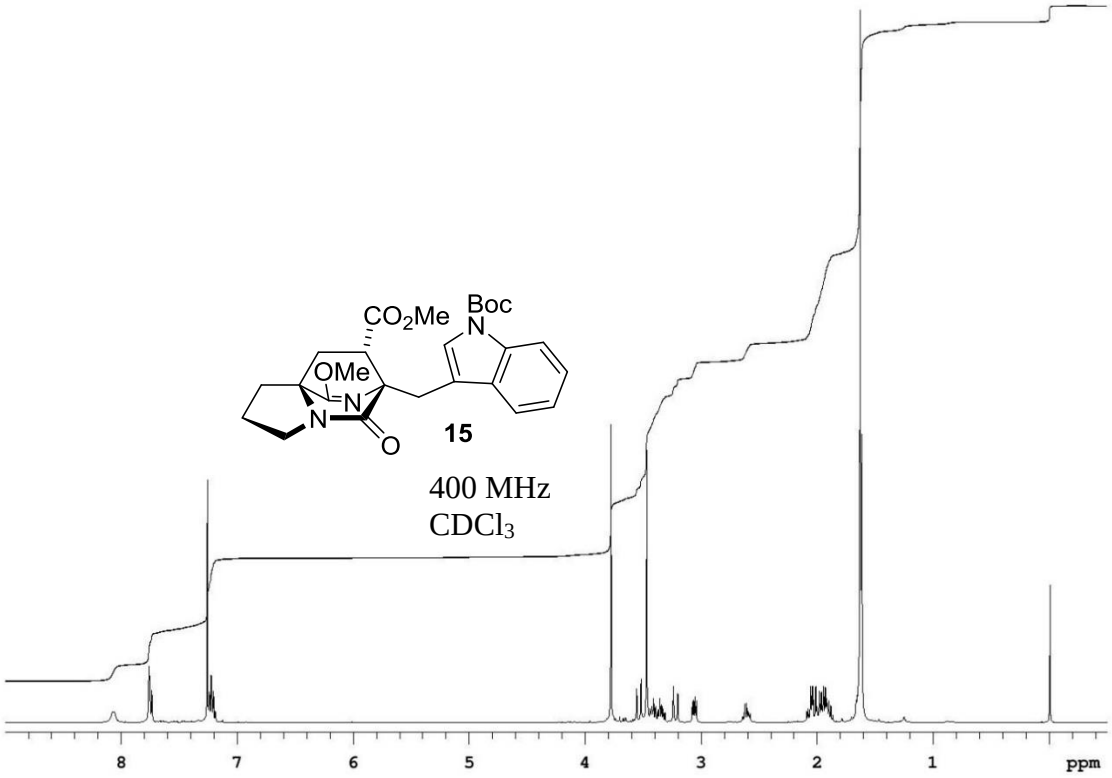
CO2Me
Boc
N
OMe
N
N
O
15
400 MHz
CDCl3
8
7
6
5
4
3
2
1
ppm

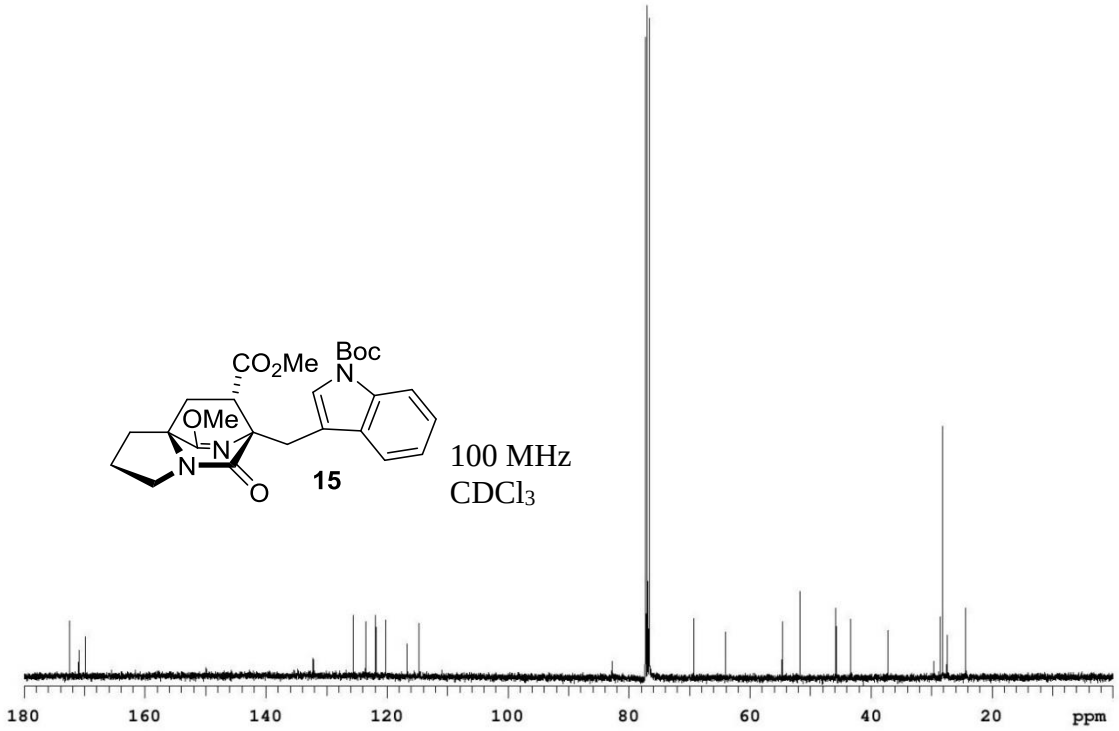
CO2Me
Boc
N
OMe
N
N
O
15
100 MHz
CDCl3
180
160
140
120
100
80
60
40
20
ppm

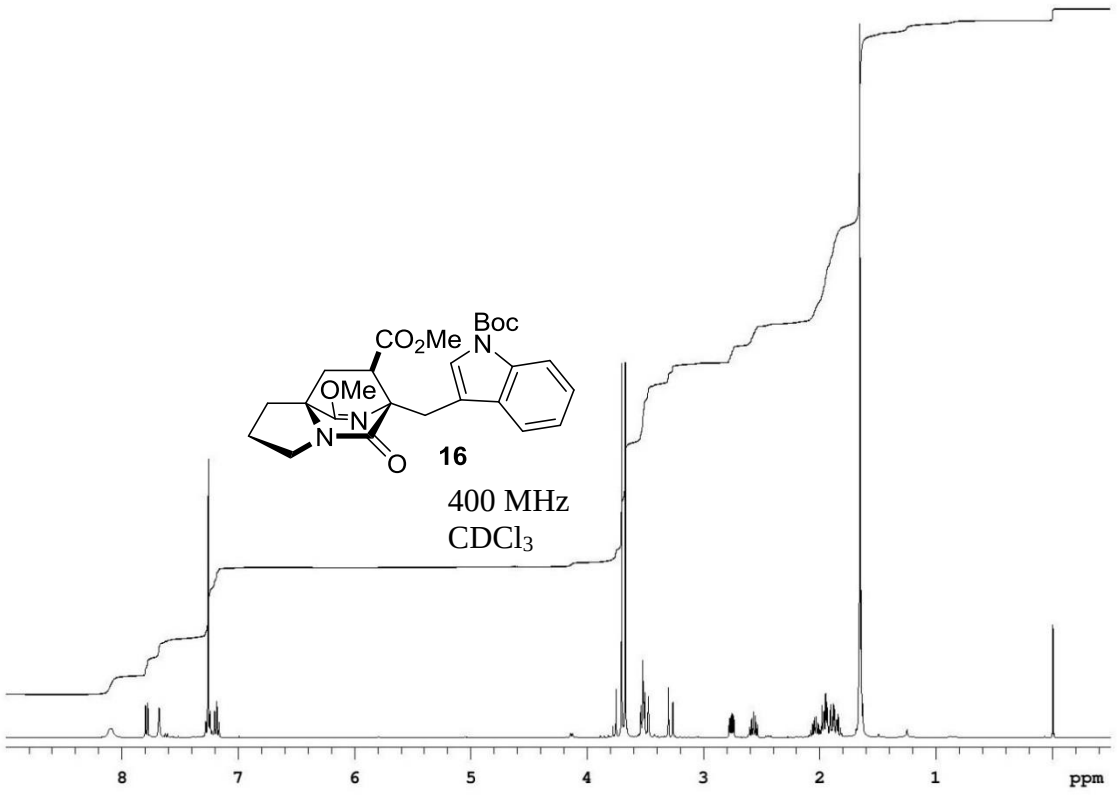
CO2Me
Boc
N
OMe
N
N
O
16
400 MHz
CDCl3
8
7
6
5
4
3
2
1
ppm

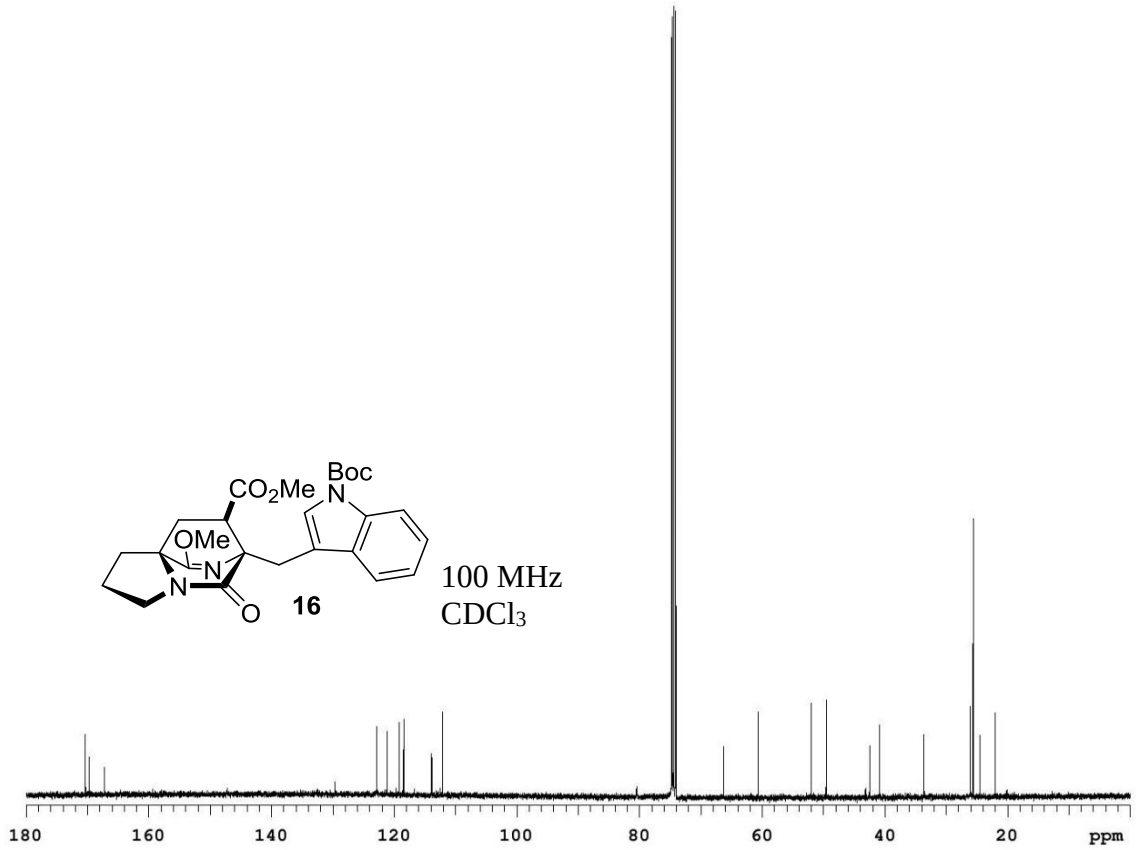
CO2Me
Boc
N
OMe
N
N
O
16
100 MHz
CDCl3
180
160
140
120
100
80
60
40
20
ppm

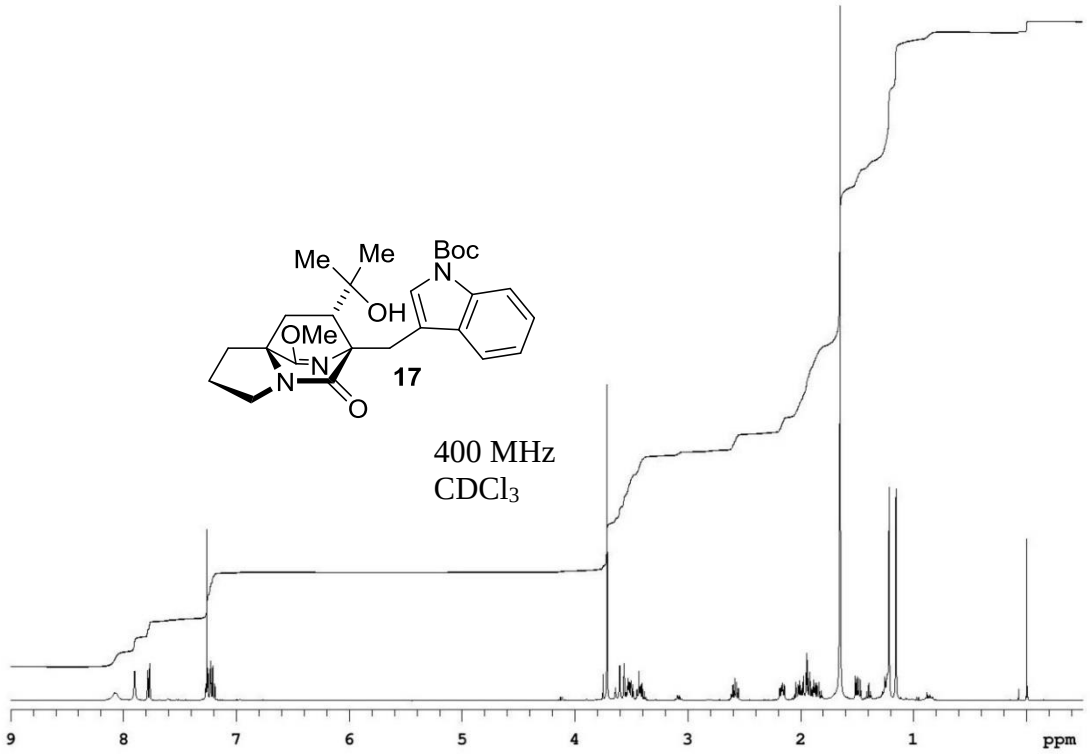
Me
Me
Boc
N
OH
OMe
N
N
O
17
400 MHz
CDCl3
9
8
7
6
5
4
3
2
1
ppm

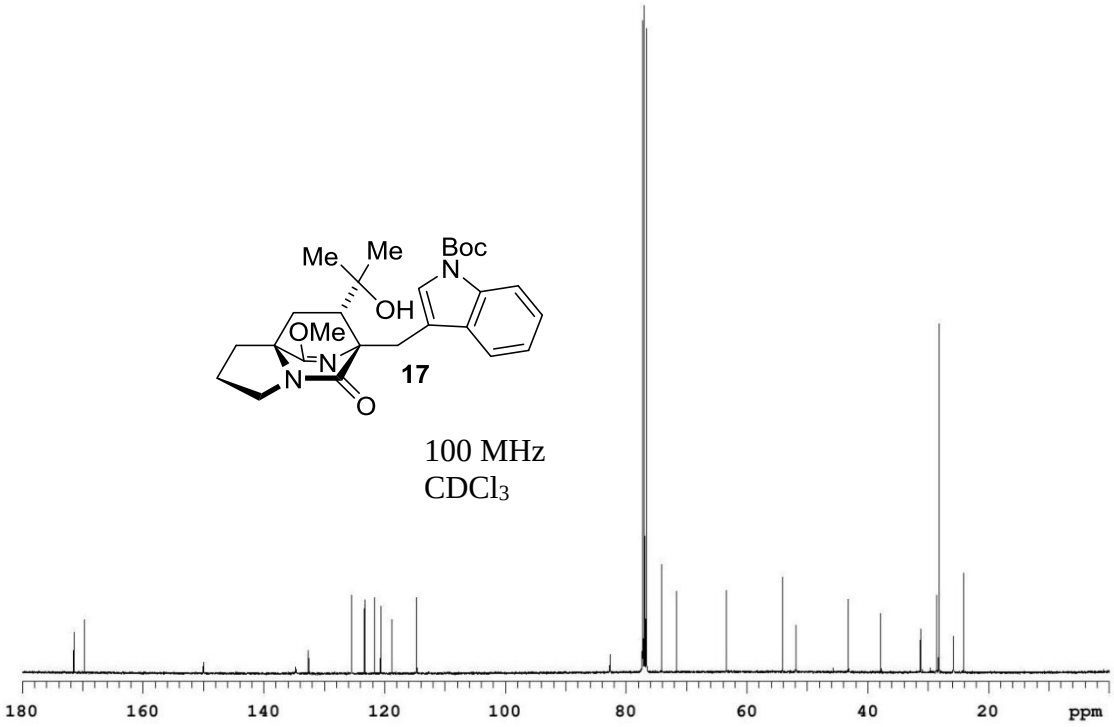
Me
Me
Boc
N
OH
OMe
N
N
O
17
100 MHz
CDCl3
180
160
140
120
100
80
60
40
20
ppm

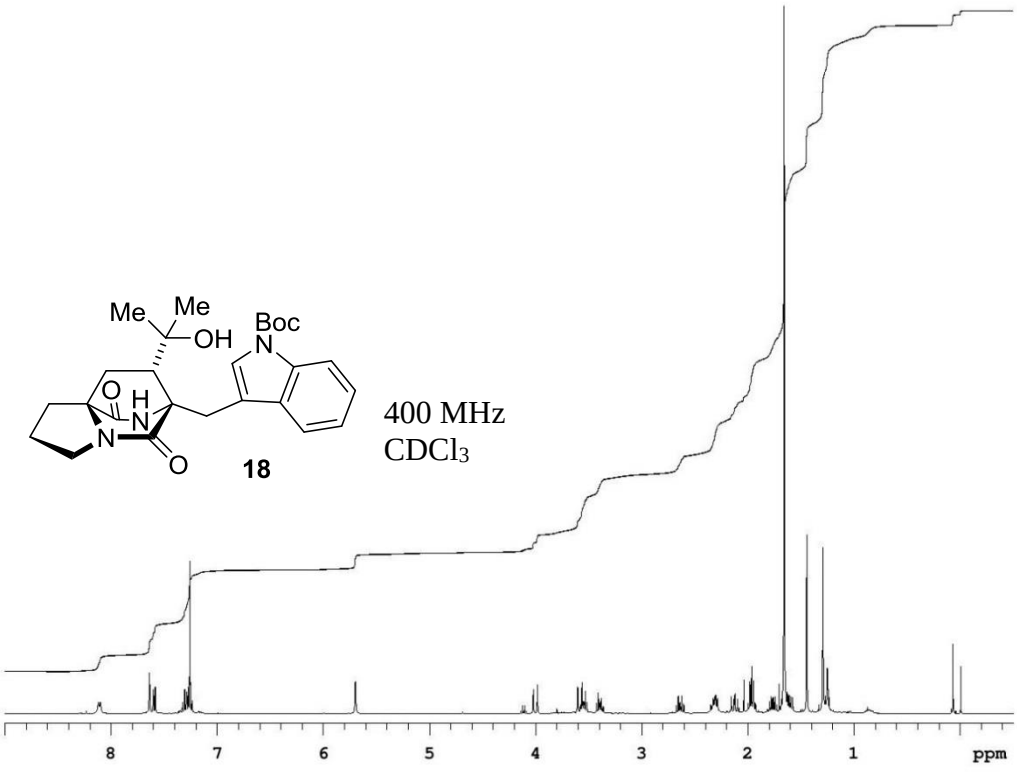
Me
Me
OH
Boc
N
O
H
N
N
O
18
400 MHz
CDCl3
8
7
6
5
4
3
2
1
ppm

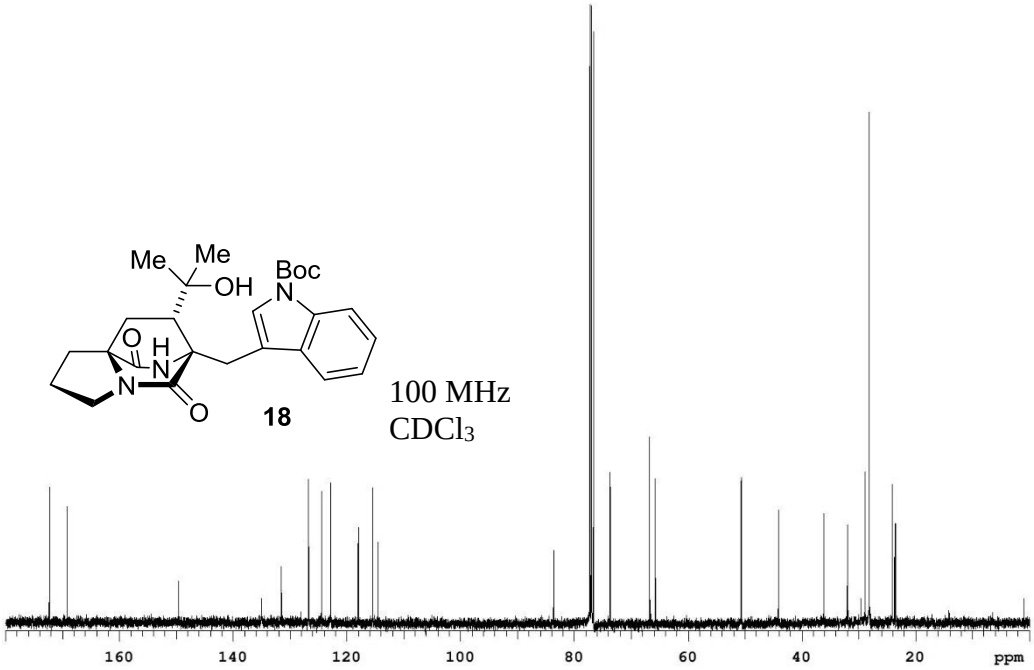
Me
Me
OH
Boc
N
O
H
N
N
O
18
100 MHz
CDCl3
160
140
120
100
80
60
40
20
ppm

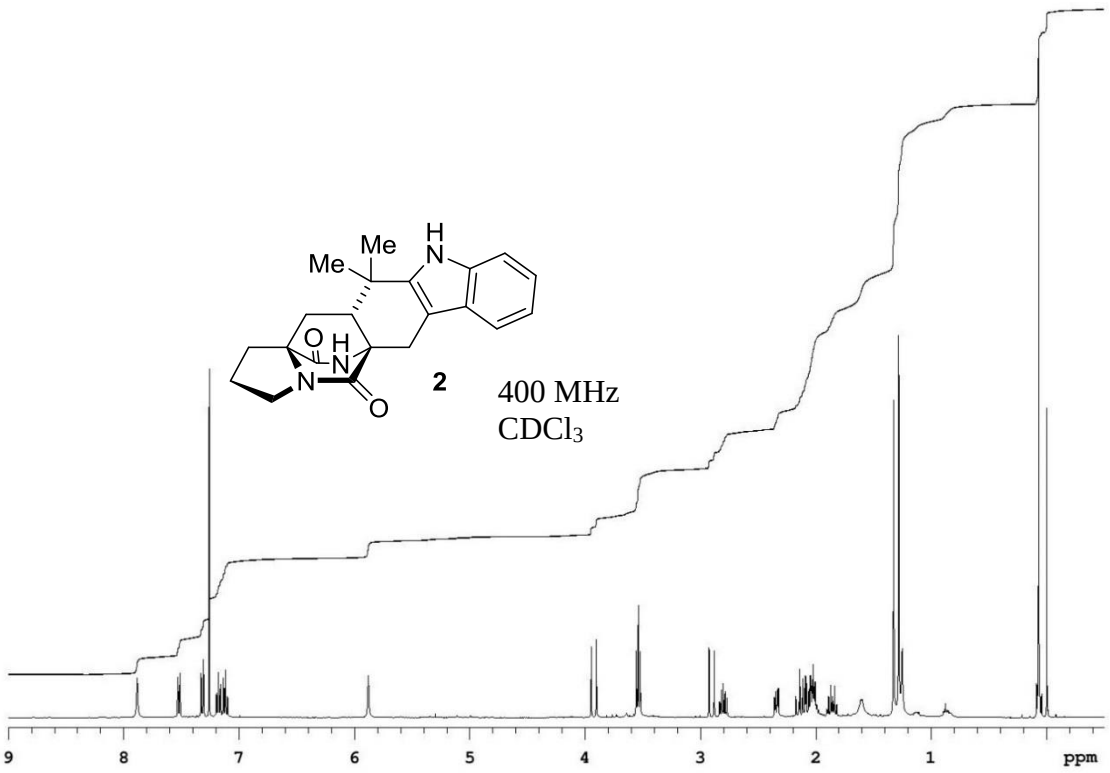
Me
Me
H
N
O
H
N
N
O
2
400 MHz
CDCl3
9
8
7
6
5
4
3
2
1
ppm

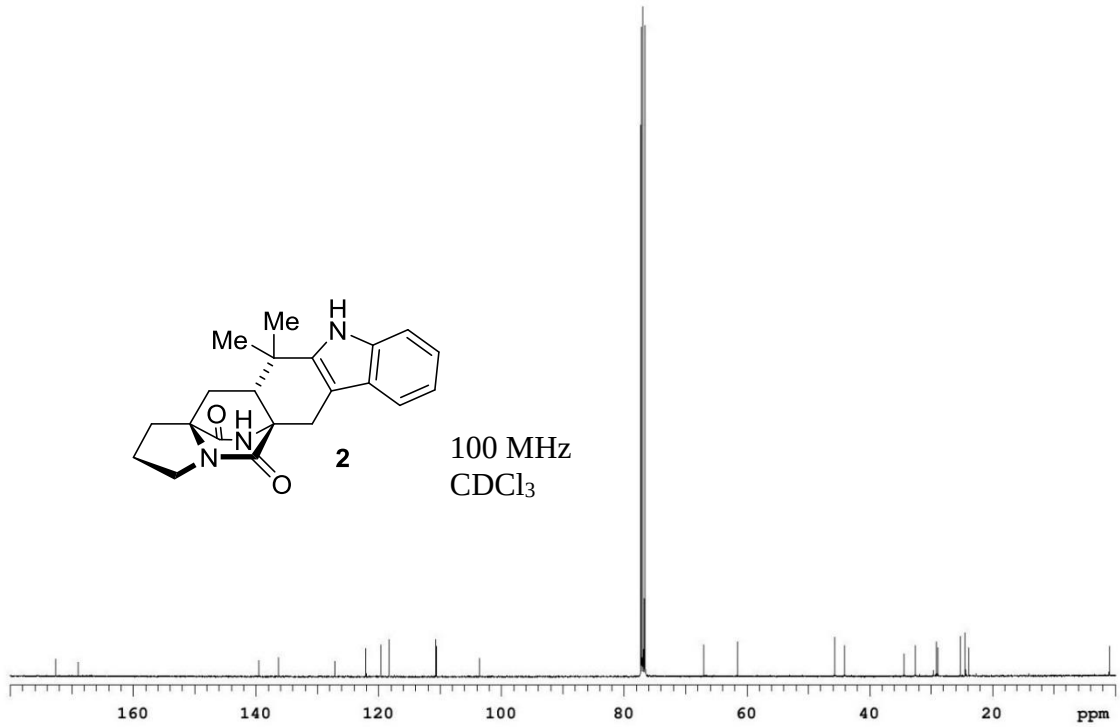
Me
Me
H
N
O
H
N
N
O
2
100 MHz
CDCl3
160
140
120
100
80
60
40
20
ppm

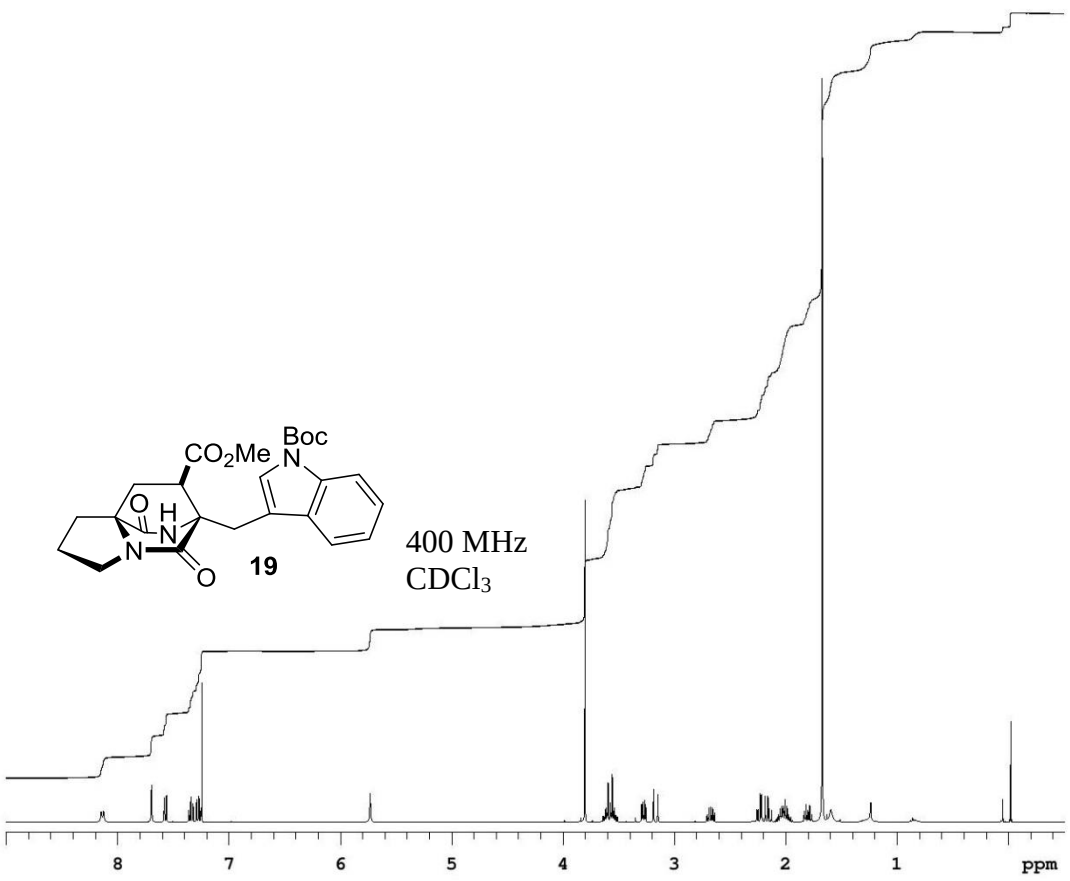
CO2Me
Boc
N
O
H
N
N
O
19
400 MHz
CDCl3
8
7
6
5
4
3
2
1
ppm

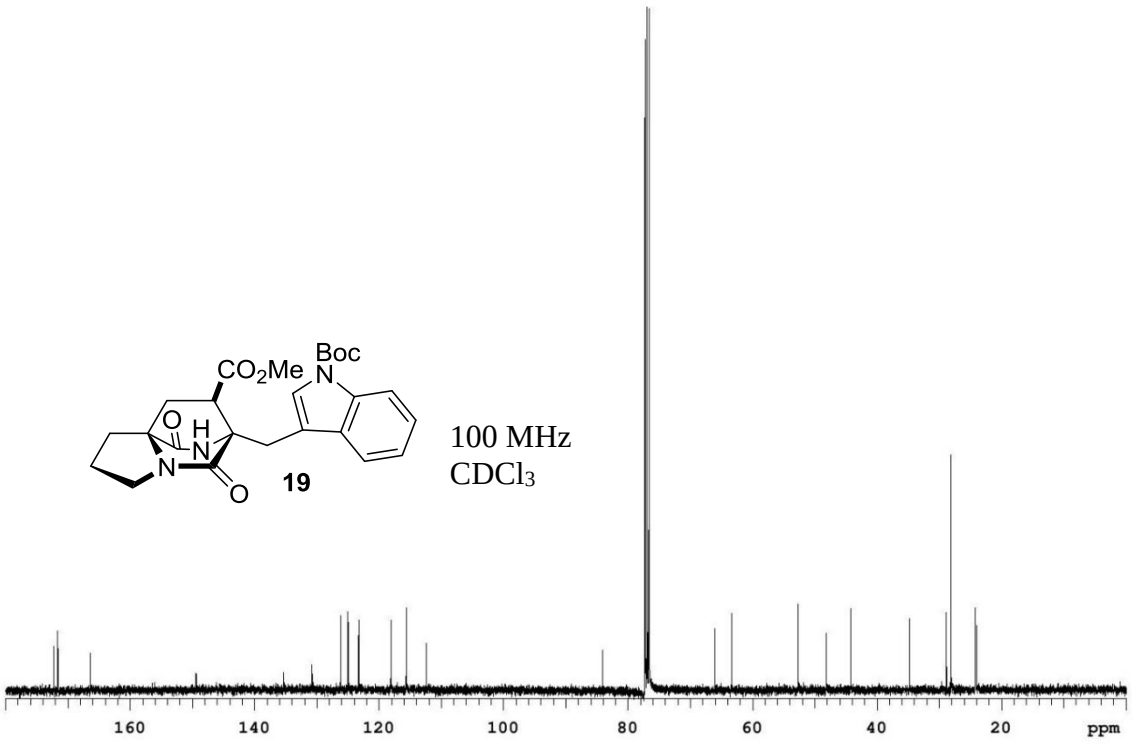
CO2Me
Boc
N
O
H
N
N
O
19
100 MHz
CDCl3
160
140
120
100
80
60
40
20
ppm

REFERENCES

1. Pangborn, A.B.; Giardello, M.A.; Grubbs, R.H.; Rosen, R.K.; Timmers, F. J., *Organometal.* **1996,** *15*, 1518–1520.
2. Still, W.C.; Kahn, M.; Mitra, A. *J. Org. Chem.* **1978,** *43*, 2923–2925.

Appendix II
Computational Data for Pyrazinone [4+2] Cyclizations

Figure A.1 [2.2.2]diazaoctanes used in computational studies

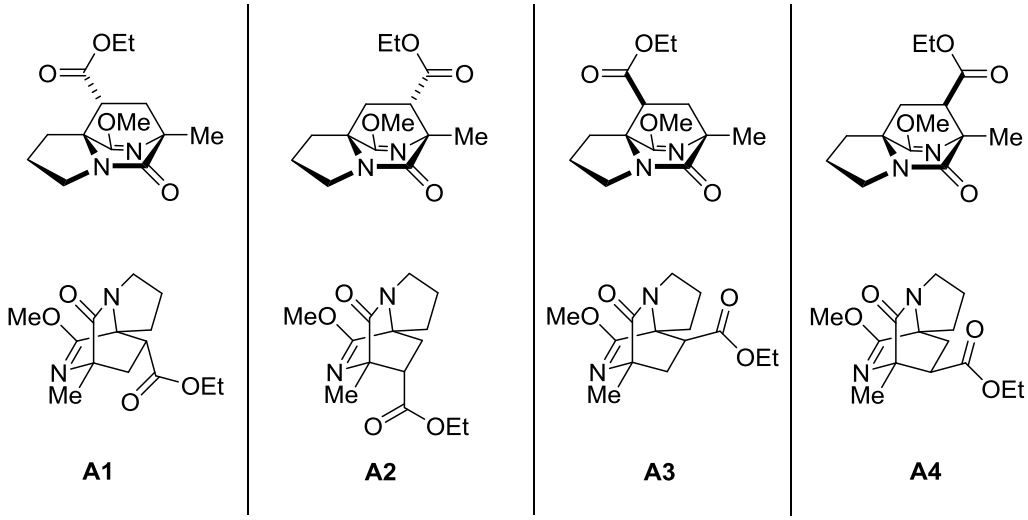

Table A.1 Comparison of computational

Product	$E_{reactants}$ (kJ mol^{-1})	E_{TS} (kJ mol^{-1})	$E_{products}$ (kJ mol^{-1})
A1	0.00	32.2	–53.8
A2	5.14	35.8	–30.7
A3	7.65	39.7	–20.8
A4	2.83	36.9	–41.7

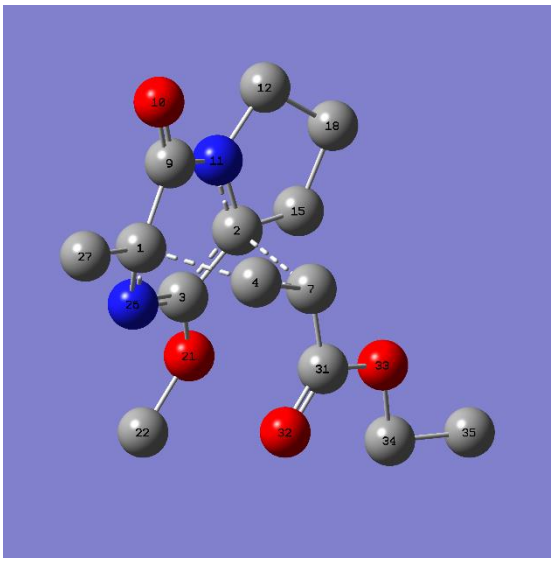

Figure A.2 Calculated transition state for **A1**

Figure A.3 Intrinsic Reaction Coordinate graph for **A1**

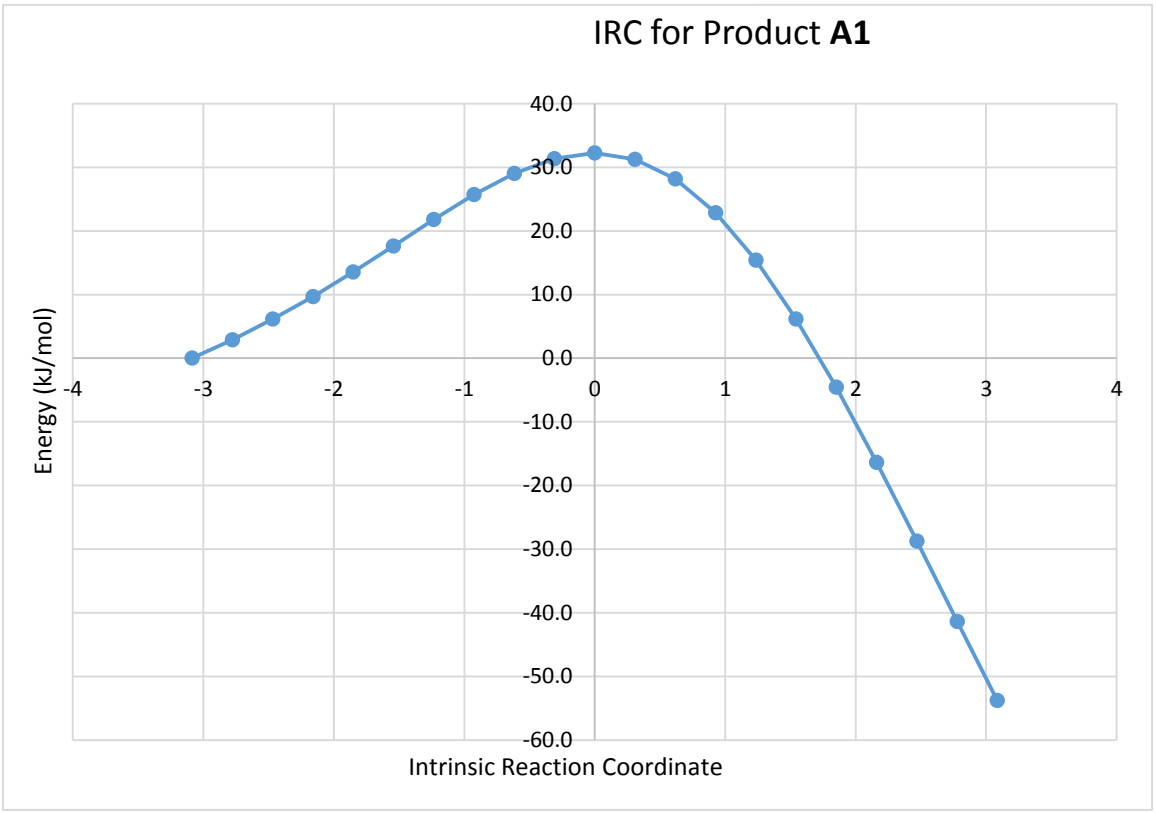

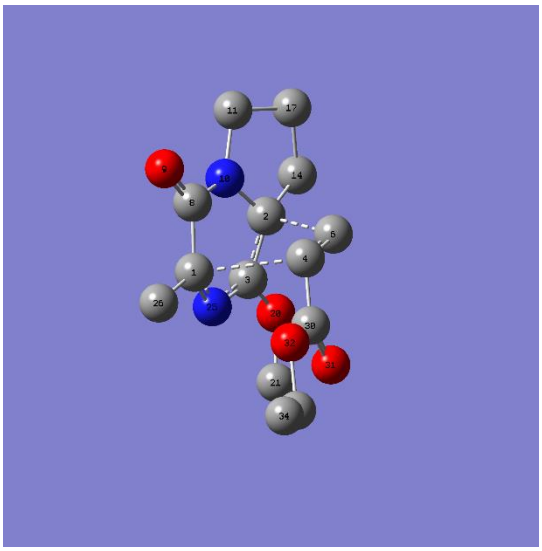

Figure A.4 Calculated transition state for **A2**

Figure A.5 Intrinsic Reaction Coordinate graph for **A2**

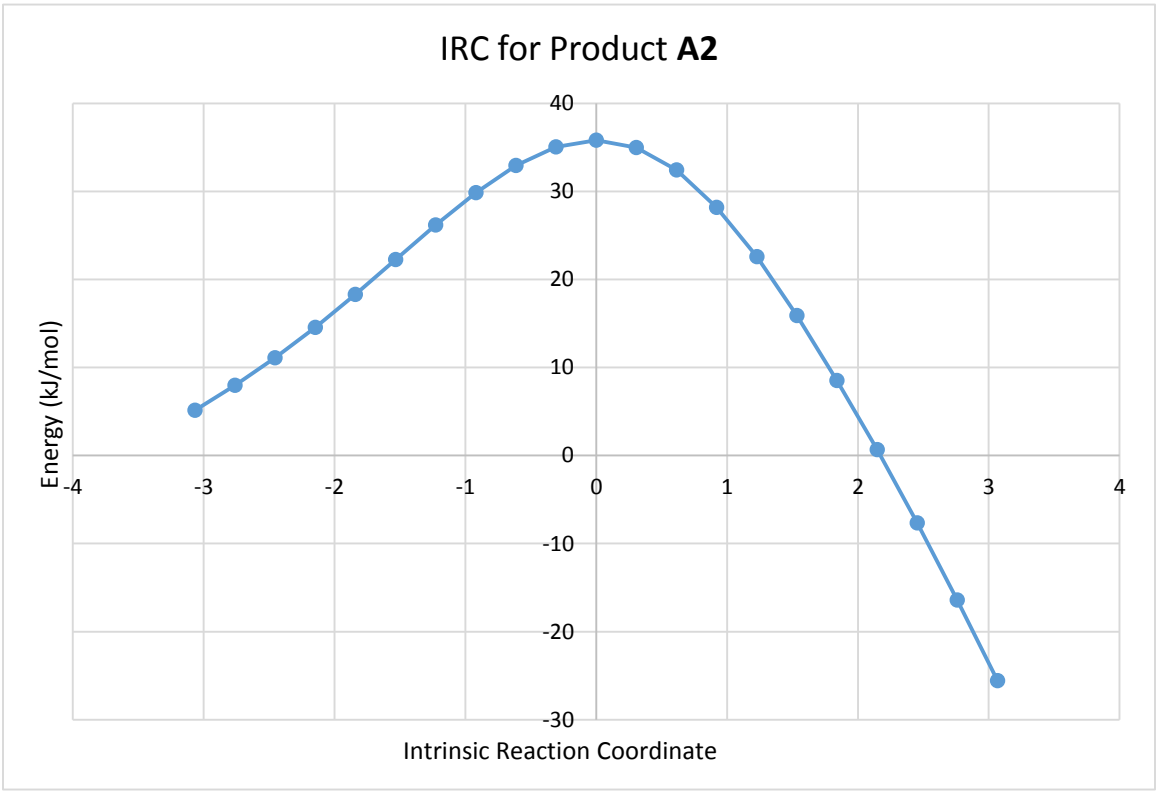

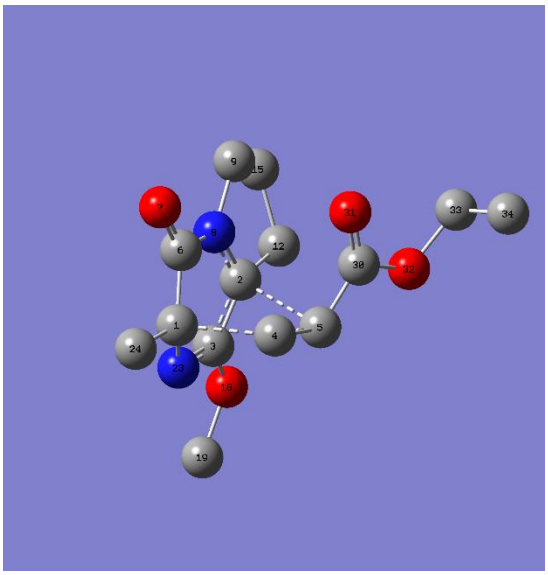

Figure A.6 Calculated transition state for **A3**

Figure A.7 Intrinsic Reaction Coordinate graph for **A3**

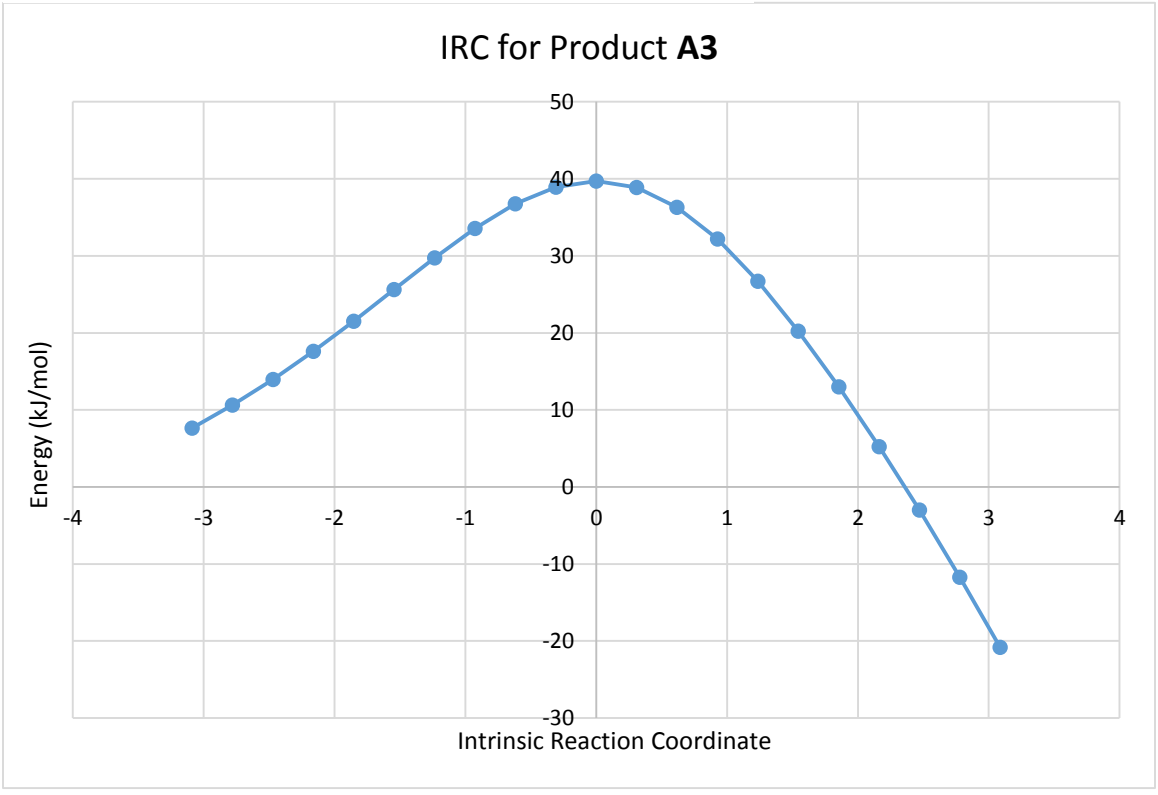

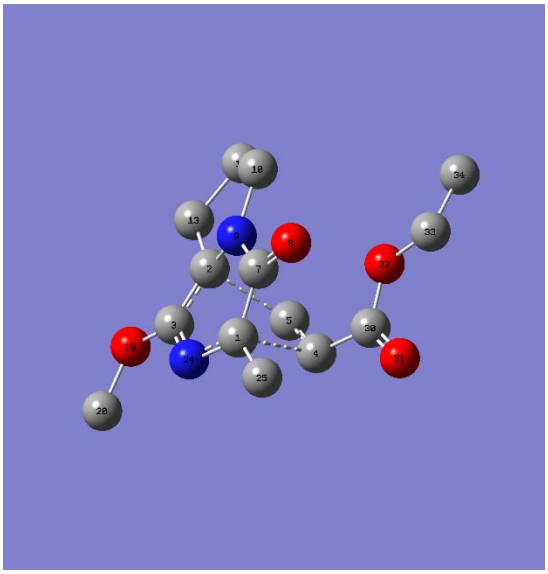

Figure A.8 Calculated transition state for **A4**

Figure A.9 Intrinsic Reaction Coordinate graph for **A4**